Understanding cessation of neural crest migration and onset of gangliogenesis

Thesis by
Hugo Urrutia

In Partial Fulfillment of the Requirements for the
Degree of
Doctor of Philosophy

CALIFORNIA INSTITUTE OF TECHNOLOGY
Pasadena, California

2025
Defended March 21, 2025

Hugo Urrutia
ORCID: 0000-0002-2970-6918

ACKNOWLEDGEMENTS

Although this thesis bears my name, I could not have done it without the unrelenting support of my mentors, friends, family, and colleagues. The past six years at Caltech have been a challenging yet deeply rewarding journey, and I'm immensely grateful for the people who ensured I never had to do it alone. As I compile this thesis, I reflect on the individuals who have played a vital role in helping me reach this moment, and I'm extremely grateful for their contributions.

First and foremost, I want to express my deepest gratitude to my parents. I would not be where I am today if not for their sacrifices and hard work in ensuring that I had every opportunity I needed to succeed in life. None of this would be possible without them, and I owe this accomplishment to their unwavering love and support.

I am profoundly grateful to my thesis advisor, Dr. Marianne Bronner, whose mentorship has shaped me into the scientist I am today. Her steadfast faith in my abilities—especially during moments when my own confidence wavered—provided the encouragement I needed to become a successful scientist. Over the years, Marianne not only instilled in me the confidence I needed to pursue my own ideas to work on in the lab, but she also guided me with wisdom and enthusiasm while emphasizing the importance of maintaining a healthy work-life balance. Her commitment and passion for science is truly inspiring, from her hands-on contributions in the lab to her tireless dedication to mentoring. To this day, I remain amazed by her expertise, especially when a project requires her steady hands to perform intricate embryo injections. Even during the challenges of the pandemic, she always made time for me, sometimes on just a few minutes' notice. She was always available to enthusiastically discuss new data or lift my spirits when it felt like nothing was working for me. I will be forever indebted to her for teaching me everything that I know about Developmental Biology, for trusting me to undertake bold projects, and for pushing me to strive for excellence. Marianne's mentoring

focused on bringing out my strengths and taught me how to think like a scientist. I will carry these lessons—both scientific and personal—throughout my career, and I am forever grateful to have had her as a mentor and role model.

I also want to extend my sincere appreciation to my thesis advisory committee members, Ellen Rothenberg, David Prober, and Joe Parker, whose insights and feedback helped shape my research at Caltech. In particular, I am especially grateful to Ellen, who chaired my thesis committee and whose infectious enthusiasm never failed to reinvigorate my excitement for science. Their guidance and support have been instrumental in my growth as a scientist, and I am deeply appreciative of their time and mentorship. I sincerely thank you all for your invaluable dedication and time you have put into serving on my committee.

To my lab mates, both past and present, in the Bronner lab, I want to thank you all for your contributions to my training, advice on my work, exciting collaborations, and for making the lab an enjoyable and supportive environment. From troubleshooting experiments to engaging in lively scientific discussions, your contributions to my journey have been invaluable. When I arrived at Caltech with very little experience in developmental biology, my first years were filled with steep learning curves, and I could not have navigated them without the patience and guidance of my fellow lab members.

No one's graduate experience in Caltech's Biology and Biological Engineering division is complete without the incredible administrative support from Liz Ayala. From the early stages of planning my in-person interview at Caltech to navigating deadlines and paperwork for graduation, I am deeply indebted to Liz for her assistance and guidance.

And finally, a special thanks to Johanna Tan-Cabugao and Constanza Gonzalez for their behind-the-scenes efforts that made my research run smoothly. Because of

their dedication and hard work, I never had to worry about ordering reagents, preparing solutions, or navigating bureaucratic hurdles, leaving me with more time to focus on doing the best science possible.

To my friends, and to those who have been my pillars of support throughout this journey, your presence has enriched my life in countless ways. I won't attempt to name everyone else, but you know who you are. Many of you come from different corners of the world, and I have cherished the cultural experiences, deep conversations, and shared adventures we have had together.

Finally, I am forever indebted to my wife, Rocio Urrutia-Angulo. Without your ongoing support, completing my PhD would have been impossible—thank you for being my biggest and greatest supporter. Rocio, you followed me through grad school and now across the country, so that I may continue to pursue my passions. Your endless patience, love, and sacrifices have made this possible, and for that, I am immensely grateful.

The research presented in this thesis was made possible by the support of the National Institutes of Health.

To everyone who has played a role in this journey—whether through mentorship, friendship, or encouragement—thank you. Now, I can proudly say that I am a developmental biologist.

ABSTRACT

The neural crest is a multipotent, vertebrate-specific embryonic cell population that originates at the border of the developing central nervous system. Often referred to as the "fourth germ layer," the neural crest gives rise to diverse cell types, including craniofacial structures and components of the peripheral nervous system. Neural crest cells from specific axial levels in the embryo generate unique sets of progeny and migrate along distinct pathways, differing from those at other axial levels. During development, the formation of key structures within the vertebrate head, such as cranial ganglia and sense organs, requires coordinated migration and interactions between two distinct embryonic cell populations: the neural crest and the ectodermal placodes. The dual embryonic origin of cranial sensory ganglia has interested investigators for some time, yet surprisingly, little is still known about the neural crest–placode relationship. Despite extensive research, the process of cranial gangliogenesis, an intriguing example of how cell–cell interactions drive the assembly of complex structures in the developing embryo, remains incompletely understood. To address this gap, I aimed to advance our understanding of neural crest contributions to cranial sensory ganglia formation and investigate how interactions between these two distinct cell populations contribute to chick trigeminal gangliogenesis.

To investigate this process, I focused on the early formation of the trigeminal ganglion, emphasizing on the transcriptional regulation of neural crest-derived cells. Using a combination of lineage labeling and *in situ* hybridization in chick embryos, we demonstrated that the transcription factor *Tlx3* is expressed in neural crest-derived cells contributing to the cranial trigeminal ganglion, coinciding with the onset of ganglion condensation. Notably, loss-of-function experiments revealed that *Tlx3* deficiency results in smaller ganglia with fewer neurons. Conversely, ectopic expression in migrating cranial neural crest cells accelerates neuronal differentiation, underscoring its critical role in neural crest-derived

neuronal development. Taken together, these results demonstrate a pivotal role for *Tlx3* in neural crest-derived cells during chick trigeminal gangliogenesis.

As an additional candidate mediator, I investigated the potential role of *Cxcl14*. The concurrent expression of CXCL14 in placodal cells and its potential cognate receptor CXCR4 in neural crest cells raised the intriguing possibility that this ligand–receptor pair mediates signaling from placodal to neural crest cells, representing an additional form of their cell-cell interactions. Loss of *Cxcl14* disrupts gangliogenesis and axonal projections, revealing an essential role for this chemokine in guiding neural crest-placode interactions during early ganglion formation. More specifically, perturbing *Cxcl14* in the placodal population resulted in increased dispersion of neural crest-derived cells in the maxillomandibular lobe but not in the ophthalmic lobe of the trigeminal ganglion, highlighting its critical role in directing neural crest-placode interactions during early ganglion formation.

In summary, the findings from my thesis advance our understanding of neural crest contributions to cranial sensory ganglia formation. By elucidating transcriptional and signaling mechanisms involved in trigeminal gangliogenesis, these results provide key insights into vertebrate neurodevelopment and lay the groundwork for further studies into neural crest biology.

PUBLISHED CONTENT AND CONTRIBUTIONS

Gandhi, S., Li, Y., Tang, W., Christensen, J.B., **Urrutia, H.A.**, Vieceli, F.M., Piacentino, M.L., and Bronner, M.E. (2021). A single-plasmid approach for genome editing coupled with long-term lineage analysis in chick embryos. *Development* 148, dev.193565. doi: 10.1242/dev.193565

H.A.U. helped conceptualize and develop the method, designed the experiments, generated experimental data, performed analyses, and wrote the paper with input from S.G. and M.E.B.

Koontz, A.*, **Urrutia, H.A.***, Bronner, M.E. (2022). Making a head: Neural crest and ectodermal placodes in cranial sensory development. *Seminars in Cell & Developmental Biology*. 138: 15-27. doi: 10.1016/j.semcdb.2022.06.009
*equal contribution

H.A.U., along with A.K., wrote the paper with input from M.E.B.

Koontz, A.*, **Urrutia, H.A.***, Bronner, M.E.* (2022). Retroviral lineage analysis reveals dual contribution from ectodermal placodes and neural crest cells to avian olfactory sensory and GnRH neurons. *Natural Sciences*. Jul;2(4): e20210037. doi: 10.1002/ntls.20210037
*equal contribution

H.A.U. assisted A.K. with generation of experimental data and H.A.U., along with A.K., wrote the paper with input from M.E.B.

Dundes, C.E., Jokhai1, R.T., Salomon-Shulman, R.E.A., Ahsan, H., Kang, R.S., Rajan, A., Kim, Y.S., Stanton, L.J., Xu, C., Do, S., Andrade López, J.M., **Urrutia, H.A.**, Greenfeld, H., Qu, Y., Miao, Y., Garcia, C., Monje, M., Wagner, D.E., Bronner, M.E., Lowe, C.J., Loh, K.M. (2024). Identification of two lineage-committed mammalian brain precursors enables derivation of human hindbrain neurons. *Nature, Resubmitted*.

H.A.U. generated experimental data, assembled figures, and helped with editing the paper.

Edens, B. M., Stundl, J., **Urrutia, H.A.**, Bronner, M.E. (2024). Neural crest origin of sympathetic neurons at the dawn of vertebrates. *Nature*. 629(8010): 121-126. doi: 10.1038/s41586-024-07297-0

H.A.U. assisted B.E. with generation of experimental data and helped with editing the paper.

Bernardi, Y.E., Sanchez-Vasquez, E, Belen Marquez, R., Piacentino, M.L., **Urrutia, H.**, Rossi, I., Alcantara Saraiva, K.L., Pereira-Neves, A., Ramirez, M.I., Bronner, M.E., de Miguel, N., Strobl-Mazzulla, P.H. (2024). miR-203 secreted in extracellular vesicles mediates the communication between neural crest and placode cells required for trigeminal ganglia formation. *PLoS Biol*ogy. 22(7): e3002074. doi: 10.1371/journal.pbio.3002074

H.A.U. assisted Y.E.B. with conceptualization, method development, and generation of experimental data.

Urrutia, H.A., Stundl, J., Bronner, M.E. (2024). Tlx3 mediates neuronal differentiation and proper condensation of the developing trigeminal ganglion. *Developmental Biology*. 515: 79-91.doi: 10.1016/j.ydbio.2024.07.005

H.A.U. conceived the project, designed the experiments, generated experimental data, performed analyses, and wrote the paper, all with input from J.S. and M.E.B.

Stundl, J., Raja, D.A.*, **Urrutia, H.A.***, Leyhr, J., Stundlova, J., Solovieva, T., Haitina, T., Sanchez, S., Musilova, Z., Martik, M., Bronner, M.E. (2024). Acquisition of neural crest in lamprey promoted thyroid evolution from chordate endostyle. *Science Advances*, *Resubmitted*.

H.A.U. assisted J.S. with experiment design, generated experimental data, performed analyses, and helped with editing the paper with input from J.S. and M.E.B.

Urrutia, H.A., Bronner, M.E. (2025). From neural crest migration to the onset of gangliogenesis. In press. *Current Topics of Developmental Biology*.

H.A.U. wrote the paper with input from M.E.B.

TABLE OF CONTENTS

LIST OF FIGURES

Number *Page*

Chapter 2

Chapter 3

Chapter 4

Chapter 5

Chapter 1

Introduction

1.1 A brief history of the neural crest

The neural crest (NC) is a transient, multipotent embryonic cell population unique to vertebrates that originates at the border of the developing central nervous system. Often described as the "fourth germ layer", the NC was first described over 150 years ago, when Wilhelm His, Sr. first identified a region at the border of the neural tube and non-neural ectoderm in chick embryos that give rise to ectomesenchymal derivatives, including craniofacial structures and components of the peripheral nervous system (Hall, 2008, 2000, 1998; His, 1868; Le Douarin and Kalcheim, 1999; Le Douarin and Dupin, 2014; Shyamala et al., 2015; Trainor et al., 2003). This unique cell population, initially coined the *Zwischenstrang* (the intermediate cord) that was later referred to as the neural crest (Baker, 2008; Bronner and LeDouarin, 2012; Couly et al., 1993; His, 1868; Le Douarin and Dupin, 2018; Sauka-Spengler and Bronner-Fraser, 2008; Trainor et al., 2003; York and McCauley, 2020; Young et al., 2014). Its evolutionary significance is highlighted by the "new head hypothesis," which suggests that neural crest acquisition enabled brain expansion and vertebrate predation (Gans and Northcutt, 1983; Northcutt, 2005).

Pioneering work by Le Douarin and colleagues has shown the immense developmental potential of the avian NC, and how these populations differ in developmental potential along the rostrocaudal (anteroposterior) body axis. In addition, lineage tracing experiments in avian embryos provided further insight into NC cell fate, enhancing our understanding of their migratory pathways, derivatives, and their axial level of origin (Le Douarin, 1980, 1973; Le Douarin and Teillet, 1974, 1973). As an amniotic system, the avian NC has served as an excellent model for understanding complex developmental processes, such as regulation of NC development by intricate gene regulatory networks (GRNs) and mechanisms governing multipotency and cell migration, and cell fate decisions (Dupin et al., 2006; Dupin and Somer, 2012; Le Douarin and Teillet, 1974; Smith, 1990; Tucker, 2004). Therefore, understanding how NC cells are specified, migrate throughout

the developing embryo, and differentiate can help us gain further insight into how these cells properly behave and function depending on their axial level of origin within the developing organism.

1.2 Thesis overview

In Chapter 2, I will discuss aspects of neural crest induction, migration and axial level differences, highlighting current knowledge on the molecular cues governing their formation, migratory behavior, and differentiation, with a particular focus on cranial sensory ganglia formation, while also emphasizing new technologies that have advanced our current understanding of the mechanisms underlying neural crest migration, its cessation, and the onset of differentiation.

In Chapter 3, I examine the early development of the cranial sensory ganglia, with a particular emphasis on the trigeminal ganglion. During formation of this ganglion, neural crest and placodal cells migrate, interact, aggregate, and condense to form the first recognizable ganglion anlage. The trigeminal ganglion has served as the ideal model system for studying neural crest-placode interactions during ganglion assembly, due to its large size, distinct semi-lunar shape, and easy accessibility. Subsequent developmental processes, including neuronal and glial differentiation, axonal projections, and specification of neuronal subtypes and functions have been studied extensively. However, the transcriptional changes that govern gangliogenesis still remain understudied. To address this gap, we examine the expression and function of T-cell leukemia homeobox 3 (*Tlx3*) in the neural crest-derived component of the developing trigeminal ganglion. Using a combination of lineage labeling with *in situ* hybridization in the chick embryo, we demonstrate that neural crest-derived cells that contribute to the cranial trigeminal ganglion express *Tlx3* at critical time points coinciding with the onset of ganglion condensation. Importantly, loss of *Tlx3* function *in vivo* reduces the overall size and abundance of neurons within the trigeminal ganglion, whereas ectopic expression of *Tlx3* in migrating cranial neural crest cells results in premature neuronal

differentiation. Taken together, these results highlight a crucial role for *Tlx3* in neural crest-derived cells during chick trigeminal gangliogenesis.

Finally in Chapter 4, I provide evidence that the orphan chemokine *Cxcl14* is expressed in the developing trigeminal ganglion of the chick embryo. Through a gene expression screen aimed at identifying factors whose onset of expression correlates ganglion condensation, we found that *Cxcl14* is expressed at the onset of aggregation, a critical stage when neural crest and placodal cells are actively interacting. Intriguingly, expression of *Cxcl14* was primarily restricted to ectodermal cells including the placodal precursors and migrating placode cells. In contrast, the receptor *Cxcr4* was exclusively expressed by neural crest cells, while its proposed ligand, *Cxcl12*, was expressed in the branchial arches, positioned some distance from the forming ganglion primordium. Importantly, loss of *Cxcl14*, including specifically in placodal cells, disrupted ganglion formation, leading to defects in gangliogenesis as well as axonal projection. Taken together, we propose that CXCL14, produced by placodal cells, binds to the receptor CXCR4 on cranial neural crest cells to properly guide the organization of the forming trigeminal ganglion. This work not only establishes a receptor-ligand interaction between CXCL14 and CXCR4 but also reveals a previously unrecognized role for this interaction in trigeminal neurogenesis.

1.3 References

Baker, C.V.H. (2008). The evolution and elaboration of vertebrate neural crest cells. Curr. Opin. Genet. Dev. *18*, 536–543.

Barondeau, D.P., Putnam, C.D., Kassmann, C.J., Tainer, J.A., Getzoff, E.D. (2003). Mechanism and energetics of green fluorescent protein chromophore synthesis revealed by trapped intermediate structures. Proc. Natl Acad. Sci. USA *100*, 12111–12116.

Bronner, M.E., Le Douarin, N.M. (2012). Development and evolution of the neural crest: An overview. Dev. Biol. *366*, 2–9.

Couly, G.F., Coltey, P.M., Le Douarin, N.M. (1993). The triple origin of skull in higher vertebrates: a study in quail-chick chimeras. Development *117*, 409–429.

Dupin, E., Creuzet, S., Le Douarin, N.M. (2006). The contribution of the neural crest to the vertebrate body. Adv. Exp. Med. Biol. *589*, 96–119.

Dupin, E., Sommer, L. (2012). Neural crest progenitors and stem cells: From early development to adulthood. Dev. Biol. *366*, 83–95.

Gans, C., Northcutt, R.G. (1983). Neural crest and the origin of vertebrates: A new head. Science *220*, 268–273.

Glenn Northcutt, R. (2005). The new head hypothesis revisited. J. Exp. Zool. B Mol. Dev. Evol. *304*, 274–297.

Hall, B.K., 2008. The neural crest and neural crest cells: discovery and significance for theories of embryonic organization. J. Biosci. *33*, 781–793.

Hall, B.K., 2000. The neural crest as a fourth germ layer and vertebrates as quadroblastic not triploblastic. Evol. Dev. *2*, 3–5.

Hall, B.K., 1998. Germ layers and the germ-layer theory revisited, in: Evolutionary Biology. Springer US, Boston, MA. pp. 121–186.

His, W., 1868. Untersuchungen über die erste Anlage des Wirbelthierleibes : die erste Entwickelung des Hühnchens im Ei/von Wilhelm His. F.C.W. Vogel.

Le Douarin, N.M. (1973). A biological cell labeling technique and its use in experimental embryology. Dev. Biol. *30*, 217–222.

Le Douarin, N.M., Teillet, M.A. (1973). The migration of neural crest cells to the wall of the digestive tract in avian embryo. J. Embryol. Exp. Morphol. *30*, 31–48.

Le Douarin, N.M., Teillet, M.A. (1974). Experimental analysis of the migration and differentiation of neuroblasts of the autonomic nervous system and of neurectodermal mesenchymal derivatives, using a biological cell marking technique. Dev. Biol. *41*, 162–184.

Le Douarin, N.M. (1980). The ontogeny of the neural crest in avian embryo chimaeras. Nature *286*, 663–669.

Le Douarin, N.M., Kalcheim, C. (1999). Developmental and cell biology series: The neural crest series number 36, 2nd ed, Developmental and cell biology series. Cambridge University Press, Cambridge, England.

Le Douarin, N.M., Dupin, E. (2014). The neural crest, a fourth germ layer of the vertebrate embryo, in: Neural Crest Cells. Elsevier, pp. 3–26.

Le Douarin, N.M., Dupin, E. (2018). The “beginnings” of the neural crest. Dev. Biol. *444*, S3–S13.

Sauka-Spengler, T., Bronner-Fraser, M. (2008). A gene regulatory network orchestrates neural crest formation. Nat. Rev. Mol. Cell Biol. *9*, 557–568.

Shyamala, K., Yanduri, S., Girish, H.C., Murgod, S. (2015). Neural crest: The fourth germ layer. J. Oral Maxillofac. Pathol. *19*, 221–229.

Smith, J. (1990). The avian neural crest as a model system for the study of cell lineages. Int. J. Dev. Biol. *34*, 157–162.

Trainor, P.A., Melton, K.R., and Manzanares, M. (2003). Origins and plasticity of neural crest cells and their roles in jaw and craniofacial evolution. Int. J. Dev. Biol. *47*, 541–553.

Tucker, R.P. (2004). Neural crest cells: A model for invasive behavior. Int. J. Biochem. Cell Biol. *36*, 173–177.

York, J.R., McCauley, D.W. (2020). The origin and evolution of vertebrate neural crest cells. Open Biol. 10, 190285.

Young, N.M., Hu, D., Lainoff, A.J., Smith, F.J., Diaz, R., Tucker, A.S., Trainor, P.A., Schneider, R.A., Hallgrímsson, B., Marcucio, R.S. (2014). Embryonic bauplans and the developmental origins of facial diversity and constraint. Dev. *141*, 1059–1063.

Chapter 2

From neural crest development to the onset of gangliogenesis

A modified version of this chapter is currently *in press* as:

Urrutia, H.A., Bronner, M.E. (2025). From neural crest migration to the onset of gangliogenesis. *Current Topics in Developmental Biology*. ***In press***.

2.1 Introduction

The neural crest (NC) is a transient, highly migratory, and multipotent embryonic cell population that contributes to many defining features of vertebrates. As a uniquely vertebrate cell type, the neural crest is an excellent model for studying cell lineage and diversification during embryonic development because of its motility and multipotency. Often referred to as the fourth germ layer, the neural crest originates from the ectoderm but has broad developmental potential to differentiate into a wide variety of distinct cell types, including ectomesenchymal cell types of the face and most of the peripheral nervous system (Hall, 2008, 2000, 1998; Le Douarin and Kalcheim, 1999; Le Douarin and Dupin, 2014; Shyamala et al., 2015). The unique capabilities of the neural crest have led to the "new head hypothesis", which proposes that acquisition of the neural crest together with ectodermal placodes in ancestral vertebrates enabled expansion of the brain which in turn aided predation (Gans and Northcutt, 1983; Glenn Northcutt, 2005).

Induction of the NC initiates during gastrulation at the border of the neural plate, juxtaposed between neural and non-neural ectoderm (Figure 2.1A). As the embryo develops, the neural crest cells undergo specification within the neural plate border, initially residing within the elevating neural folds during neurulation and subsequently positioned within the dorsal neural tube (Figure 2.1A-C) (Erickson and Reedy, 1998; Milet and Monsoro-Burq, 2012; Steventon et al., 2005). By the time these cells are fully specified to a neural crest fate, they express characteristic neural crest marker genes – *FoxD3*, *Snai2*, and *Sox9*, among others. Upon closure of the neural tube, avian NC cells undergo an epithelial-to-mesenchymal transition (EMT), whereby they lose their epithelial characteristics, such as apicobasal polarity and tight junctions, and assume invasive and migratory mesenchymal characteristics, thus becoming a mesenchymal population distinct from the neural tube or non-neural ectoderm (Figure 2.1C) (Duband and Thiery, 1982; Hall, 2009; Kerosuo and Bronner-Fraser, 2012; Le Douarin and Kalcheim, 1999; Lim and Thiery, 2012; Sauka-Spengler

and Bronner-Fraser, 2008; Simoes-Costa and Bronner, 2016; Steventon et al., 2005; Théveneau et al., 2007; Theveneau and Mayor, 2012; Thiery and Sleeman, 2006).

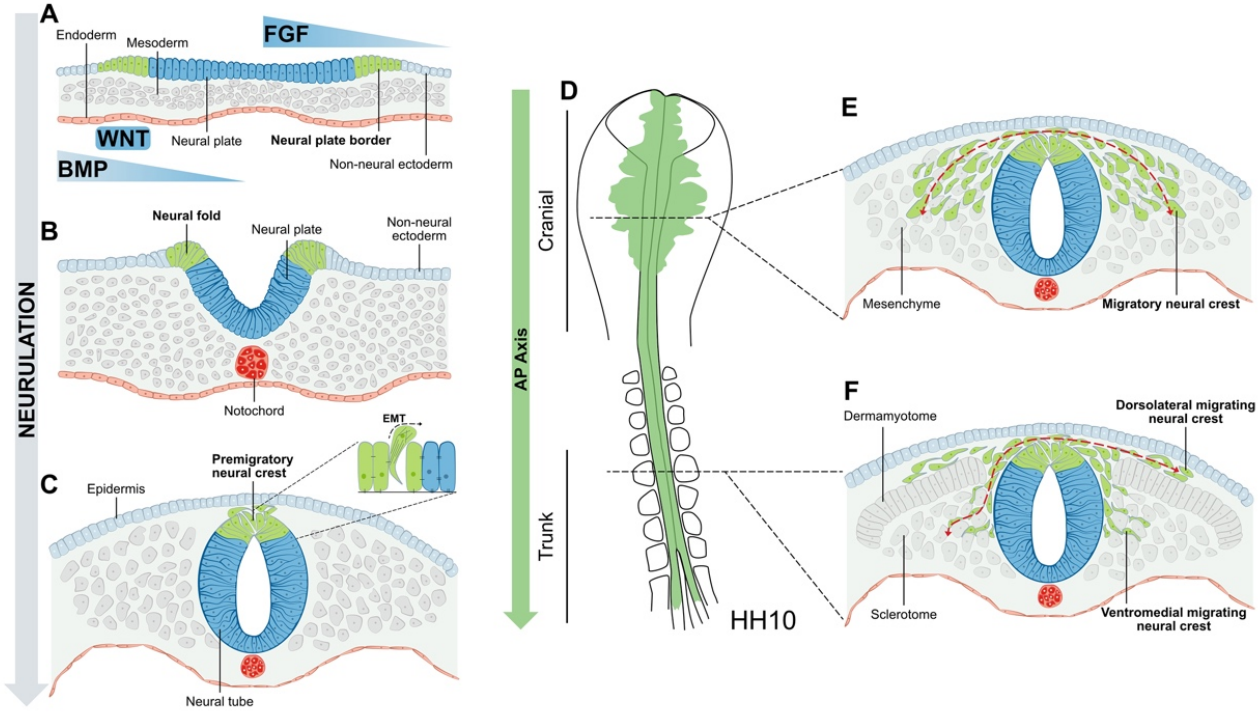

Figure 2.1 Generalized morphogenetic stages during early neural crest development. (A) Schematic diagram of transverse sections through chick embryo during neurulation. Prospective neural crest (NC) cells reside in the neural plate border (green), a territory between the neural plate and the non-neural ectoderm. NC is induced by signals (mainly BMPs, WNT, and/or FGFs) at the neural plate border. (B) As neurulation proceeds, the neural plate invaginates, resulting in the elevation of the neural folds, which contain NC precursors. (C) After neural tube closure, NC cells lose intercellular connections and undergo an epithelial to mesenchymal transition (EMT). (D) Schematic dorsal view of a stage 10 chicken embryo, showing the NC (green) in the vicinity of the midline. Dotted lines delimit the embryonic region represented in cross-section (E & F). (E-F) Schematic of migratory NC cells following stereotypical pathways to diverse destinations. HH: Hamburger and Hamilton developmental stages,
AP: anteroposterior.

Following EMT and delamination from the neuroepithelium, NC cells emigrate from the dorsal neural tube, either collectively or individually. The process of neural tube closure initiates in the head and proceeds tailward, as the embryo develops. Following this rostral to caudal sequence, neural crest emigration extends along the body axis in a rostrocaudal wave (Figure 2.1D). Subsequently, NC cells migrate extensively throughout the embryo along well-defined routes (Figure 2.1D-F), responding to local environmental and morphogenetic cues, enabling their invasion of distinct tissues, where they will differentiate into a wide range of cell types (Figure

2.2) (Dupin et al., 2006; Grenier et al., 2009; Le Douarin and Teillet, 1974; Minoux and Rijli, 2010; Theveneau and Mayor, 2012).

Pioneering work by Le Douarin and colleagues has shown that avian neural crest populations differ in developmental potential along the rostrocaudal (anteroposterior) body axis, such that they can be sub-categorized into four distinct regions, based on their axial level of origin (Figure 2.2). For example, the cranial NC, which arises from the cranial neural tube (posterior forebrain to the anterior hindbrain) migrate dorsolaterally between the presumptive epidermis and the mesodermal mesenchyme (Figure 2.1E) to populate the head, forming the craniofacial skeleton and contributing to cranial sensory ganglia (Figure 2.2) (Johnston, 1966; Noden, 1975). The vagal neural crest contributes to portions of the heart as well as the enteric ganglia and, in birds, the nerve of Remak of the gut (Johnston, 1966; Noden, 1975). The vagal NC population arises from the posterior hindbrain to somite 7 (Figure 2.2). Just below the vagal region is the trunk NC, arising from the presumptive spinal cord adjacent to somites 8-28. These NC cells contribute to the dorsal root ganglion, sympathetic ganglia, and the adrenal medulla (Figure 2.2) (Dupin et al., 2006; Grenier et al., 2009; Le Douarin and Teillet, 1974; Minoux and Rijli, 2010; Theveneau and Mayor, 2012). Finally, the lumbosacral neural crest arise posterior to the 28th somite and contributes to the enteric nervous system of the post-umbilical gut.

The best studied of these neural crest subpopulations is the cranial (cephalic) neural crest (CNC) which arises from the dorsal side of the diencephalon (posterior forebrain) extending to the caudal rhombencephalon (hindbrain) in avian embryos (Figure 2.2 & 2.3) (Couly and Le Douarin, 1987). After delaminating, these cells predominantly migrate as one continuous wave from the dorsal midline of the neural tube, and then split into three discrete, segregated streams: first, ranging from the diencephalon to rhombomeres (r) 1 and r2; second, laterally from r4; third, laterally from r6-r8 (Figure 2.3). These streams populate specific regions of the developing craniofacial and neck region. In particular, the first cranial-most (mandibular) stream populates the frontal-nasal and periocular regions, along with the first branchial

(pharyngeal) arch (BA) (Figure 2.3). The second (hyoid) stream emerging from r4 contributes extensively to BA2, while the third (branchial) stream originating from r6 populates BA3, the heart and enteric nervous system (Figure 2.3) (Le Douarin and Kalcheim, 1999).

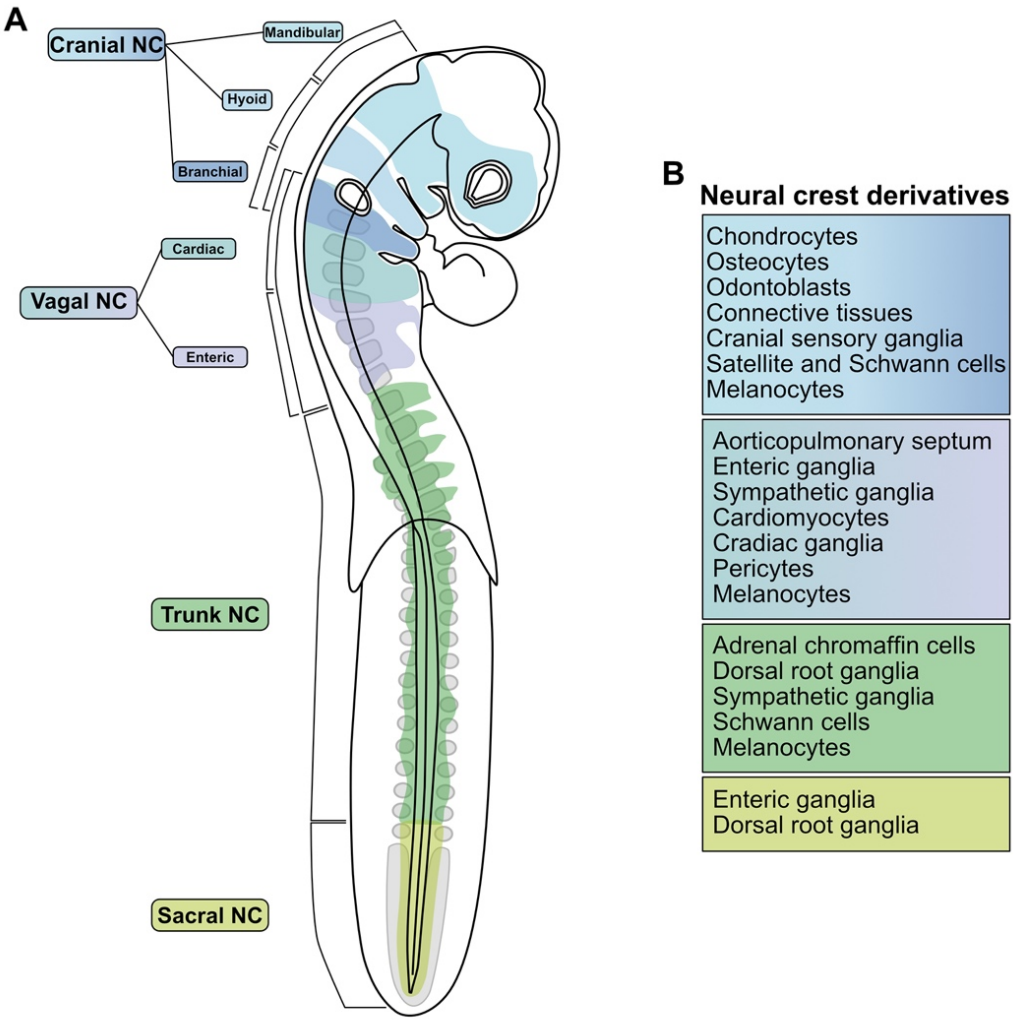

Figure 2.2 Overview of NC subpopulations along the anteroposterior axis. (A) Schematic of NC subpopulations in an HH16 chick embryo. These populations are subdivided into several unique subpopulations along the body axis, designated on their axial level of origin - cranial, vagal, trunk, and sacral NC. The cranial NC includes NC cells that are formed between the forebrain and the 6th rhombomere of the hindbrain. The vagal crest emerges from the first seven somites. The trunk neural crest spans from the 8th to the 27th somite, while the sacral neural crest is positioned posterior to this boundary. (B) Major derivatives of NC subpopulations.

2.2 Neural crest induction and formation

The neural crest was first described in the literature over 150 years ago, when Wilhelm His, Sr. identified this strand of cells emerging from the dorsal neural tube. Initially, His coined the term *Zwischenstrang* (the intermediate cord) that was later referred to as the neural crest (Baker, 2008; Bronner and LeDouarin, 2012; Couly et al., 1993; His, 1868; Le Douarin and Dupin, 2018; Sauka-Spengler and Bronner-Fraser, 2008; Trainor et al., 2003; York and McCauley, 2020; Young et al., 2014). The ectoderm of gastrulating embryos will form four distinct cell types – epidermal cells, placodal cells, cells of the nervous system, and neural crest cells (Bronner-Fraser, 1995). Induction of the neural crest initiates at the neural plate border under the influence of extracellular signals like bone morphogenetic protein (BMP), fibroblast growth factor (FGF), Notch, retinoic acid, and WNT, which emanate from both the surrounding ectoderm and underlying mesoderm (Figure 2.1A) (Betancur et al., 2010; Bronner and LeDouarin, 2012; Sauka-Spengler and Bronner-Fraser, 2008; Simões-Costa and Bronner, 2015; Thawani and Groves, 2020). Importantly, induction of the NC is governed by intermediate levels of BMP, controlled by BMP antagonists – Chordin, Noggin or Follistatin, originating from the mesoderm (Sauka-Spengler and Bronner-Fraser, 2008; Teraoka et al., 2009).

Neural tube closure (Figure 2.1A-C) progresses in an anteroposterior (rostrocaudal) sequence within the developing avian embryo (Figure 2.1D), a progression closely followed by neural crest specification. In response to the signaling cascades, neural plate border and neural crest specifiers are activated. This includes various transcription factors such as *FoxD3*, *Pax3/7*, and *Tfap2*, which in turn further solidify NC formation (Betancur et al., 2010; Bronner and LeDouarin, 2012; Sauka-Spengler and Bronner-Fraser, 2008; Simões-Costa and Bronner, 2015). For instance, *FoxD3* has been implicated in the induction and specification of pre-migratory NC cells (Lukoseviciute et al., 2018). In addition, *Pax3/7* has been shown to be required for NC specification (Basch et al., 2006; Hong and Saint-Jeannet, 2007; Mayran et al., 2018). Conversely, the pioneer factor, *Tfap2* has been shown to affect chromatin

landscape, further solidifying NC specification (Kenny et al., 2021; Wang et al., 2011). Nevertheless, combinatorial expression of various other transcription factors (e.g., *FoxD3*, *Id2*, *Pax3/7*, *Msx1/2*, *Sox9*, *Zic1/2*) within these territories also regulate NC specification and actively repressed alternative fates. For example, *FoxD3* mediates repression of neural and pre-placodal fates (Hochgreb-Hägele and Bronner, 2013; Lukoseviciute et al., 2018; Thomas and Erickson, 2009). Following specification, the NC are then positioned in the dorsal neural tube (Figure 2.1C).

After induction and specification, the axial level-specific identity of NC cells is regulated by expression of different transcription factors. For instance, *Dmbx1* and *Otx2* play vital roles in specification of cranial NC identity, whereas anterior Hox genes, such as *HoxA2* and *HoxB2*, influence NC cells within the anterior hindbrain, while subsequent Hox genes (e.g., *HoxA3/4*, *HoxB3/4, HoxB5*), along with Retinoic Acid receptors and *Cdx1/2*, establish vagal and trunk NC identity (Frith et al., 2018; Minoux and Rijli, 2010; Rothstein et al., 2018; Simoes-Costa and Bronner, 2016; Williams et al., 2019). These signals activate expression of gene regulatory networks that define NC territories, and the subsequent steps required for NC development (Marchant et al., 1998; Mayor et al., 1995, 1997; Prasad et al., 2012; Sauka-Spengler and Bronner-Fraser, 2008; Steventon et al., 2009; Stuhlmiller and García-Castro, 2012). For example, ectopic expression of cranial crest-specific transcription factors (*Sox8*, *Tfap2β* and *Ets1*) in the trunk NC activates a partial reprogramming of avian trunk NC cells, resulting in formation of chondroblasts, a cell type that trunk neural crest cells normally are unable to make (Simoes-Costa and Bronner, 2016).

The neural plate border not only gives rise to NC cells, but also placodal precursors which arise adjacent and lateral to the neural crest in the pre-placodal domain (Betancur et al., 2010; Bhattacharyya et al., 2004; LaBonne and Bronner-Fraser, 1998; Pieper et al., 2011; Prasad et al., 2012; Streit, 2002; H. Xu et al., 2008). Whether presumptive neural crest and placode cells are predetermined within the neural plate border remains a matter of debate (Krispin et al., 2010; Roellig et al., 2017; Williams et al., 2022). The distinction between these cell types becomes

apparent only at the end of neurulation when the midline of the ectoderm thickens and begins to invaginate, giving rise to the central nervous system (brain and spinal cord) along the body axis of the embryo (Figure 2.1B) (Bronner-Fraser, 1995).

2.3 Neural crest EMT and onset of migration

Upon neural tube closure, pre-migratory neural crest cells undergo EMT, during which their transcriptional landscape and cellular properties change dramatically. They lose their epithelial characteristics and acquire mesenchymal properties to delaminate from the neural tube and migrate extensively throughout the developing embryo (Figure 2.1D-1F) (Betancur et al., 2010; Martik and Bronner, 2017; Martinsen and Bronner-Fraser, 1998; Minoux et al., 2017; Minoux and Rijli, 2010; Prasad et al., 2012; Sauka-Spengler and Bronner-Fraser, 2008; Simões-Costa and Bronner, 2015; Steventon et al., 2014; Theveneau and Mayor, 2012). Neural crest cells then emigrate from the dorsal neural tube in a rostrocaudal progression along the body axis with cells at the midline of the caudal forebrain and midbrain emerging prior to those adjacent to the hindbrain (Figure 2.1D). Extracellular matrix (ECM) remodeling and loss of adherens junctions occur during EMT, via changes in cadherin expression. In particular, neural crest specification is complete when these cells switch from type I cadherins (E- and N-cadherin) and begin expressing type II cadherins (e.g., Cadherin-6B/7/10/11), which are essential for acquisition of contact inhibition of locomotion (CIL) and cell repolarization (Dady et al., 2012; Piloto and Schilling, 2010; Rogers et al., 2013; Scarpa et al., 2015; Theveneau et al., 2010; Théveneau et al., 2007).

Cranial NC cells have been shown to collectively migrate, which is defined either as coordinated migration of tightly clustered cells or small loose groups of cells, where communication and cooperation between these cells contribute to their overall directionality (Etienne-Manneville, 2014; Revenu et al., 2014; Theveneau and Mayor, 2012). Cadherin based contacts have been shown to control collective migration of cranial NC cells. These contacts act as key regulators of molecular communication, allowing cells to polarize, collectively migrate with high directionality, and coalesce

upon reaching their destination (Carmona-Fontaine et al., 2008; Desai et al., 2009; Dupin et al., 2009; Friedl and Gilmour, 2009; Revenu et al., 2014; Theveneau et al., 2010).

EMT is controlled by NC specifier genes; e.g., in the trunk region, *Snai1/2*, *FoxD3*, and *Sox9/10* govern EMT. In contrast, these transcription factors work in conjunction with *Ets1*, *Sox5* and *p53* to mediate EMT in the cranial region (Cheung et al., 2005; del Barrio and Nieto, 2002; McKeown et al., 2013; Perez-Alcala et al., 2004; Rinon et al., 2011; Taneyhill et al., 2007; Théveneau et al., 2007). WNT signaling activates expression of *Snai1/2*, which is crucial for the initial delamination of NC cells via repression of cadherin molecules (Vallin et al., 2001; Yook et al., 2006). In *Xenopus*, cranial NC cells mainly express both type I E-cadherin and N-cadherin. At the onset of migration, E-cadherin expression is reduced while N-cadherin expression is only slightly reduced, through expression of the transcription factor, *Twist.* Similarly, expression of *Sip1/Zeb2* in chick is required for two phases of neural crest EMT. This transcription factor actively represses expression of E-cadherin in the presumptive NC, thereby allowing detachment from the neural tube, and activation and maintenance of N-cadherin expression during migration (Barriga et al., 2013; Rogers et al., 2013; Theveneau et al., 2013).

In chick, *Snai2* is essential for cranial NC EMT as it transcriptionally represses Cadherin-6B, mainly by functioning in conjunction with *Ets1* (Taneyhill et al., 2007; Théveneau et al., 2007). NC specifiers *FoxD3* and *Sox10* repress N-cadherin expression (Cheung et al., 2005; Dottori et al., 2001). In addition, *FoxD3* has been shown to further contribute to EMT by repressing other transmembrane proteins, like *Tspan18*, which is crucial for establishment and maintenance of tight cell junctions (Fairchild et al., 2014; Fairchild and Gammill, 2013). Conversely, as expression of type I cadherins is reduced, type II cadherins (e.g., Cadherin-7/11/19/20) are upregulated in migratory NC (Chalpe et al., 2010; Faulkner-Jones et al., 1999; Moore and Larue, 2004; Nakagawa and Takeichi, 1995; Pla et al., 2001; Takahashi and Osumi, 2005; Wu et al., 2014; Wu and Taneyhill, 2019). Finally, upon completion of

EMT, NC cells begin receiving and integrating both positive and negative signals from surrounding tissues, via cell-cell and cell-ECM contact interactions, allowing these cells to migrate extensively, exhibiting both collective and individual migratory behaviors (Hall, 2008; Le Douarin and Kalcheim, 1999).

2.4 Cranial neural crest migration

Although the general sequence of induction, delamination, and initiation of migration appear similar along most of the anteroposterior axis, NC migration and the range of derivatives vary among different axial regions and in different species (Alfandari et al., 2010; Hall, 2009; Le Douarin and Kalcheim, 1999; Minoux and Rijli, 2010; Théveneau et al., 2007). Various lineage tracing methods marking different populations of NC cells have significantly enhanced our understanding of the migratory paths and derivatives these cells form.

In avian embryos, advent of the quail-chick chimeras by Le Douarin and colleagues (Le Douarin, 1973; Le Douarin and Teillet, 1974, 1973) enabled precise mapping of neural crest migratory paths, axial levels of origin, and range of derivatives. Neural crest migration has also been extensively studied in *Xenopus* and zebrafish embryos. In frogs, cranial neural crest cells undergo collective migration, whereas in chick and zebrafish, they migrate more as individual cells that have leader and follower cells (Kulesa and Gammill, 2010; Kuriyama and Mayor, 2008; Olsson and Hanken, 1996; Richardson et al., 2016; Schroeder, 1970). Tracing neural crest cell behavior by both static and live imaging has provided invaluable insight into their migratory patterns (Davis and Trinkaus, 1981; Le Douarin and Kalcheim, 1999; Newgreen et al., 1982). Moreover, comparative studies across different species have highlighted the complexity of cranial NC migratory behaviors, the nature of their migratory streams with respect to individual or collective cell migration, and the role of environmental cues in providing attractive and repulsive signals (Bronner-Fraser, 1993; Erickson, 1985; Erickson et al., 1980; Le Douarin, 1982; Newgreen, 1989; Noden, 1975; Thiery et al., 1982; Tosney, 1982).

Cranial neural crest cells emerge from the length of the posterior forebrain (diencephalon) to the rostral hindbrain (rhombencephalon) (Figure 2.2 & 2.3). These cells predominantly migrate along a dorsolateral route, under the presumptive ectoderm (Figure 2.1E), and eventually occupy the craniofacial/frontonasal region and branchial arches (BA) of the developing avian embryo (Figure 2.3) (Bajpai et al., 2010; Creuzet et al., 2002; Johnston, 1966; Kerosuo and Bronner, 2016; Kulesa et al., 2010; Le Douarin, 1973; Noden, 1975; Weston, 1963; Weston and Butler, 1966). Cranial NC migrate in three distinct streams. The mandibular stream emerges from the level of the posterior forebrain to rhombomere (r) 2, with a small contribution from the adjacent region, r3, which is predominantly NC-free (Figure 2.3). The cells in this stream migrate dorsolaterally for the initial portion of their migration to populate the frontal-nasal and periocular regions, along with BA1 (Figure 2.3). The hyoid stream of cranial NC cells arises from r4 and eventually populates BA2, with neural crest cells migrating downward from r3 and upward from r5 contributing small portions to this stream (Figure 2.3). The branchial cranial NC stream originates from r6-r8, with contribution from both r5 and r7, and populates BA3 and BA4 (Figure 2.3) (Kuriyama and Mayor, 2008; Le Douarin and Kalcheim, 1999). In part, the main reason for these

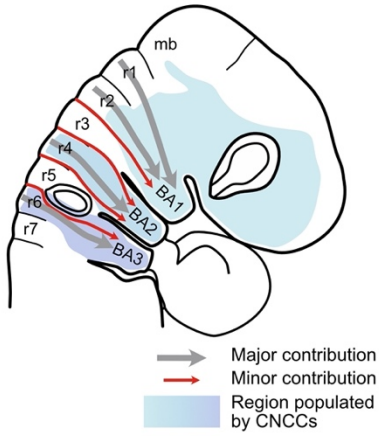

Figure 2.3 Overview of cranial neural crest migratory route. Beginning at stage 10, cranial NC cells migrate dorsolaterally, between the ectoderm and the underlying paraxial mesoderm. The major migratory streams of the cranial NC originate from rhombomeres 2, 4 and 6 (r2, r4, r6; gray arrows) to populate the branchial arches 1, 2 and 3 (BA1, BA2, BA3), respectively. Some NC cells from r3 and r5 (red arrows) contribute minimally to BA1, BA2 and BA3. mb: midbrain.

well-segregated streams is the lack of NC cells originating and migrating from r3 and r5, due to the existence of focal apoptosis mainly mediated by BMP4, although some aspects of this proposed signaling cascade have been challenged (Farlie et al., 1999; Lumsden et al., 1994; Smith and Graham, 2001). BMP receptors BMPR1A and BMPR2 are expressed in both the hindbrain and NC cells that arise from these axial levels, but BMP4 is only expressed at the level of r3 and r5. Studies have shown that when r4 NC cells are transplanted to either r3 or r5, they failed to properly migrate, suggesting that these spaces are devoid of NC due to environmental cues rather than cell-autonomous effects (Farlie et al., 1999). *In vivo* time-lapses have shown that NC cells emerging from r3 or r5 rarely migrate, instead rounding up and collapsing their filopodia and lamellipodia, and reversing their migration to join adjacent NC streams (Kulesa and Fraser, 2000, 1998).

The combination of high resolution live imaging using vital dyes or transgenics together with molecular/genetic perturbations, has illuminated the molecular mechanisms governing the migratory behavior of NC cells. Largely focusing on the cranial neural crest in chick, *Xenopus*, and zebrafish embryos, several studies have shown that the cranial NC navigates through complex environments. Migrating neural crest cells are influenced by factors secreted by neighboring cells including the cranial placodes, rhombomeres and surrounding mesenchyme (Baker, 2008; Minoux and Rijli, 2010; Steventon et al., 2014; Szabó et al., 2019; Theveneau and Mayor, 2012).

Three main mechanisms provide guidance to the cranial neural crest as they navigate through their environment and interact with neighboring neural crest and other cell types. These mechanisms – contact inhibition of locomotion (CIL), co-attraction, and chemotaxis – function cooperatively to pattern the cranial NC into their migratory streams. In particular, the collective migration of the cranial NC depends on co-attraction and contact inhibition of locomotion (Carmona-Fontaine et al., 2008; Rogers et al., 2013; Scarpa et al., 2015). CIL, first described in an *in vitro* study of fibroblast cells, has been shown to be important for explaining neural crest migration (Abercrombie and Heaysman, 1953). This phenomenon is best described as when a

cell ceases moving in the same direction upon contact with another cell and instead moves away in the opposite direction (Abercrombie, 1979). Mayor and colleagues, using live imaging in both *Xenopus* and zebrafish embryos, have shown the importance of CIL during the directional migration of CNC cells both *in vitro* and *in vivo* (Carmona-Fontaine et al., 2011, 2008). They found that the leading edge of *Xenopus* NC explants stopped their migration upon contact with NC cells from another NC explant, but were able to consume mesodermal explants, demonstrating that NC-NC interactions are homotypic. Live time-lapse microscopy has shown that NC cells collapse their lamellipodia upon contact with other NC cells, an observation similarly shown in fibroblast cells (Carmona-Fontaine et al., 2011, 2008). Thus, NC cells exposed at the leading edge of the explants migrate away from the cluster, leading to directional migration of the entire explant. Similarly, live imaging of zebrafish neural crest has demonstrated collapse of protrusions and changes in migratory direction when two NC cells make contact *in vivo*. Altogether, both *in vitro* and *in vivo* studies have shown that the directionality of NC migration is highly dependent on cell-cell interactions, from either another NC or other cell types, and CIL is required for normal neural crest migration.

The WNT/Planar Cell Polarity (PCP) pathway has been shown to mediates contact inhibition in *Xenopus* neural crest (Carmona-Fontaine et al., 2008; Mayor and Theveneau, 2014). Disruption of the PCP pathway results in failure of lamellipodial collapse when NC cells collide, resulting in maintenance of their direction of migration rather than CIL. N-cadherin plays a vital role in this process, mainly by inhibiting protrusion and *Rac1* activity at sites of cell contact while increasing *Rac1* activity at the leading edges. The polarized distribution of *Rac1* activity at the leading edge of the NC cell has also been shown to be crucial for responding to chemoattractants (Theveneau et al., 2010). In particular, the Stromal cell-derived factor 1 (*Sdf1*/*Cxcl12)* chemokine influences the migratory direction of NC cells *in vivo*, as demonstrated via loss-of-function experiments of either *Cxcl12* or its receptor *Cxcr4* in *Xenopus* embryos (Theveneau et al., 2010). *Cxcl12* binds to *Cxcr4* on the cell membrane and promotes intracellular *Rac1*, a key player in the activation and

stabilization of the cell motility structures (e.g., filopodia, pseudopodia) that promote cell movement. Consistent with this, N-cadherin function-blocking antibodies cause a loss of attraction toward *Cxcl12*, emphasizing the importance of N-cadherin in maintaining functional cell–cell contacts during NC migration (Theveneau et al., 2013, 2010). *Sdf1*/*Cxcl12* interactions stabilize the large cell protrusions present at the leading edge through an increase in *Rac1* activity (Theveneau et al., 2013, 2010). Thus, *Cxcl12* may amplify and stabilize contact-dependent cell polarity to result in directional collective migration. Moreover, *Cxcl12* and its receptors *Cxcr4* and *Cxcr7* not only direct cranial neural crest cells into the branchial arches but also play a role in the condensation of the ventral cartilages in zebrafish (Olesnicky Killian et al., 2009).

Another factor important for neural crest chemotaxis and collective migration in *Xenopus* is the complement factor C3a and its receptor C3aR (Carmona-Fontaine et al., 2011; Theveneau et al., 2010). These act together with *Cxcl12*/*Cxcr4* to maintain co-attraction via cohesive clustering of migrating cranial crest cells. This phenomenon of co-attraction allows collective migration of neural crest cells despite low cell–cell adhesion and dispersion induced by CIL. As NC cells migrate, they may stray from the stream to which they belong. When this occurs, these cells are quickly attracted back to the stream via C3a-dependent chemotaxis which activates *Rac1*, polarizing the NC cells to return to the bulk of migratory stream.

Other cell types also influence collective cell migration. For example, the presence of cranial ectodermal placodes help shape the migratory behavior of cranial NC cells as they migrate through the developing *Xenopus* head. Collective cell migration occurs when NC cells “chase” placodal cells that in turn “run” upon contact with NC cells (Theveneau et al., 2013, 2010). When cultured separately *in vitro*, NC cells migrate randomly whereas placodes cells remain stationary. However, when co-cultured together, the placodal cells express the chemoattractant *Cxcl12* that attracts NC cells, resulting in the formation of transient, but functional, cell–cell adhesion complexes between NC and placode cells. Similar to CIL and dependent on N-

cadherin PCP signaling, placode cell protrusions become destabilized upon physical contact with NC cells and in turn the placode cells "run" from the NC. Thus, the "chase-and-run" interaction between NC and placodal cells also promotes NC migration and patterning of the placode.

Another type of interaction between avian neural crest cells and the environment that results in the formation of segregated migratory "streams" is influenced by Ephrin-Eph signaling. These inhibitory signals parse NC cells into distinct streams such that they migrate through regions that lack the inhibitory Eph ligand (Gammill et al., 2007). For instance, neural crest cells expressing the tyrosine kinase receptor *EphA4+/EphB1+* invade only BA3 and BA4, while neural crest cells expressing *Ephrin-B2* are repelled and migrate into BA2 (Osborne et al., 2005). In *Xenopus*, cranial neural crest cells do not form distinct streams, but do not intermix as they migrate, due to Eph/ephrin signaling (Smith et al., 1997). In the mouse, *Ephrin-B2* is expressed in the ectoderm of the branchial arches and neural epithelium. Its knock down results in failure of neural crest cells to migrate and populate BA2, even though the migratory streams remain segregated (Adams et al., 2001). On the other hand, knock-down of *Ephrin-B1* in cranial neural crest cells results in cells wandering between streams and migrating into BA3 and BA4 (Davy et al., 2004). It is not yet known which *Eph* receptors are involved or where they are expressed, but *in situ* hybridization in the chick suggests that complementary expression of *EphA* and *B* receptors on the cranial crest and *Ephrin-B1* and *EphB2* ligands on non-neural cells in the crest-free regions may play a role in segregating the streams thus promoting directional migration into the branchial arches (Mellott and Burke, 2008). Among other inhibitory signals, *Semaphorins*, *Plexins*, *Neuropilins*, and *Slit-Robo* interactions also influence NC migratory streams (reviewed in Minoux and Rijli, 2010).

Endothelin signaling also influences migration and final localization of NC cells. Many migratory cranial and cardiac NC cells express *Cxcr4* and endothelin receptors *EdnrA/B*. These cells are guided by neighboring tissues that express the cognate ligands, such as *Edn3* and *Sdf1*/*Cxcl12* (Square et al., 2020; Theveneau and

Mayor, 2012). These ligand-receptor pairs have been shown to guide the migration and development of NC-derived to the heart and gut, respectively, to form the enteric nervous system (Ling and Sauka-Spengler, 2019; Square et al., 2020; Theveneau and Mayor, 2012). Additionally, other chemoattractants implicated to NC migration include VEGF, which is critical for CNC migration in the avian embryos (McLennan et al., 2015) and GDNF, critical for migration of vagal neural crest cells in populating the enteric nervous system (Sasselli et al., 2012). These signals, both attractive and inhibitory, help prevent dispersion and maintain the high density of the NC cells within their migration routes as they reach to their final destinations.

2.5 Trunk neural crest migration

In the trunk of the avian embryo, neural crest cells are thought to be specified by similar mechanisms as in the head but undergo different types of EMT and follow very different migratory pathways. Although avian cranial NC cells depart from the neural tube nearly all at once, the trunk NC delaminate progressively in a single chainlike manner after detaching from the neural tube (Cheung et al., 2005; Hall, 2008; Johnston, 1966; Le Douarin and Kalcheim, 1999; Le Douarin and Teillet, 1974; Noden, 1975; Théveneau et al., 2007). Upon closure of the neural tube, the trunk NC cells delaminate and migrate away along two main routes – either dorsolaterally under the ectoderm or ventromedially along the side of the neural tube (Figure 2.1F). Interestingly, NC migration in the trunk is tightly linked with differentiation of the somites (Sela-Donenfeld and Kalcheim, 1999). Quail–chick chimeras have shown that the dorsolateral stream is primarily comprised of presumptive melanocytes. While the NC cells from the ventromedial stream mainly contribute to the sensory ganglia, sympathetic ganglia, adrenal medulla, aortic plexus, and some cells of the metanephric mesenchyme (George et al., 2010, 2007; Lefcort and George, 2007).

Initial studies focused on the migratory routes taken by the ventromedially migrating NC cells came from analyses using the HNK1 antibody, which labels most migratory NC cells (Bronner-Fraser, 1986; Rickmann et al., 1985). These studies

revealed that avian trunk NC cells invade the sclerotomes and migrate throughout rostral half of each somitic sclerotome, while being restricted from the caudal half, resulting in segmental migration. These observations propelled a search for possible rostrally localized attractants and/or caudally localized repellants. The caudal sclerotome expresses *Ephrins* and *Semaphorins*, along with inhibitory ECM molecules, such as *Versicans*, and *F-spondin* (Newgreen et al., 1986; Newgreen and Gooday, 1985). *Semaphorins* expressed in the caudal half of each sclerotome appear to be the primary reason for exclusion of neural crest cells from the caudal sclerotome by interacting with *Neuropilin2* receptors on neural crest cells, thus confining them to the rostral half of each somite which is repressor-free (Davy and Soriano, 2007; Gammill et al., 2007; Krull, 1998; Wang and Anderson, 1997). After migration, ventromedially migrating NC cells differentiate into dorsal root ganglia, with high levels of *Notch* promoting a glial fate, while high levels of *Delta* lead to a neuronal fate (Harris and Erickson, 2007; Krull, 1998; Krull et al., 1997; Wang and Anderson, 1997; Yu and Moens, 2005). Migration of these cells is also controlled temporally in a chemotactic fashion by the levels of *Cxcl12* along the ventro-dorsal axis, suggesting that a combination of attractive and repulsive cues guide trunk NC migration (Kasemeier-Kulesa et al., 2010).

The dorsolateral pathway, located between the future epidermis and dorsal somite/dermomyotome, is followed by avian neural crest cells destined to become melanocytes (Tosney, 2004). Repressors like *Slit1*, *Endothelin-3*, and *EphrinB1* are initially expressed under the epidermis on the dorsolateral route in the chick. Thus, early migrating trunk neural crest cells are initially excluded from this pathway. Later trunk NC cells, that express the receptor, *EphB2*, are able to migrate through these regions, as *Ephrins* are down-regulated. Cells moving along the dorsolateral pathway express *FoxD3* which induces MITF, a transcription factor necessary for the differentiation of neural crest cells into melanocytes (Thomas and Erickson, 2009).

Taken together, it is clear that various strategies guide neural crest cells along their migratory journey to their final destinations. The different mechanisms described above are under complex regulatory control that leads to intricate and stereotypic cell

behaviors unique to each axial level. These not only guide neural crest cells to the proper locations but also are instrumental in ensuring appropriate differentiation. Despite many studies on neural crest migration, open questions remain about what direct these cells away from the neural tube and what signals cause cessation of migration and the transition to differentiation. While several signaling systems have been identified, there are others likely to be discovered in the future.

2.6 Onset of cranial neural crest ectomesenchymal differentiation

Following extensive migration throughout the developing embryo, guided by local environmental cues, neural crest cells progressively settle in diverse distal sites and utilize distinct gene regulatory networks to regulate their terminal differentiation. Although any given NC cell may have substantial flexibility to differentiate into various cell types, there is also evidence for lineage restrictions along the anteroposterior axis. The transition to a differentiated state is regulated by multiple transcription factors that co-bind to downstream loci to effectuate cell fate commitment and differentiation into a plethora of neural crest derivatives, ranging from chondrocytes, smooth muscle, peripheral neurons to glia, and melanocytes, among others (Le Douarin, 1982; Le Douarin and Kalcheim, 1999; reviewed in Martik and Bronner, 2017). Similar to NC induction, the gene regulatory networks for differentiation are highly dependent upon extracellular signaling cues. For example, chondrocyte differentiation is regulated by transforming growth factor (TGF-β) signaling (Furumatsu et al., 2005), while autonomic neurons are dependent on cues from BMP signaling (Morikawa et al., 2009) and melanocyte differentiation is regulated by WNT signaling (Jin et al., 2001; Takeda et al., 2000). Interestingly, transcription factors are often reused reiteratively to drive various developmental lineages. For instance, *Sox10*, plus *Mitf* and *Tfap2* regulate melanocyte differentiation in the periphery, while in the central nervous system, *Sox10* with *Olig1/2* mediate the differentiation of oligodendrocytes (Green et al., 2015; Potterf et al., 2001; Seberg et al., 2017; Simoes-Costa and Bronner, 2016; Soldatov et al., 2019). These environmental cues and distinct gene batteries result in the activation or repression of

effector genes, and in turn alter the transcriptional outputs of these cells (Simões-Costa and Bronner, 2015). Despite ample studies focused on how NC cells migrate to different regions of the embryo and how they are subjected to different spatial signaling cues, many open questions remain regarding what ultimately dictates their terminal fate commitment.

Classical lineage tracing approaches in chick have shown that the cranial neural crest contributes to cartilage and bone of the head, cranial nerves (CN), Schwann cells, the ossicles of the middle ear and periocular structures, smooth muscles, and connective tissues of the blood vessels. Additionally, these cells contribute to formation of the dermis of the head, teeth, melanocytes, and forebrain meninges (Figure 2.2) (Couly et al., 1993; Evans and Noden, 2006; Gross and Hanken, 2008, 2005; Hall, 2008; Helms and Schneider, 2003; Le Douarin and Kalcheim, 1999; Le Lièvre, 1978; Minoux and Rijli, 2010; Moody and Heaton, 1983c, 1983b, 1983a; Trainor and Tam, 1995). Finally, these cells also form multiple parts of the teeth, including dentin which is deposited and mineralized by NC-derived odontoblasts (Graveson et al., 1997; Lumsden, 1988; Lumsden and Buchanan, 1986; Smith and Hall, 1990). These derivatives are exclusive to the cranial NC population.

The cranial NC is thought to be a developmentally heterogeneous comprised of a combination of multipotent and partially fate-restricted cells (Cohen and Konigsberg, 1975; Dupin et al., 1990; Ito et al., 1993; Sieber-Blum, 1989; Sieber-Blum and Cohen, 1980). For example, lineage tracing approaches in zebrafish have revealed a spatial correspondence between the time of emigration and final fate of cranial NC cells (Schilling and Kimmel, 1994). Whereas early-migratory cranial NC cells give rise to skeletal and connective tissue, late-migrating cranial NC tend to assume neuronal fates. In both avian and mice embryos, lineage tracing and clonal neural crest cell differentiation studies have shown that these cells have both ectomesenchymal and neural potential, providing evidence that cranial neural crest cells are multipotent but become fate-restricted as they migrate towards their final destinations (Calloni et al., 2009). Consistent with these findings, cranial NC cells

express *Sox10* and *FoxD3* (Britsch et al., 2001; Dottori et al., 2001) but these genes are down-regulated as the cells enter the branchial arches where expression of ectomesenchymal markers is upregulated.

Unlike the cranial neural crest, avian trunk NC cells do not form cartilage and are unable to differentiate into cartilage when grafted to the cranial region (Chibon, 1967; Le Douarin, 1982; Lwigale, 2001; Nakamura and Lievre, 1982; Simoes-Costa and Bronner, 2016). The core regulatory network driving chondrocyte differentiation involves TGF-β signaling and the expression of *Sox5/6* and *Sox9*, which directly activate *Col2a1* and *Agc1*, both cartilage differentiation markers (Bell et al., 1997; Furumatsu et al., 2005; Ito et al., 2002; Lefebvre et al., 1998).

Taking advantage of this knowledge, Simões-Costa & Bronner utilized cranial versus trunk avian NC-specific enhancers to isolate pure populations of NC cells. Transcriptional profiling identified various transcription factors enriched in the cranial NC compared to the trunk NC: *Brn3c*, *Lhx5*, *Dmbx1*, *Ets1*, *Sox8*, and *Tfap2β* (Simoes-Costa and Bronner, 2016). Through a series of loss-of-function and promoter-chromatin immunoprecipitation (ChIP) assays, the regulatory linkage between these factors was established. It was revealed that ectopic expression of *Ets1*, *Sox8*, and *Tfap2β* in the trunk NC resulted in upregulation of chondrogenic genes, such as *Alx1* and *Runx2*, while concomitantly downregulating trunk NC genes, such as *Dbx2* and *Hes6*. Following reprogramming and transplantation into the cranial region, these cells gave rise to ectopic cartilage nodules. This was among the first demonstration that neural crest cells from other axial levels can be successfully reprogrammed into a cranial-like fate in avian embryos (Simoes-Costa and Bronner, 2016). Murine single cell profiling of cranial NC revealed that this population may transiently reactivate Yamanaka pluripotency factors (*Nanog*, *Oct4* and *Sox2*) before NC formation (Zalc et al., 2021). Thus, an *in vivo* programming event may be redirecting cranial NC towards multipotency via extensive epigenomic priming and chromatin remodeling and allowing these cells to generate ectomesenchymal derivatives and pattern the vertebrate head (Scerbo and Monsoro-Burq, 2020).

2.7 Cranial neural crest and placode contribution to peripheral nervous systems

Within the developing vertebrate head, the peripheral nervous systems (PNS) originates from two transient cell populations: the neural crest and ectodermal placode. Several cranial sensory ganglia are a mosaic of these two populations, organized together not only morphologically but also functionally as coherent structures. For example, both neural crest- and placode-derived cells contribute to distinct proximal and distal components, respectively, of facial (VII), glossopharyngeal (IX), and vagus (X) cranial nerves (Figure 2.4) (Barlow, 2002; D'Amico-Martel and Noden, 1983; Steventon et al., 2014). In the case of the trigeminal ganglion, placode cells give rise to sensory neurons mostly within the distal region, while neural crest cells generate neurons within the proximal region and glia throughout (Hamburger, 1961; Lwigale, 2001).

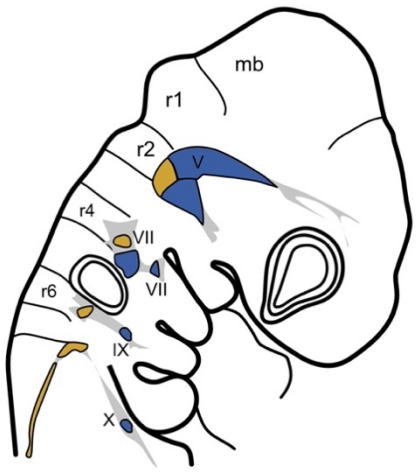

Figure 2.4 Organization of cranial sensory ganglia. Schematic representing the ganglia and major nerve branches of the Vth, VIIth, VIIIth, IXth and Xth cranial nerves, as well as their embryonic origins (yellow, neural crest; blue, epibranchial placode). Neurons from the epibranchial, trigeminal, and otic placodes coalesce to form the distal aspects of the sensory ganglia (blue). Cranial NC cells form the proximal aspects (yellow), as well as ectomesenchymal cells, Schwann cells, melanocytes, and neurons

During early development, placodal cells thicken within the ectoderm, delaminate, and migrate into the cranial mesenchyme, after neural crest migration is well underway. In cases where both populations contribute to the same ganglia, placodal cells are in close proximity to migratory cranial NC cells, while other placodal populations, such as the otic, potentially act as barriers shaping the migratory streams of NC cells emerging from the hindbrain and heading towards the branchial arches (reviewed in Steventon et al., 2014). On the other hand, cranial neural crest cells may physically segregate and individualize placode-derived ganglionic clusters, which in turn enables formation of the NC streams within the head (Szabó et al., 2019; Theveneau et al., 2013). These types of intercellular interactions are also thought to be governed by the "chase-and-run" which aid in the proper migration and shaping of each cell population into ganglia (Szabó et al., 2019; Theveneau et al., 2013, 2010).

More recently, biomechanical studies have identified mechanical forces as 'trigger and guidance' cues for collective NC migration and differentiation (Barriga et al., 2018; Shellard and Mayor, 2021, 2019; Zhu et al., 2019). In particular, higher cell density of the cranial mesenchyme in *Xenopus* results in tissue stiffening, which neural crest cells detect. This in turn initiates collective cranial neural crest migration (Barriga et al., 2018). Furthermore, these studies have revealed that NC cells establish their migratory routes by detecting and following a stiffness gradient across adjacent tissues (Shellard and Mayor, 2021, 2019). In *Xenopus* embryos, this gradient is partly established by attractive signals from ventrally localized placode cells adjacent to cranial neural crest cells (Theveneau et al., 2013). Mechanical forces from placode cells also contribute to NC directional migration (Shellard and Mayor, 2021). Cranial NC cells 'soften' placode cells via N-cadherin interactions, thereby creating a collective durotaxis gradient that NC cells probe and follow during embryonic development. Ectopic stiffness gradients or absence of these gradients result in erratic NC migration *in vivo* (Shellard and Mayor, 2021). NC differentiation in mice is also affected by the rigidity of substrates. Stiff substrates result in smooth muscle differentiation whereas softer environments lead to glial differentiation (Li et al., 2011; Zhu et al., 2019). Taken together, these results demonstrate that mechanical cues

drive collective migration and differentiation of NC cells. The molecular mechanisms driving the detection of these mechanical forces will be an interesting topic for further exploration.

Both modern and classical embryological experiments have demonstrated the interdependence of NC and placodal cell populations, both required for proper patterning of the cranial PNS (Bina et al., 2023; Gammill et al., 2007; Halmi et al., 2024; Hines and Taneyhill, 2024; Shiau et al., 2008; Shiau and Bronner-Fraser, 2009; Theveneau et al., 2013, 2010; Urrutia et al., 2024; Wu and Taneyhill, 2019). Ablation of the NC population does not lead to loss of cranial ganglia, but rather causes inappropriate morphology and positioning of ganglion, with evident abnormal or absent proximal components that lack projections to the CNS (Begbie and Graham, 2001; Cheng et al., 2000; Kuratani et al., 1991; Shiau et al., 2008; Yntema, 1944). Genetic ablation of the neural crest or perturbation of proper neural crest migration can lead to inappropriate fusions of otherwise physically separated ganglia in avian embryos (Bina et al., 2023; Gassmann et al., 1995; Golding et al., 2004; Hines and Taneyhill, 2024; Osborne et al., 2005; Schwarz et al., 2008; Shiau et al., 2008; Shiau and Bronner-Fraser, 2009; Urrutia et al., 2024; Wu and Taneyhill, 2019). On the other hand when placodes populations are ablated, NC cells are able to properly migrate but fail to produce cranial ganglia, with normal distal portions (Begbie and Graham, 2001; Cheng et al., 2000; Shiau et al., 2008). Finally, there is evidence that cranial NC cells actively guide placode cells by creating “corridors” that orchestrate the patterning of sensory neurons derived from both NC and placode cells (Freter et al., 2013). Altogether, these results point to the crucial role for NC and placode interactions during formation of cranial sensory ganglia.

2.7.1 Epibranchial ganglia

The epibranchial placodes contribute to sensory neurons in the distal portion of cranial ganglia VII, IXth and Xth (geniculate, petrosal and nodose placodes, respectively) (Figure 2.4). These neurons innervate the taste buds of the oropharyngeal

cavity, along with the heart, respiratory system, gastrointestinal tract and external ear. They relay vital sensory information via central projections to the hindbrain (D'Amico-Martel and Noden, 1983; Harlow et al., 2011; Harlow and Barlow, 2007; Schlosser and Northcutt, 2000). Lineage labeling with CM-DiI and CM-DiO of NC and placode cells, respectively, has revealed that placode-derived neurons overlap with neurogliogenic neural crest cells (Begbie and Graham, 2001). In addition to placodally derived neurons, NC cells contribute to proximal region of these ganglia, forming both peripheral glial cells (Schwann cells) and sensory neurons (D'Amico-Martel and Noden, 1983; Harlow et al., 2011; Harlow and Barlow, 2007; Le Douarin et al., 1991; Le Douarin, 1986; Schoenwolf et al., 2009).

Classical embryological studies have provided a clear understanding of the cellular contributions of neural crest and placode cells in the formation of epibranchial ganglia. In particular, ablation of prospective geniculate ectoderm in the chick results in ventrolateral displacement and loss or reduction of the central connections to the CNS (Yntema, 1944). Similarly, ablation of the cardiac neural crest results in similar phenotypes in the petrosal and nodose ganglia. In these instances, the distal portion of the ganglia develops in complete isolation, but the proximal and central regions are entirely lost. Later studies also confirmed these observations in the chick (Begbie and Graham, 2001; Kuratani et al., 1991; Yntema, 1944). In addition, placode-derived neurons fail to internally migrate resulting in displaced ganglia (Begbie and Graham, 2001). Thus, neural crest cells are required for accurate positioning of the epibranchial ganglia, as well as for establishing appropriate connections with the CNS.

In developing mouse embryos, proneural genes *Neurog1* and *Neurog2* are transiently expressed in distinct cranial ganglia. In particular, the geniculate and petrosal ganglia express *Neurog2*, while the nodose ganglia express both *Neurog1* and *Neurog2* (Fode et al., 1998; Ma et al., 1998). In *Neurog2* null mutant mice, the delamination and differentiation of the geniculate and petrosal placode progenitors are altered, resulting in delayed development of the distal portion of the geniculate ganglia and loss of the petrosal ganglia, mainly due to epibranchial neuroblasts failing to

delaminate (Coppola, 2010). While the nodose ganglion remains unaffected with single mutants, *Neurog1* and *Neurog2* double mutants result in loss of the ganglion, suggesting that there may function redundantly (Espinosa-Medina et al., 2014; Fode et al., 1998; Ma et al., 1998; Takano-Maruyama et al., 2012). Thus, *Neurog1/2* are proneural factors critical for initiating and balancing the neuronal differentiation of progenitors within the epibranchial ganglia (Bertrand et al., 2002; Huang et al., 2014). Coppola and colleagues (2010) observed not only a loss of the geniculate ganglia in *Ngn2* knock-out mice, but also of the sphenopalatine sympathetic ganglion, raising the possibility that placodal neurons provide a survival signal for NC-derived neurons which they innervate. Together, these studies further point to reciprocal interaction between neural crest and placodes cells in the establishment of correct circuits within the peripheral nervous system.

2.7.2 Trigeminal ganglia

There is rich literature regarding the reciprocal interactions between NC and placode cells that have also been investigated during formation of the trigeminal ganglion. Unlike the epibranchial ganglia, which have clear NC and placodal contribution to the proximal and distal regions, respectively, the trigeminal ganglion is comprised of a mixture of neurons derived from both embryonic populations (Baker, 2006; Blentic et al., 2011; D'Amico-Martel, 1982; D'Amico-Martel and Noden, 1983; Hamburger, 1961; Jidigam and Gunhaga, 2013; Knecht and Bronner-Fraser, 2002; Lwigale, 2001; Saint-Jeannet and Moody, 2014; Shiau et al., 2008). As the largest of the cranial ganglia, the trigeminal ganglion is a bi-lobed structure comprised of ophthalmic (OpV) and maxillo-mandibular (MmV) branches, which contains sensory neurons originating from both NC and placodal cells, with the placode (the OpV and MmV placodes in amniotes) contributing predominantly to the distal regions of the ganglion, while neural crest cells contribute proximally, along with associated glia throughout in developing birds (D'Amico-Martel and Noden, 1983; Hamburger, 1961; Moody et al., 1989; Moody and Heaton, 1983a, 1983b, 1983c; Noden, 1975; Serbedzija et al., 1992; Shiau et al., 2008).

The trigeminal ganglion arises from both migratory cranial NC cells and the trigeminal placode (D'Amico-Martel and Noden, 1983; Hamburger, 1961). In chick embryos, placodal cells begin to ingress ~HH12 as individuals or in short chains, maintaining contact with one another as they migrate into the cranial mesenchyme and immediately intermingle with HNK1+ migratory NC cells (Figure 2.5A, arrow) (D'Amico-Martel and Noden, 1983; Shiau et al., 2008). Prior to ingression, placodal cells begin to co-express neuronal markers such as Islet1 and β-neurotubulin (TUJ1) and continue to express these markers throughout gangliogenesis (Begbie et al., 2002; Moody et al., 1989; Shiau et al., 2008). While these cells express neuronal markers by the time they intermingle with NC cells, they are not necessarily post-mitotic, as these markers also label dividing neuroblasts (Begbie et al., 2002; Moody et al., 1989). At HH13, placode-derived neuroblasts exhibit short, randomly oriented axons primarily in the developing OpV lobe (Figure 2.5B, arrow) (Shiau et al., 2008). As development progresses, placodal cell ingression peaks between HH14–16 and ceases entirely at ~HH21 (D'Amico-Martel and Noden, 1983). By HH14, the placode neuroblasts begin to organize within the OpV lobe of the trigeminal ganglion, while the most proximal region (asterisk) appears to be exclusively occupied by NC-derived cells (Figure 2.5C, arrow) (Shiau et al., 2008). Additionally, by this stage, a few placodal neurons from the MmV lobe have started to extend towards the base of the first pharyngeal arch (Figure 2.5C, dashed arrow). By HH15, some placodal neurons within the OpV lobe extend towards the posterior region of the eye, occasionally making contact with the epidermis near the eye (Figure 2.5D, arrowhead). Concurrently, additional neuroblasts from the maxillomandibular placode begin to emerge and cluster ventrally to the OpV placodal neurons (Figure 2.5D, arrow). By HH16, post-mitotic neurons derived from the placode first appear (Figure 2.5E), with the OpV neurons continuing to extend dorsomedially and anteriorly, reaching a position approximately halfway between the retina and the telencephalon (Figure 2.5E, dashed arrow) (D'Amico-Martel and Noden, 1983).

By HH17, the majority of placode-derived neurons have clustered around the peripheral and distal regions of the NC–derived ganglionic core (Figure 2.5F,

asterisk). At this stage, more neurons are typically present in the OpV lobe than in the MmV lobe, and the NC–derived cells have not yet begun to differentiate (Figure 2.5F, arrows). At these developmental stages, the trigeminal ganglion now appears more as a stereotypic, bi-lobed structure with clearly defined OpV and MmV branches aligned along the proximodistal axis, with the OpV lobe continuing to develop ahead of the MmV lobe.

At HH18, the trigeminal NC cells are entirely intermixed with placode neurons (Figure 2.5G) and have segregated from the rest of the migratory cranial NC stream that now surround the eye and occupy the first pharyngeal arch. By this stage, both NC and placode cells observed throughout the ganglion, with exception of the most

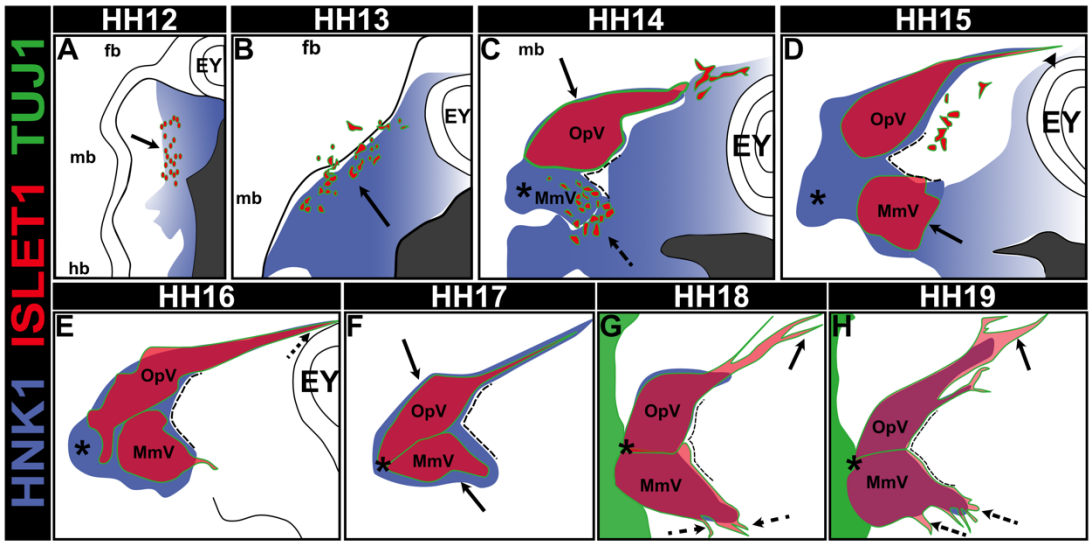

Figure 2.5 Chick trigeminal ganglion development at successive stages. (A-H) Schematic representing

Successive stages between HH12-19. During these stages, extensive overlap and intermixing of both placodal and neural crest cells is evident, as represented by antibodies against ISLET1 and TUJ1 for placodes and HNK1 for NC cells. (A) At HH12, several placodal cells can be seen distributed along the dorsal edge of the NC stream (arrow), between the developing eye and anterior hindbrain. (A-D) At HH12–15, the OpV placodal neurons appear first and are located more dorsally than the MmV placodal cells. (C) By HH14, most of the most proximal region (asterisk) is occupied by only neural crest cells. (E) At HH16, the interlobic region (demarcated by the black dashed lines) that lies between the OpV

and MmV lobes is mostly devoid of placodal neurons, and the NC have started to segregate from the periocular NC stream. As development progresses, this becomes an increasingly more defined trigeminal morphology. (F-H) By HH17-19, placodal and NC cells are well condensed into the ganglion. EY, eye; fb, forebrain; mb, midbrain; hb, hindbrain; OpV, ophthalmic; MmV, maxillo-mandibular; *, most proximal region to hindbrain.

proximal portion, which is solely NC-derived. Additionally, at this stage the MmV lobe begins to subdivide into smaller branches (Figure 2.5G-H, dashed arrow), that reflect the origins of the two major branches of the maxillary and mandibular nerves. Meanwhile, NC-derived cells begin differentiating into neurons, satellite glia, and Schwann cells around embryonic day 4 (~HH22–24) (D'Amico-Martel and Noden, 1980; 1983). By HH18-19, placodal and NC cells are well condensed into the trigeminal ganglion and few placodal cell bodies are found along the OpV projection (Figure 2.5G-H, dashed arrows). This prefigures the mature organization seen at embryonic day 12 (HH38), where NC-derived neurons occupy the proximal region and placode-derived neurons the distal region. This developmental timeline shows that throughout trigeminal gangliogenesis, both NC and placodal cells, intermingle and are in direct contact with one another, resulting in proper development of the ganglion.

Interestingly, within both the epibranchial and trigeminal ganglia, terminal differentiation of placodally-derived neurons precedes that of NC-derived neurons. As a result, cranial neural crest cells do not undergo large-scale neuronal differentiation until after the trigeminal ganglion has fully condensed (Begbie et al., 2002; d'Amico-Martel and Noden, 1980; D'Amico-Martel and Noden, 1983; Hamburger, 1961; Moody et al., 1989; Moody and Heaton, 1983a, 1983b, 1983c; Noden, 1975; Serbedzija et al., 1992; Shiau et al., 2008). To determine whether NC cells play a role in the induction of ophthalmic placode cells, ablation studies in chick, followed by analysis of *Pax3* expression, revealed that loss of NC cells did not change *Pax3* expression but instead resulted in ganglia that were abnormal and misshaped (D'Amico-Martel and Noden, 1983; Gammill et al., 2007; Hamburger, 1961; Shiau et al., 2008; Stark et al., 1997). Later NC ablations result in formation of slightly reduced, but overall normal ganglia. However, condensation of the ganglia was affected, along with a lack of axon projections to the hindbrain (Hamburger, 1961; Moody and Heaton, 1983c). Disruption of NC migration due to changes in *Neuropilin*/*Semaphorin* signaling or loss of cadherin molecules also disrupt trigeminal condensation and gangliogenesis, further supporting a role for NC cells in facilitating the aggregation of placodal neurons into the trigeminal ganglion (Akitaya and Bronner-Fraser, 1992;

D'Amico-Martel and Noden, 1983; Gammill et al., 2007; Saint-Jeannet and Moody, 2014; Shiau et al., 2008; Shiau and Bronner-Fraser, 2009). Together, these results illustrate the vital role of reciprocal interactions between NC and placode cells in ganglion condensation and establishment of appropriate central connections.

At a molecular level, various adhesion and signaling molecules have been shown to facilitate trigeminal ganglion formation. In avian embryos, *Slit-Robo* interactions are one of these molecular mechanism by which NC and placode interactions aid in the condensation and formation of the ganglia (Shiau et al., 2008; Shiau and Bronner-Fraser, 2009). Loss-of-function experiments have shown that loss of either component results in malformation of the ganglion (Shiau et al., 2008). It was later determined that N-cadherin may be acting downstream of *Slit-Robo*, aiding in the aggregation of the trigeminal ganglion (Shiau and Bronner-Fraser, 2009). Electroporation of morpholinos against N-cadherin into the presumptive trigeminal ectoderm, leads to dispersed and mislocalized trigeminal neuronal projections; however, ingression of these placodally-derived neurons remained unaffected (Shiau and Bronner-Fraser, 2009). Interestingly, it was confirmed that N-cadherin expression is downstream of *Robo2*, as *Slit1* overexpression results in ectopic aggregates of N-cadherin positive and *Robo2* negative neurons (Shiau and Bronner-Fraser, 2009).

In addition, previous studies have also shown that intercellular interactions during trigeminal ganglion formation are mediated, in part, by cadherin-based adhesion. In particular, Cadherin-7 and N-cadherin are expressed in neural crest and placode cells, respectively, during formation of the chick trigeminal ganglia (Hatta et al., 1987; Nakagawa and Takeichi, 1995; Shiau and Bronner-Fraser, 2009; Wu and Taneyhill, 2019). Neither depletion nor ectopic expression of Cadherin-7 impacts the overall morphology of the ganglion. While knockdown of N-cadherin does not affect initial placode cell ingression and delamination, it leads to increased placodal neuron dispersal during trigeminal gangliogenesis (Wu et al., 2014; Wu and Taneyhill, 2019). Overall, the interactions between Cadherin-7, expressed in NC cells, and N-cadherin,

present in placodal neurons, is required for coalescing of NC and placodal neurons during trigeminal gangliogenesis.

Additional signaling molecules have been implicated in the role of NC and placode interactions during cranial ganglion formation. In particular, disruption of *Neuropilin*/*Semaphorin* signaling affect cranial NC migratory behaviors (Osborne et al., 2005; Schwarz et al., 2008). In mice lacking the *Neuropilin* receptors NRP1/2, NC cells invade NC-free territories between the mandibular and hyoid NC streams, resulting in fused trigeminal and facial ganglia (Schwarz et al., 2008). Additionally, inhibition of the *Semaphorins Sema3A/3F* results in loss of NC migration and inhibits placodal aggregation in both the epibranchial and trigeminal ganglion (Osborne et al., 2005). Similarly, loss of the tyrosine kinase receptor, *erbB4* in either mice or chick embryos results in misrouting of r4 NC cells and production of ectopic cranial nerves (Gassmann et al., 1995; Golding et al., 2004).

Another signaling molecule implicated in promoting NC and placode condensation during chick trigeminal gangliogenesis is WNT6, along with its WNT modulator, *Wise* (Beaudoin et al., 2005; Guidato and Itasaki, 2007; Shigetani and Itasaki, 2007). Previous studies have shown that ectopic expression of *Wise* results in the formation of ectopic ganglia, a phenotype similar to the ectopic expression of *Wnt6*, suggesting that both *Wise* and *Wnt6* may act synergistically and thus may be inducing both placode and NC earlier than intended, resulting in these ectopic ganglia (Bastidas et al., 2004; Canning et al., 2008; García-Castro et al., 2002; Lassiter et al., 2007; Lewis et al., 2004; Shigetani and Itasaki, 2007).

In addition to adhesion and signaling molecules, multiple transcription factors have been implicated in promoting the condensation and differentiation of neurons with the trigeminal ganglion. Vertebrate neurogenesis is governed, in part, by proneural genes that regulate cell type determination and terminal differentiation. Basic Helix-Loop-Helix (bHLH) transcription factors, *Neurog1/2*, along with downstream transcription factors, such as *NeuroD1*, have been identified in

differentiating post-mitotic neuronal precursors and contribute to the establishment or maintenance of the neuronal program (Bertrand et al., 2002; Bina et al., 2023; Ma et al., 1998, 1996; Sommer et al., 1996; Ventéo et al., 2019). Depletion of *Neurog2* or *NeuroD1* from chick trigeminal placode cells results in malformation of the trigeminal ganglion. In particular, *Neurog2* and *NeuroD1* are shown to be critical for the development of the trigeminal ganglion, controlling neuronal differentiation, and precise axon outgrowth and innervation of target tissues as well as neuron morphology (Bina et al., 2023).

Another transcription factor implicated in differentiation and fate specification of sensory neurons in the peripheral nervous systems is *Tlx3* (Cheng et al., 2004; Hornbruch et al., 2005; Kondo et al., 2008; Logan et al., 1998; Y. Xu et al., 2008). In the chick, previous studies have shown that *Tlx3* is expressed in placodally derived components of the trigeminal ganglion, serving as a post-mitotic selector gene propelling these cells towards a neuronal fate (Cheng et al., 2004; Kondo et al., 2008; Logan et al., 1998). In addition, recent studies have revealed that, in the chick, *Tlx3* is expressed by both NC cells and placode cells and required for proper gangliogenesis. Moreover, ectopic expression of *Tlx3* leads to premature expression of neural markers, while its depletion results in improper condensation and size reduction of the ganglion. This suggests that *Tlx3* is necessary for specification of neural crest- and placode-derived sensory neurons during development of the trigeminal ganglion (Urrutia et al., 2024).

Taken together, neural crest cells play a vital role in the correct aggregation and condensation to form the trigeminal ganglion and establish correct connections to the hindbrain. Importantly, these results suggest a dual role for the NC in guiding the initial migration of placodal neurons to the appropriate sites as well as contributing to neurons and glia within the trigeminal ganglion.

2.8 Conclusion

In this chapter, I summarize our current knowledge of neural crest formation, migratory behaviors, and contribution to cranial sensory gangliogenesis. The neural crest is a captivating embryonic population, due to its migratory ability, plethora of derivatives, and broad developmental potential. This unique cell population is responsible for formation of craniofacial cartilage and bones and the peripheral nervous system, both defining features of vertebrates, effectively parting them from invertebrate chordates. Through a network of transcription factors and signaling cascades, different events in neural crest development are tightly regulated. Regardless of axial level of origin, many neural crest cells are multipotent and are capable of differentiating into a diverse array of derivatives (Baggiolini et al., 2015). Our current understanding of the NC and its transcriptional regulation has revealed multiple layers of control. While it is clear that there are both direct and indirect interactions between different neural crest transcription factors, adhesion, and signaling molecules, our grasp of the precise regulation of normal NC development and differentiation, and how their dysregulation can contribute to disease remains a mystery.

The use of high-throughput sequencing together with classical perturbation techniques has greatly enhanced our knowledge of how the neural crest develops. Additionally, technologies such as ATAC-seq, ChIP-seq, single cell RNA-seq, CRISPR/Cas9, and high-resolution microscopy have opened the possibility to dig deeper into some of the fundamental questions in neural crest biology, for example, better detailing the contribution of neural crest and placode interactions to morphogenetic events. These new methodologies hold the promise of providing further insights into the molecular mechanisms that control complex tissue rearrangements during vertebrate development. These techniques also can be applied to understand the cues involved in assembling ganglia in correct positions, as well as overall morphogenesis of other neural crest-derived structures and how their dysregulation can cause tissue deformities. Finally, I expect that future work will continue expanding our understanding of how the assembly of peripheral structures is

coordinated with their central targets. Recent studies suggest that some of the early mechanisms that pattern the CNS are equally involved in patterning the periphery, and vice versa.

2.9 References

Abercrombie, M. (1979). Contact inhibition and malignancy. Nature *281*, 259–262.

Abercrombie, M., Heaysman, J.E. (1953). Observations on the social behaviour of cells in tissue culture. I. Speed of movement of chick heart fibroblasts in relation to their mutual contacts. Exp. Cell Res. *5*, 111–131.

Adams, R.H., Diella, F., Hennig, S., Helmbacher, F., Deutsch, U., Klein, R. (2001). The cytoplasmic domain of the ligand ephrinB2 is required for vascular morphogenesis but not cranial neural crest migration. Cell *104*, 57–69.

Akitaya, T., Bronner-Fraser, M. (1992). Expression of cell adhesion molecules during initiation and cessation of neural crest cell migration. Dev. Dyn. *194*, 12–20.

Alfandari, D., Cousin, H., Marsden, M. (2010). Mechanism of Xenopus cranial neural crest cell migration. Cell Adh. Migr. *4*, 553–560.

Baggiolini, A., Varum, S., Mateos, J.M., Bettosini, D., John, N., Bonalli, M., Ziegler, U., Dimou, L., Clevers, H., Furrer, R., Sommer, L. (2015). Premigratory and migratory neural crest cells are multipotent in vivo. Cell Stem Cell *16*, 314–322.

Bajpai, R., Chen, D.A., Rada-Iglesias, A., Zhang, J., Xiong, Y., Helms, J., Chang, C.-P., Zhao, Y., Swigut, T., Wysocka, J. (2010). CHD7 cooperates with PBAF to control multipotent neural crest formation. Nature *463*, 958–962.

Baker, C. (2006). Neural Crest and Cranial Ectodermal Placodes, in: Developmental Neurobiology. Kluwer Academic Publishers-Plenum Publishers, New York, pp. 67–127.

Baker, C.V.H. (2008). The evolution and elaboration of vertebrate neural crest cells. Curr. Opin. Genet. Dev. *18*, 536–543.

Barlow, L.A. (2002). Cranial nerve development: placodal neurons ride the crest. Curr. Biol. *12*, R171-3.

Barriga, E.H., Franze, K., Charras, G., Mayor, R. (2018). Tissue stiffening coordinates morphogenesis by triggering collective cell migration in vivo. Nature *554*, 523–527.

Barriga, E.H., Maxwell, P.H., Reyes, A.E., Mayor, R. (2013). The hypoxia factor Hif-1α controls neural crest chemotaxis and epithelial to mesenchymal transition. J. Cell Biol. *201*, 759–776.

Basch, M.L., Bronner-Fraser, M., García-Castro, M.I. (2006). Specification of the neural crest occurs during gastrulation and requires Pax7. Nature *441*, 218–222.

Bastidas, F., De Calisto, J., Mayor, R. (2004). Identification of neural crest competence territory: role of Wnt signaling. Dev. Dyn. *229*, 109–117.

Beaudoin, G.M.J., 3rd, Sisk, J.M., Coulombe, P.A., Thompson, C.C. (2005). Hairless triggers reactivation of hair growth by promoting Wnt signaling. Proc. Natl. Acad. Sci. U. S. A. *102*, 14653–14658.

Begbie, J., Ballivet, M., Graham, A. (2002). Early steps in the production of sensory neurons by the neurogenic placodes. Mol. Cell. Neurosci. *21*, 502–511.

Begbie, J., Graham, A. (2001). Integration between the epibranchial placodes and the hindbrain. Science *294*, 595–598.

Bell, D.M., Leung, K.K., Wheatley, S.C., Ng, L.J., Zhou, S., Ling, K.W., Sham, M.H., Koopman, P., Tam, P.P., Cheah, K.S. (1997). SOX9 directly regulates the type-II collagen gene. Nat. Genet. *16*, 174–178.

Bertrand, N., Castro, D.S., Guillemot, F. (2002). Proneural genes and the specification of neural cell types. Nat. Rev. Neurosci. *3*, 517–530.

Betancur, P., Bronner-Fraser, M., Sauka-Spengler, T. (2010). Assembling neural crest regulatory circuits into a gene regulatory network. Annu. Rev. Cell Dev. Biol. *26*, 581–603.

Bhattacharyya, S., Bailey, A.P., Bronner-Fraser, M., Streit, A. (2004). Segregation of lens and olfactory precursors from a common territory: cell sorting and reciprocity of Dlx5 and Pax6 expression. Dev. Biol. *271*, 403–414.

Bina, P., Hines, M.A., Sanyal, J., Taneyhill, L.A. (2023). Neurogenin 2 and Neuronal Differentiation 1 control proper development of the chick trigeminal ganglion and its nerve branches. J. Dev. Biol. *11*.

Blentic, A., Chambers, D., Skinner, A., Begbie, J., Graham, A. (2011). The formation of the cranial ganglia by placodally-derived sensory neuronal precursors. Mol. Cell. Neurosci. *46*, 452–459.

Britsch, S., Goerich, D.E., Riethmacher, D., Peirano, R.I., Rossner, M., Nave, K.A., Birchmeier, C., Wegner, M. (2001). The transcription factor Sox10 is a key regulator of peripheral glial development. Genes Dev. *15*, 66–78.

Bronner, M.E., LeDouarin, N.M. (2012). Development and evolution of the neural crest: an overview. Dev. Biol. *366*, 2–9.

Bronner-Fraser, M. (1995). Origin of the avian neural crest. Stem Cells *13*, 640–646.

Bronner-Fraser, M. (1993). Neural crest cell migration in the developing embryo. Trends Cell Biol. *3*, 392–397.

Bronner-Fraser, M. (1986). Analysis of the early stages of trunk neural crest migration in avian embryos using monoclonal antibody HNK-1. Dev. Biol. *115*, 44–55.

Calloni, G.W., Le Douarin, N.M., Dupin, E. (2009). High frequency of cephalic neural crest cells shows coexistence of neurogenic, melanogenic, and osteogenic differentiation capacities. Proc. Natl. Acad. Sci. U. S. A. *106*, 8947–8952.

Canning, C.A., Lee, L., Luo, S.X., Graham, A., Jones, C.M. (2008). Neural tube derived Wnt signals cooperate with FGF signaling in the formation and differentiation of the trigeminal placodes. Neural Dev. *3*, 35.

Carmona-Fontaine, C., Matthews, H.K., Kuriyama, S., Moreno, M., Dunn, G.A., Parsons, M., Stern, C.D., Mayor, R. (2008). Contact inhibition of locomotion in vivo controls neural crest directional migration. Nature *456*, 957–961.

Carmona-Fontaine, C., Theveneau, E., Tzekou, A., Tada, M., Woods, M., Page, K.M., Parsons, M., Lambris, J.D., Mayor, R. (2011). Complement fragment C3a controls mutual cell attraction during collective cell migration. Dev. Cell *21*, 1026–1037.

Chalpe, A.J., Prasad, M., Henke, A.J., Paulson, A.F. (2010). Regulation of cadherin expression in the chicken neural crest by the Wnt/β-catenin signaling pathway. Cell Adh. Migr. *4*, 431–438.

Cheng, L., Arata, A., Mizuguchi, R., Qian, Y., Karunaratne, A., Gray, P.A., Arata, S., Shirasawa, S., Bouchard, M., Luo, P., Chen, C.-L., Busslinger, M., Goulding, M., Onimaru, H., Ma, Q. (2004). Tlx3 and Tlx1 are post-mitotic selector genes determining glutamatergic over GABAergic cell fates. Nature Neuroscience.

Cheng, Y., Cheung, M., Abu-Elmagd, M.M., Orme, A., Scotting, P.J. (2000). Chick sox10, a transcription factor expressed in both early neural crest cells and central nervous system. Brain Res. Dev. Brain Res. *121*, 233–241.

Cheung, M., Chaboissier, M.-C., Mynett, A., Hirst, E., Schedl, A., Briscoe, J. (2005). The transcriptional control of trunk neural crest induction, survival, and delamination. Dev. Cell *8*, 179–192.

Chibon, P. (1967). Nuclear labelling by tritiated thymidine of neural crest derivatives in the amphibian Urodele Pleurodeles waltlii Michah. J. Embryol. Exp. Morphol. *18*, 343–358.

Cohen, A.M., Konigsberg, I.R. (1975). A clonal approach to the problem of neural crest determination. Dev. Biol. *46*, 262–280.

Couly, G.F., Coltey, P.M., Le Douarin, N.M. (1993). The triple origin of skull in higher vertebrates: A study in quail-chick chimeras. Development *117*, 409–429.

Couly, G.F., Le Douarin, N.M. (1987). Mapping of the early neural primordium in quail-chick chimeras. II. The prosencephalic neural plate and neural folds: Implications for the genesis of cephalic human congenital abnormalities. Dev. Biol. *120*, 198–214.

Creuzet, S., Couly, G., Vincent, C., Le Douarin, N.M. (2002). Negative effect of Hox gene expression on the development of the neural crest-derived facial skeleton. Development *129*, 4301–4313.

Dady, A., Blavet, C., Duband, J.-L. (2012). Timing and kinetics of E- to N-cadherin switch during neurulation in the avian embryo. Dev. Dyn. *241*, 1333–1349.

D'Amico-Martel, A., Noden, D.M. (1980). An autoradiographic analysis of the development of the chick trigeminal ganglion. J. Embryol. Exp. Morphol. *55*, 167–182.

D'Amico-Martel, A. (1982). Temporal patterns of neurogenesis in avian cranial sensory and autonomic ganglia. Am. J. Anat. *163*, 351–372.

D'Amico-Martel, A., Noden, D.M. (1983). Contributions of placodal and neural crest cells to avian cranial peripheral ganglia. Am. J. Anat. *166*, 445–468.

Davis, E.M., Trinkaus, J.P. (1981). Significance of cell-to-cell contacts for the directional movement of neural crest cells within a hydrated collagen lattice. Development *63*, 29–51.

Davy, A., Aubin, J., Soriano, P. (2004). Ephrin-B1 forward and reverse signaling are required during mouse development. Genes Dev. *18*, 572–583.

Davy, A., Soriano, P. (2007). Ephrin-B2 forward signaling regulates somite patterning and neural crest cell development. Dev. Biol. *304*, 182–193.

Del Barrio, M.G., Nieto, M.A. (2002). Overexpression of Snail family members highlights their ability to promote chick neural crest formation. Development *129*, 1583–1593.

Desai, R.A., Gao, L., Raghavan, S., Liu, W.F., Chen, C.S. (2009). Cell polarity triggered by cell-cell adhesion via E-cadherin. J. Cell Sci. *122*, 905–911.

Dottori, M., Gross, M.K., Labosky, P., Goulding, M. (2001). The winged-helix transcription factor Foxd3 suppresses interneuron differentiation and promotes neural crest cell fate. Development *128*, 4127–4138.

Duband, J.L., Thiery, J.P. (1982). Distribution of fibronectin in the early phase of avian cephalic neural crest cell migration. Dev. Biol. *93*, 308–323.

Dupin, E., Baroffio, A., Dulac, C., Cameron-Curry, P., Le Douarin, N.M. (1990). Schwann-cell differentiation in clonal cultures of the neural crest, as evidenced by the anti-Schwann cell myelin protein monoclonal antibody. Proc. Natl. Acad. Sci. U. S. A. *87*, 1119–1123.

Dupin, E., Creuzet, S., Le Douarin, N.M. (2006). The contribution of the neural crest to the vertebrate body. Adv. Exp. Med. Biol. *589*, 96–119.

Dupin, I., Camand, E., Etienne-Manneville, S. (2009). Classical cadherins control nucleus and centrosome position and cell polarity. J. Cell Biol. *185*, 779–786.

Erickson, C.A. (1985). Control of neural crest cell dispersion in the trunk of the avian embryo. Dev. Biol. *111*, 138–157.

Erickson, C.A., Reedy, M.V. (1998). Neural crest development: The interplay between morphogenesis and cell differentiation. Curr. Top. Dev. Biol. *40*, 177–209.

Erickson, C.A., Tosney, K.W., Weston, J.A. (1980). Analysis of migratory behavior of neural crest and fibroblastic cells in embryonic tissues. Dev. Biol. *77*, 142–156.

Espinosa-Medina, I., Outin, E., Picard, C.A., Chettouh, Z., Dymecki, S., Consalez, G.G., Coppola, E., Brunet, J.-F. (2014). Neurodevelopment. Parasympathetic ganglia derive from Schwann cell precursors. Science *345*, 87–90.

Etienne-Manneville, S. (2014). Neighborly relations during collective migration. Curr. Opin. Cell Biol. *30*, 51–59.

Evans, D.J.R., Noden, D.M. (2006). Spatial relations between avian craniofacial neural crest and paraxial mesoderm cells. Dev. Dyn. *235*, 1310–1325.

Fairchild, C.L., Conway, J.P., Schiffmacher, A.T., Taneyhill, L.A., Gammill, L.S. (2014). FoxD3 regulates cranial neural crest EMT via downregulation of tetraspanin18 independent of its functions during neural crest formation. Mech. Dev. *132*, 1–12.

Fairchild, C.L., Gammill, L.S. (2013). Tetraspanin18 is a FoxD3-responsive antagonist of cranial neural crest epithelial-to-mesenchymal transition that maintains cadherin-6B protein. J. Cell Sci. *126*, 1464–1476.

Farlie, P.G., Kerr, R., Thomas, P., Symes, T., Minichiello, J., Hearn, C.J., Newgreen, D. (1999). A paraxial exclusion zone creates patterned cranial neural crest cell outgrowth adjacent to rhombomeres 3 and 5. Dev. Biol. *213*, 70–84.

Faulkner-Jones, B.E., Godinho, L.N., Reese, B.E., Pasquini, G.F., Ruefli, A., Tan, S.S. (1999). Cloning and expression of mouse Cadherin-7, a type-II cadherin isolated from the developing eye. Mol. Cell. Neurosci. *14*, 1–16.

Fode, C., Gradwohl, G., Morin, X., Dierich, A., LeMeur, M., Goridis, C., Guillemot, F. (1998). The bHLH protein NEUROGENIN 2 is a determination factor for epibranchial placode-derived sensory neurons. Neuron *20*, 483–494.

Freter, S., Fleenor, S.J., Freter, R., Liu, K.J., Begbie, J. (2013). Cranial neural crest cells form corridors prefiguring sensory neuroblast migration. Development *140*, 3595–3600.

Friedl, P., Gilmour, D. (2009). Collective cell migration in morphogenesis, regeneration and cancer. Nat. Rev. Mol. Cell Biol. *10*, 445–457.

Frith, T., Jr, Granata, I., Wind, M., Stout, E., Thompson, O., Neumann, K., Stavish, D., Heath, P.R., Ortmann, D., Hackland, J.O., Anastassiadis, K., Gouti, M., Briscoe, J., Wilson, V., Johnson, S.L., Placzek, M., Guarracino, M.R., Andrews, P.W., Tsakiridis, A. (2018). Human axial progenitors generate trunk neural crest cells in vitro. Elife *7*.

Furumatsu, T., Tsuda, M., Taniguchi, N., Tajima, Y., Asahara, H. (2005). Smad3 induces chondrogenesis through the activation of SOX9 via CREB-binding protein/p300 recruitment. J. Biol. Chem. *280*, 8343–8350.

Gammill, L.S., Gonzalez, C., Bronner-Fraser, M. (2007). Neuropilin 2/semaphorin 3F signaling is essential for cranial neural crest migration and trigeminal ganglion condensation. Dev. Neurobiol. *67*, 47–56.

Gans, C., Northcutt, R.G. (1983). Neural crest and the origin of vertebrates: A new head. Science *220*, 268–273.

García-Castro, M.I., Marcelle, C., Bronner-Fraser, M. (2002). Ectodermal Wnt function as a neural crest inducer. Science *297*, 848–851.

Gassmann, M., Casagranda, F., Orioli, D., Simon, H., Lai, C., Klein, R., Lemke, G. (1995). Aberrant neural and cardiac development in mice lacking the ErbB4 neuregulin receptor. Nature *378*, 390–394.

George, L., Chaverra, M., Todd, V., Lansford, R., Lefcort, F. (2007). Nociceptive sensory neurons derive from contralaterally migrating, fate-restricted neural crest cells. Nat. Neurosci. *10*, 1287–1293.

George, L., Kasemeier-Kulesa, J., Nelson, B.R., Koyano-Nakagawa, N., Lefcort, F. (2010). Patterned assembly and neurogenesis in the chick dorsal root ganglion. J. Comp. Neurol. *518*, 405–422.

Glenn Northcutt, R. (2005). The new head hypothesis revisited. J. Exp. Zool. B Mol. Dev. Evol. 304, 274–297.

Golding, J.P., Sobieszczuk, D., Dixon, M., Coles, E., Christiansen, J., Wilkinson, D., Gassmann, M. (2004). Roles of erbB4, rhombomere-specific, and rhombomere-independent cues in maintaining neural crest-free zones in the embryonic head. Dev. Biol. *266*, 361–372.

Graveson, A.C., Smith, M.M., Hall, B.K. (1997). Neural crest potential for tooth development in a urodele amphibian: Developmental and evolutionary significance. Dev. Biol. *188*, 34–42.

Green, S.A., Simoes-Costa, M., Bronner, M.E. (2015). Evolution of vertebrates as viewed from the crest. Nature *520*, 474–482.

Grenier, J., Teillet, M.-A., Grifone, R., Kelly, R.G., Duprez, D. (2009). Relationship between neural crest cells and cranial mesoderm during head muscle development. PLoS One *4*, e4381.

Gross, J.B., Hanken, J. (2008). Review of fate-mapping studies of osteogenic cranial neural crest in vertebrates. Dev. Biol. *317*, 389–400.

Gross, J.B., Hanken, J. (2005). Cranial neural crest contributes to the bony skull vault in adult Xenopus laevis: Insights from cell labeling studies. J. Exp. Zool. B Mol. Dev. Evol. *304*, 169–176.

Guidato, S., Itasaki, N. (2007). Wise retained in the endoplasmic reticulum inhibits Wnt signaling by reducing cell surface LRP6. Dev. Biol. *310*, 250–263.

Hall, B.K. (2009). The neural crest and neural crest cells in vertebrate development and evolution. Springer, New York, NY.

Hall, B.K. (2008). The neural crest and neural crest cells: Discovery and significance for theories of embryonic organization. J. Biosci. *33*, 781–793.

Hall, B.K. (2000). The neural crest as a fourth germ layer and vertebrates as quadroblastic not triploblastic. Evol. Dev. *2*, 3–5.

Hall, B.K. (1998). Germ layers and the germ-layer theory revisited, in: Evolutionary Biology. Springer US, Boston, MA, pp. 121–186.

Halmi, C.A., Leonard, C.E., McIntosh, A.T., Taneyhill, L.A. (2024). N-cadherin facilitates trigeminal sensory neuron outgrowth and target tissue innervation. bioRxiv.

Hamburger, V. (1961). Experimental analysis of the dual origin of the trigeminal ganglion in the chick embryo. J. Exp. Zool. *148*, 91–123.

Harlow, D.E., Barlow, L.A. (2007). Embryonic origin of gustatory cranial sensory neurons. Dev. Biol. *310*, 317–328.

Harlow, D.E., Yang, H., Williams, T., Barlow, L.A. (2011). Epibranchial placode-derived neurons produce BDNF required for early sensory neuron development. Dev. Dyn. *240*, 309–323.

Harris, M.L., Erickson, C.A. (2007). Lineage specification in neural crest cell pathfinding. Dev. Dyn. *236*, 1–19.

Hatta, K., Takagi, S., Fujisawa, H., Takeichi, M. (1987). Spatial and temporal expression pattern of N-cadherin cell adhesion molecules correlated with morphogenetic processes of chicken embryos. Dev. Biol. *120*, 215–227.

Helms, J.A., Schneider, R.A. (2003). Cranial skeletal biology. Nature *423*, 326–331.

Hines, M.A., Taneyhill, L.A. (2024). Elp1 function in placode-derived neurons is critical for proper trigeminal ganglion development. Dev. Dyn.

His, W. (1868). Untersuchungen über die erste Anlage des Wirbelthierleibes : die erste Entwickelung des Hühnchens im Ei / von Wilhelm His. F.C.W. Vogel, Leipzig.

Hochgreb-Hägele, T., Bronner, M.E. (2013). A novel FoxD3 gene trap line reveals neural crest precursor movement and a role for FoxD3 in their specification. Dev. Biol. *374*, 1–11.

Hong, C.-S., Saint-Jeannet, J.-P. (2007). The activity of Pax3 and Zic1 regulates three distinct cell fates at the neural plate border. Mol. Biol. Cell *18*, 2192–2202.

Hornbruch, A., Ma, G., Ballermann, M.A., Tumova, K., Liu, D., Cairine Logan, C. (2005). A BMP-mediated transcriptional cascade involving Cash1 and Tlx-3 specifies first-order relay sensory neurons in the developing hindbrain. Mech. Dev. *122*, 900–913.

Huang, C., Chan, J.A., Schuurmans, C. (2014). Proneural bHLH genes in development and disease. Curr. Top. Dev. Biol. *110*, 75–127.

Ito, K., Morita, T., Sieber-Blum, M. (1993). In vitro clonal analysis of mouse neural crest development. Dev. Biol. *157*, 517–525.

Ito, Y., Bringas, P., Jr, Mogharei, A., Zhao, J., Deng, C., Chai, Y. (2002). Receptor-regulated and inhibitory Smads are critical in regulating transforming growth factor beta-mediated Meckel's cartilage development. Dev. Dyn. *224*, 69–78.

Jidigam, V.K., Gunhaga, L. (2013). Development of cranial placodes: insights from studies in chick. Dev. Growth Differ. *55*, 79–95.

Jin, E.J., Erickson, C.A., Takada, S., Burrus, L.W. (2001). Wnt and BMP signaling govern lineage segregation of melanocytes in the avian embryo. Dev. Biol. *233*, 22–37.

Johnston, M.C. (1966). A radioautographic study of the migration and fate of cranial neural crest cells in the chick embryo. Anat. Rec. *156*, 143–155.

Kasemeier-Kulesa, J.C., McLennan, R., Romine, M.H., Kulesa, P.M., Lefcort, F. (2010). CXCR4 controls ventral migration of sympathetic precursor cells. J. Neurosci. *30*, 13078–13088.

Kenny, C., Dilshat, R., Seberg, H., Van Otterloo, E., Bonde, G., Helverson, A., Franke, C.M., Steingrímsson, E., Cornell, R.A. (2022). TFAP2 Paralogs Facilitate Chromatin Access for MITF at Pigmentation and Cell Proliferation Genes. PLoS Gen. *18*, 5: e1010207.

Kerosuo, L., Bronner, M.E. (2016). CMyc regulates the size of the premigratory neural crest stem cell pool. Cell Rep. *17*, 2648–2659.

Kerosuo, L., Bronner-Fraser, M. (2012). What is bad in cancer is good in the embryo: Importance of EMT in neural crest development. Semin. Cell Dev. Biol. *23*, 320–332.

Knecht, A.K., Bronner-Fraser, M. (2002). Induction of the neural crest: a multigene process. Nat. Rev. Genet. *3*, 453–461.

Kondo, T., Sheets, P.L., Zopf, D.A., Aloor, H.L., Cummins, T.R., Chan, R.J., Hashino, E. (2008). Tlx3 exerts context-dependent transcriptional regulation and

promotes neuronal differentiation from embryonic stem cells. Proc. Natl. Acad. Sci. U. S. A. *105*, 5780–5785.

Krispin, S., Nitzan, E., Kalcheim, C. (2010). The dorsal neural tube: A dynamic setting for cell fate decisions. Dev. Neurobiol. *70*, 796–812.

Krull, C.E. (1998). Inhibitory interactions in the patterning of trunk neural crest migration. Ann. N. Y. Acad. Sci. *857*, 13–22.

Krull, C.E., Lansford, R., Gale, N.W., Collazo, A., Marcelle, C., Yancopoulos, G.D., Fraser, S.E., Bronner-Fraser, M. (1997). Interactions of Eph-related receptors and ligands confer rostrocaudal pattern to trunk neural crest migration. Curr. Biol. *7*, 571–580.

Kulesa, P.M., Bailey, C.M., Kasemeier-Kulesa, J.C., McLennan, R. (2010). Cranial neural crest migration: New rules for an old road. Dev. Biol. *344*, 543–554.

Kulesa, P.M., Fraser, S.E. (2000). In ovo time-lapse analysis of chick hindbrain neural crest cell migration shows cell interactions during migration to the branchial arches. Development *127*, 1161–1172.

Kulesa, P.M., Fraser, S.E. (1998). Neural crest cell dynamics revealed by time-lapse video microscopy of whole embryo chick explant cultures. Dev. Biol. *204*, 327–344.

Kulesa, P.M., Gammill, L.S. (2010). Neural crest migration: Patterns, phases and signals. Dev. Biol. *344*, 566–568.

Kuratani, S.C., Miyagawa-Tomita, S., Kirby, M.L. (1991). Development of cranial nerves in the chick embryo with special reference to the alterations of cardiac branches after ablation of the cardiac neural crest. Anat. Embryol. (Berl.) *183*, 501–514.

Kuriyama, S., Mayor, R. (2008). Molecular analysis of neural crest migration. Philos. Trans. R. Soc. Lond. B Biol. Sci. *363*, 1349–1362.

LaBonne, C., Bronner-Fraser, M. (1998). Neural crest induction in Xenopus: Evidence for a two-signal model. Development *125*, 2403–2414.

Lassiter, R.N.T., Dude, C.M., Reynolds, S.B., Winters, N.I., Baker, C.V.H., Stark, M.R. (2007). Canonical Wnt signaling is required for ophthalmic trigeminal placode cell fate determination and maintenance. Dev. Biol. *308*, 392–406.

Le Douarin, N.M. (1982). Developmental and cell biology series: The neural crest series number 12, Developmental and cell biology series. Cambridge University Press, Cambridge, England.

Le Douarin, N.M. (1973). A biological cell labeling technique and its use in expermental embryology. Dev. Biol. *30*, 217–222.

Le Douarin, N.M., Dulac, C., Dupin, E., Cameron-Curry, P. (1991). Glial cell lineages in the neural crest. Glia *4*, 175–184.

Le Douarin, N., Kalcheim, C. (1999). Developmental and cell biology series: The neural crest series number *36*, 2nd ed, Developmental and cell biology series. Cambridge University Press, Cambridge, England.

Le Douarin, N.M. (1986). Cell line segregation during peripheral nervous system ontogeny. Science *231*, 1515–1522.

Le Douarin, N.M., Dupin, E. (2018). The “beginnings” of the neural crest. Dev. Biol. *444*, S3–S13.

Le Douarin, N.M., Dupin, E. (2014). The neural crest, a fourth germ layer of the vertebrate embryo, in: Neural Crest Cells. Elsevier, pp. 3–26.

Le Douarin, N.M., Teillet, M.A. (1974). Experimental analysis of the migration and differentiation of neuroblasts of the autonomic nervous system and of neurectodermal mesenchymal derivatives, using a biological cell marking technique. Dev. Biol. *41*, 162–184.

Le Douarin, N.M., Teillet, M.A. (1973). The migration of neural crest cells to the wall of the digestive tract in avian embryo. J. Embryol. Exp. Morphol. *30*, 31–48.

Le Lièvre, C.S. (1978). Participation of neural crest-derived cells in the genesis of the skull in birds. J. Embryol. Exp. Morphol. *47*, 17–37.

Lefcort, F., George, L. (2007). Neural crest cell fate: To be or not to be prespecified. Cell Adh. Migr. *1*, 199–201.

Lefebvre, V., Li, P., de Crombrugghe, B. (1998). A new long form of Sox5 (L-Sox5), Sox6 and Sox9 are coexpressed in chondrogenesis and cooperatively activate the type II collagen gene. EMBO J. *17*, 5718–5733.

Lewis, J.L., Bonner, J., Modrell, M., Ragland, J.W., Moon, R.T., Dorsky, R.I., Raible, D.W. (2004). Reiterated Wnt signaling during zebrafish neural crest development. Development *131*, 1299–1308.

Li, X., Chu, J., Wang, A., Zhu, Y., Chu, W.K., Yang, L., Li, S. (2011). Uniaxial mechanical strain modulates the differentiation of neural crest stem cells into smooth muscle lineage on micropatterned surfaces. PLoS One *6*, e26029.

Lim, J., Thiery, J.P. (2012). Epithelial-mesenchymal transitions: Insights from development. Development *139*, 3471–3486.

Ling, I.T.C., Sauka-Spengler, T. (2019). Early chromatin shaping predetermines multipotent vagal neural crest into neural, neuronal and mesenchymal lineages. Nat. Cell Biol. *21*, 1504–1517.

Logan, C., Wingate, R.J., McKay, I.J., Lumsden, A. (1998). Tlx-1 and Tlx-3 homeobox gene expression in cranial sensory ganglia and hindbrain of the chick embryo: markers of patterned connectivity. J. Neurosci. *18*, 5389–5402.

Lukoseviciute, M., Gavriouchkina, D., Williams, R.M., Hochgreb-Hagele, T., Senanayake, U., Chong-Morrison, V., Thongjuea, S., Repapi, E., Mead, A., Sauka-Spengler, T. (2018). From pioneer to repressor: Bimodal foxd3 activity dynamically remodels neural crest regulatory landscape in vivo. Dev. Cell *47*, 608-628.e6.

Lumsden, A., Clarke, J.D., Keynes, R., Fraser, S. (1994). Early phenotypic choices by neuronal precursors, revealed by clonal analysis of the chick embryo hindbrain. Development *120*, 1581–1589.

Lumsden, A.G. (1988). Spatial organization of the epithelium and the role of neural crest cells in the initiation of the mammalian tooth germ. Development *103* Suppl, 155–169.

Lumsden, A.G., Buchanan, J.A. (1986). An experimental study of timing and topography of early tooth development in the mouse embryo with an analysis of the role of innervation. Arch. Oral Biol. *31*, 301–311.

Lwigale, P.Y. (2001). Embryonic origin of avian corneal sensory nerves. Dev. Biol. *239*, 323–337.

Ma, Q., Chen, Z., del Barco Barrantes, I., de la Pompa, J.L., Anderson, D.J. (1998). Neurogenin1 is essential for the determination of neuronal precursors for proximal cranial sensory ganglia. Neuron *20*, 469–482.

Ma, Q., Kintner, C., Anderson, D.J. (1996). Identification of neurogenin, a vertebrate neuronal determination gene. Cell *87*, 43–52.

Marchant, L., Linker, C., Ruiz, P., Guerrero, N., Mayor, R. (1998). The inductive properties of mesoderm suggest that the neural crest cells are specified by a BMP gradient. Dev. Biol. *198*, 319–329.

Martik, M.L., Bronner, M.E. (2017). Regulatory logic underlying diversification of the neural crest. Trends Genet. *33*, 715–727.

Martinsen, B.J., Bronner-Fraser, M. (1998). Neural crest specification regulated by the helix-loop-helix repressor Id2. Science *281*, 988–991.

Mayor, R., Guerrero, N., Martínez, C. (1997). Role of FGF and noggin in neural crest induction. Dev. Biol. *189*, 1–12.

Mayor, R., Morgan, R., Sargent, M.G. (1995). Induction of the prospective neural crest of Xenopus. Development *121*, 767–777.

Mayor, R., Theveneau, E. (2014). The role of the non-canonical Wnt-planar cell polarity pathway in neural crest migration. Biochem. J. *457*, 19–26. https://doi.org/10.1042/BJ20131182

Mayran, A., Khetchoumian, K., Hariri, F., Pastinen, T., Gauthier, Y., Balsalobre, A., Drouin, J. (2018). Pioneer factor Pax7 deploys a stable enhancer repertoire for specification of cell fate. Nat. Genet. *50*, 259–269.

McKeown, S.J., Wallace, A.S., Anderson, R.B. (2013). Expression and function of cell adhesion molecules during neural crest migration. Dev. Biol. *373*, 244–257.

McLennan, R., Schumacher, L.J., Morrison, J.A., Teddy, J.M., Ridenour, D.A., Box, A.C., Semerad, C.L., Li, H., McDowell, W., Kay, D., Maini, P.K., Baker, R.E., Kulesa, P.M. (2015). VEGF signals induce trailblazer cell identity that drives neural crest migration. Dev. Biol. *407*, 12–25.

Mellott, D.O., Burke, R.D. (2008). Divergent roles for Eph and ephrin in avian cranial neural crest. BMC Dev. Biol. *8*, 56.

Milet, C., Monsoro-Burq, A.H. (2012). Neural crest induction at the neural plate border in vertebrates. Dev. Biol. *366*, 22–33.

Minoux, M., Holwerda, S., Vitobello, A., Kitazawa, T., Kohler, H., Stadler, M.B., Rijli, F.M. (2017). Gene bivalency at Polycomb domains regulates cranial neural crest positional identity. Science *355*, eaal2913.

Minoux, M., Rijli, F.M. (2010). Molecular mechanisms of cranial neural crest cell migration and patterning in craniofacial development. Development *137,* 2605–2621.

Moody, S.A., Heaton, M.B. (1983c). Developmental relationships between trigeminal ganglia and trigeminal motoneurons in chick embryos. I. Ganglion development is necessary for motoneuron migration. J. Comp. Neurol. *213*, 327–343.

Moody, S.A., Heaton, M.B. (1983b). Developmental relationships between trigeminal ganglia and trigeminal motoneurons in chick embryos. II. Ganglion axon ingrowth guides motoneuron migration. J. Comp. Neurol. *213*, 344–349.

Moody, S.A., Heaton, M.B., (1983a). Developmental relationships between trigeminal ganglia and trigeminal motoneurons in chick embryos. III. Ganglion perikarya direct motor axon growth in the periphery. J. Comp. Neurol. *213*, 350–364.

Moody, S.A., Quigg, M.S., Frankfurter, A. (1989). Development of the peripheral trigeminal system in the chick revealed by an isotype-specific anti-beta-tubulin monoclonal antibody. The Journal of Comparative Neurology.

Moore, R., Larue, L. (2004). Cell surface molecules and truncal neural crest ontogeny: A perspective. Birth Defects Res. C Embryo Today *72*, 140–150.

Morikawa, Y., Zehir, A., Maska, E., Deng, C., Schneider, M.D., Mishina, Y., Cserjesi, P. (2009). BMP signaling regulates sympathetic nervous system development through Smad4-dependent and -independent pathways. Development *136*, 3575–3584.

Nakagawa, S., Takeichi, M. (1995). Neural crest cell-cell adhesion controlled by sequential and subpopulation-specific expression of novel cadherins. Development *121*, 1321–1332.

Nakamura, H., Lievre, C.S.A.-L. (1982). Mesectodermal capabilities of the trunk neural crest of birds. Development *70*, 1–18.

Newgreen, D.F. (1989). Physical influences on neural crest cell migration in avian embryos: Contact guidance and spatial restriction. Dev. Biol. *131*, 136–148.

Newgreen, D.F., Gibbins, I.L., Sauter, J., Wallenfels, B., Wütz, R. (1982). Ultrastructural and tissue-culture studies on the role of fibronectin, collagen and glycosaminoglycans in the migration of neural crest cells in the fowl embryo. Cell Tissue Res. *221*, 521–549.

Newgreen, D.F., Gooday, D. (1985). Control of the onset of migration of neural crest cells in avian embryos. Role of Ca++-dependent cell adhesions. Cell Tissue Res. *239*, 329–336.

Newgreen, D.F., Scheel, M., Kastner, V. (1986). Anatomical and experimental studies on early morphogenesis of the avian perichordal region: Differential effect of notochordal chondroitinase-sensitive material on neural crest and sclerotome cells. Cell Tiss. Res.

Noden, D.M. (1975). An analysis of migratory behavior of avian cephalic neural crest cells. Dev. Biol. *42*, 106–130.

Olesnicky Killian, E.C., Birkholz, D.A., Artinger, K.B. (2009). A role for chemokine signaling in neural crest cell migration and craniofacial development. Dev. Biol. *333*, 161–172.

Olsson, L., Hanken, J. (1996). Cranial neural-crest migration and chondrogenic fate in the oriental fire-bellied toad Bombina orientalis: Defining the ancestral pattern of head development in anuran amphibians. J. Morphol. *229*, 105–120.

Osborne, N.J., Begbie, J., Chilton, J.K., Schmidt, H., Eickholt, B.J. (2005). Semaphorin/neuropilin signaling influences the positioning of migratory neural crest cells within the hindbrain region of the chick. Dev. Dyn. *232*, 939–949.

Perez-Alcala, S., Nieto, M.A., Barbas, J.A. (2004). LSox5 regulates RhoB expression in the neural tube and promotes generation of the neural crest. Development *131*, 4455–4465.

Pieper, M., Eagleson, G.W., Wosniok, W., Schlosser, G. (2011). Origin and segregation of cranial placodes in Xenopus laevis. Dev. Biol. *360*, 257–275.

Piloto, S., Schilling, T.F. (2010). Ovo1 links Wnt signaling with N-cadherin localization during neural crest migration. Development *137*, 2603–2603.

Pla, P., Moore, R., Morali, O.G., Grille, S., Martinozzi, S., Delmas, V., Larue, L. (2001). Cadherins in neural crest cell development and transformation. J. Cell. Physiol. *189*, 121–132.

Potterf, S.B., Mollaaghababa, R., Hou, L., Southard-Smith, E.M., Hornyak, T.J., Arnheiter, H., Pavan, W.J. (2001). Analysis of SOX10 function in neural crest-derived melanocyte development: SOX10-dependent transcriptional control of dopachrome tautomerase. Dev. Biol. *237*, 245–257.

Prasad, M.S., Sauka-Spengler, T., LaBonne, C. (2012). Induction of the neural crest state: control of stem cell attributes by gene regulatory, post-transcriptional and epigenetic interactions. Dev. Biol. *366*, 10–21.

Revenu, C., Streichan, S., Donà, E., Lecaudey, V., Hufnagel, L., Gilmour, D. (2014). Quantitative cell polarity imaging defines leader-to-follower transitions during collective migration and the key role of microtubule-dependent adherens junction formation. Development *141*, 1282–1291.

Richardson, J., Gauert, A., Briones Montecinos, L., Fanlo, L., Alhashem, Z.M., Assar, R., Marti, E., Kabla, A., Härtel, S., Linker, C. (2016). Leader cells define directionality of trunk, but not cranial, neural crest cell migration. Cell Rep. *15*, 2076–2088.

Rickmann, M., Fawcett, J.W., Keynes, R.J. (1985). The migration of neural crest cells and the growth of motor axons through the rostral half of the chick somite. Development *90*, 437–455.

Rinon, A., Molchadsky, A., Nathan, E., Yovel, G., Rotter, V., Sarig, R., Tzahor, E. (2011). P53 coordinates cranial neural crest cell growth and epithelial-mesenchymal transition/delamination processes. Development *138*, 1827–1838.

Roellig, D., Tan-Cabugao, J., Esaian, S., Bronner, M.E. (2017). Dynamic transcriptional signature and cell fate analysis reveals plasticity of individual neural plate border cells. Elife *6*.

Rogers, C.D., Saxena, A., Bronner, M.E. (2013). Sip1 mediates an E-cadherin-to-N-cadherin switch during cranial neural crest EMT. J. Cell Biol. *203*, 835–847.

Rothstein, M., Bhattacharya, D., Simoes-Costa, M. (2018). The molecular basis of neural crest axial identity. Dev. Biol. 444 Suppl *1*, S170–S180.

Saint-Jeannet, J.-P., Moody, S.A. (2014). Establishing the pre-placodal region and breaking it into placodes with distinct identities. Dev. Biol. *389*, 13–27.

Sasselli, V., Pachnis, V., Burns, A.J., 2012. The enteric nervous system. Dev. Biol. 366, 64–73. https://doi.org/10.1016/j.ydbio.2012.01.012

Sauka-Spengler, T., Bronner-Fraser, M. (2008). A gene regulatory network orchestrates neural crest formation. Nat. Rev. Mol. Cell Biol. *9*, 557–568.

Scarpa, E., Szabó, A., Bibonne, A., Theveneau, E., Parsons, M., Mayor, R. (2015). Cadherin switch during EMT in neural crest cells leads to contact inhibition of locomotion via repolarization of forces. Dev. Cell *34*, 421–434.

Scerbo, P., Monsoro-Burq, A.H. (2020). The vertebrate-specific VENTX/NANOG gene empowers neural crest with ectomesenchyme potential. Sci. Adv. *6*, eaaz1469.

Schilling, T.F., Kimmel, C.B. (1994). Segment and cell type lineage restrictions during pharyngeal arch development in the zebrafish embryo. Development *120*, 483–494.

Schlosser, G., Northcutt, R.G. (2000). Development of neurogenic placodes in Xenopus laevis. J. Comp. Neurol. *418*, 121–146.

Schoenwolf, G.C., Bleyl, S.B., Brauer, P.R., Francis-West, P.H. (2009). Development of the peripheral nervous system, in: Larsen's Human Embryology. Elsevier, pp. 297–318.

Schroeder, T.E. (1970). Neurulation in Xenopus laevis. An analysis and model based upon light and electron microscopy. J. Embryol. Exp. Morphol. *23*, 427–462.

Schwarz, Q., Vieira, J.M., Howard, B., Eickholt, B.J., Ruhrberg, C. (2008). Neuropilin 1 and 2 control cranial gangliogenesis and axon guidance through neural crest cells. Development *135*, 1605–1613.

Seberg, H.E., Van Otterloo, E., Loftus, S.K., Liu, H., Bonde, G., Sompallae, R., Gildea, D.E., Santana, J.F., Manak, J.R., Pavan, W.J., Williams, T., Cornell, R.A. (2017). TFAP2 paralogs regulate melanocyte differentiation in parallel with MITF. PLoS Genet. *13*, e1006636.

Sela-Donenfeld, D., Kalcheim, C. (1999). Regulation of the onset of neural crest migration by coordinated activity of BMP4 and Noggin in the dorsal neural tube. Development *126*, 4749–4762.

Serbedzija, G.N., Bronner-Fraser, M., Fraser, S.E. (1992). Vital dye analysis of cranial neural crest cell migration in the mouse embryo. Development *116*, 297–307.

Shellard, A., Mayor, R. (2021). Collective durotaxis along a self-generated stiffness gradient in vivo. Nature *600*, 690–694.

Shellard, A., Mayor, R. (2019). Integrating chemical and mechanical signals in neural crest cell migration. Curr. Opin. Genet. Dev. *57*, 16–24.

Shiau, C.E., Bronner-Fraser, M. (2009). N-cadherin acts in concert with Slit1-Robo2 signaling in regulating aggregation of placode-derived cranial sensory neurons. Development *136*, 4155–4164.

Shiau, C.E., Lwigale, P.Y., Das, R.M., Wilson, S.A., Bronner-Fraser, M. (2008). Robo2-Slit1 dependent cell-cell interactions mediate assembly of the trigeminal ganglion. Nat. Neurosci. *11*, 269–276.

Shigetani, Y., Itasaki, N. (2007). Expression of Wise in chick embryos. Dev. Dyn. *236*, 2277–2284.

Shyamala, K., Yanduri, S., Girish, H.C., Murgod, S. (2015). Neural crest: The fourth germ layer. J. Oral Maxillofac. Pathol. *19*, 221–229.

Sieber-Blum, M. (1989). Commitment of neural crest cells to the sensory neuron lineage. Science *243*, 1608–1611.

Sieber-Blum, M., Cohen, A.M. (1980). Clonal analysis of quail neural crest cells: They are pluripotent and differentiate in vitro in the absence of noncrest cells. Dev. Biol. *80*, 96–106.

Simoes-Costa, M., Bronner, M.E. (2016). Reprogramming of avian neural crest axial identity and cell fate. Science *352*, 1570–1573.

Simões-Costa, M., Bronner, M.E. (2015). Establishing neural crest identity: A gene regulatory recipe. Development *142*, 242–257.

Smith, A., Graham, A. (2001). Restricting Bmp-4 mediated apoptosis in hindbrain neural crest. Dev. Dyn. *220*, 276–283.

Smith, A., Robinson, V., Patel, K., Wilkinson, D.G. (1997). The EphA4 and EphB1 receptor tyrosine kinases and ephrin-B2 ligand regulate targeted migration of branchial neural crest cells. Curr. Biol. *7*, 561–570.

Smith, M.M., Hall, B.K. (1990). Development and evolutionary origins of vertebrate skeletogenic and odontogenic tissues. Biol. Rev. Camb. Philos. Soc. *65*, 277–373.

Soldatov, R., Kaucka, M., Kastriti, M.E., Petersen, J., Chontorotzea, T., Englmaier, L., Akkuratova, N., Yang, Y., Häring, M., Dyachuk, V., Bock, C., Farlik, M., Piacentino, M.L., Boismoreau, F., Hilscher, M.M., Yokota, C., Qian, X., Nilsson, M., Bronner, M.E., Croci, L., Hsiao, W.-Y., Guertin, D.A., Brunet, J.-F., Consalez, G.G., Ernfors, P., Fried, K., Kharchenko, P.V., Adameyko, I. (2019). Spatiotemporal structure of cell fate decisions in murine neural crest. Science *364*, eaas9536.

Sommer, L., Ma, Q., Anderson, D.J. (1996). neurogenins, a novel family of atonal-related bHLH transcription factors, are putative mammalian neuronal determination genes that reveal progenitor cell heterogeneity in the developing CNS and PNS. Mol. Cell. Neurosci. *8*, 221–241.

Square, T.A., Jandzik, D., Massey, J.L., Romášek, M., Stein, H.P., Hansen, A.W., Purkayastha, A., Cattell, M.V., Medeiros, D.M. (2020). Evolution of the endothelin pathway drove neural crest cell diversification. Nature *585*, 563–568.

Stark, M.R., Sechrist, J., Bronner-Fraser, M., Marcelle, C. (1997). Neural tube-ectoderm interactions are required for trigeminal placode formation. Development *124*, 4287–4295.

Steventon, B., Araya, C., Linker, C., Kuriyama, S., Mayor, R. (2009). Differential requirements of BMP and Wnt signalling during gastrulation and neurulation define two steps in neural crest induction. Development *136*, 771–779.

Steventon, B., Carmona-Fontaine, C., Mayor, R. (2005). Genetic network during neural crest induction: From cell specification to cell survival. Semin. Cell Dev. Biol. *16*, 647–654.

Steventon, B., Mayor, R., Streit, A. (2014). Neural crest and placode interaction during the development of the cranial sensory system. Dev. Biol. *389*, 28–38.

Streit, A. (2002). Extensive cell movements accompany formation of the otic placode. Dev. Biol. *249*, 237–254.

Stuhlmiller, T.J., García-Castro, M.I. (2012). Current perspectives of the signaling pathways directing neural crest induction. Cell. Mol. Life Sci. *69*, 3715–3737.

Szabó, A., Theveneau, E., Turan, M., Mayor, R. (2019). Neural crest streaming as an emergent property of tissue interactions during morphogenesis. PLoS Comput. Biol. *15*, e1007002.

Takahashi, M., Osumi, N. (2005). Identification of a novel type II classical cadherin: Rat cadherin19 is expressed in the cranial ganglia and Schwann cell precursors during development. Dev. Dyn. *232*, 200–208.

Takano-Maruyama, M., Chen, Y., Gaufo, G.O. (2012). Differential contribution of Neurog1 and Neurog2 on the formation of cranial ganglia along the anterior-posterior axis. Dev. Dyn. *241*, 229–241.

Takeda, K., Yasumoto, K., Takada, R., Takada, S., Watanabe, K., Udono, T., Saito, H., Takahashi, K., Shibahara, S. (2000). Induction of melanocyte-specific microphthalmia-associated transcription factor by Wnt-3a. J. Biol. Chem. *275*, 14013–14016.

Taneyhill, L.A., Coles, E.G., Bronner-Fraser, M. (2007). Snail2 directly represses cadherin6B during epithelial-to-mesenchymal transitions of the neural crest. Development *134*, 1481–1490.

Teraoka, M.E., Paschaki, M., Muta, Y., Ladher, R.K. (2009). Rostral paraxial mesoderm regulates refinement of the eye field through the bone morphogenetic protein (BMP) pathway. Dev. Biol. *330*, 389–398.

Thawani, A., Groves, A.K. (2020). Building the border: Development of the chordate neural plate border region and its derivatives. Front. Physiol. 11, 608880.

Théveneau, E., Duband, J.-L., Altabef, M. (2007). Ets-1 confers cranial features on neural crest delamination. PLoS One *2*, e1142.

Theveneau, E., Marchant, L., Kuriyama, S., Gull, M., Moepps, B., Parsons, M., Mayor, R. (2010). Collective chemotaxis requires contact-dependent cell polarity. Dev. Cell *19*, 39–53.

Theveneau, E., Mayor, R. (2012). Neural crest delamination and migration: from epithelium-to-mesenchyme transition to collective cell migration. Dev. Biol. *366*, 34–54.

Theveneau, E., Steventon, B., Scarpa, E., Garcia, S., Trepat, X., Streit, A., Mayor, R. (2013). Chase-and-run between adjacent cell populations promotes directional collective migration. Nat. Cell Biol. *15*, 763–772.

Thiery, J.P., Duband, J.L., Delouvée, A. (1982). Pathways and mechanisms of avian trunk neural crest cell migration and localization. Dev. Biol. *93*, 324–343.

Thiery, J.P., Sleeman, J.P. (2006). Complex networks orchestrate epithelial-mesenchymal transitions. Nat. Rev. Mol. Cell Biol. *7*, 131–142.

Thomas, A.J., Erickson, C.A. (2009). FOXD3 regulates the lineage switch between neural crest-derived glial cells and pigment cells by repressing MITF through a non-canonical mechanism. Development *136*, 1849–1858.

Tosney, K.W. (2004). Long-distance cue from emerging dermis stimulates neural crest melanoblast migration. Dev. Dyn. *229*, 99–108.

Tosney, K.W. (1982). The segregation and early migration of cranial neural crest cells in the avian embryo. Dev. Biol. *89*, 13–24.

Trainor, P.A., Melton, K.R., Manzanares, M. (2003). Origins and plasticity of neural crest cells and their roles in jaw and craniofacial evolution. Int. J. Dev. Biol. *47*, 541–553.

Trainor, P.A., Tam, P.P. (1995). Cranial paraxial mesoderm and neural crest cells of the mouse embryo: Co-distribution in the craniofacial mesenchyme but distinct segregation in branchial arches. Development *121*, 2569–2582.

Urrutia, H.A., Stundl, J., Bronner, M.E. (2024). Tlx3 mediates neuronal differentiation and proper condensation of the developing trigeminal ganglion. Dev. Biol. *515*, 79–91.

Vallin, J., Thuret, R., Giacomello, E., Faraldo, M.M., Thiery, J.P., Broders, F. (2001). Cloning and characterization of three Xenopus slug promoters reveal direct regulation by Lef/beta-catenin signaling. J. Biol. Chem. *276*, 30350–30358.

Ventéo, S., Desiderio, S., Cabochette, P., Deslys, A., Carroll, P., Pattyn, A. (2019). Neurog2 deficiency uncovers a critical period of cell fate plasticity and vulnerability among neural-crest-derived somatosensory progenitors. Cell Rep. *29*, 2953-2960.e2.

Wang, H.U., Anderson, D.J. (1997). Eph family transmembrane ligands can mediate repulsive guidance of trunk neural crest migration and motor axon outgrowth. Neuron *18*, 383–396.

Wang, W.-D., Melville, D.B., Montero-Balaguer, M., Hatzopoulos, A.K., Knapik, E.W. (2011). Tfap2a and Foxd3 regulate early steps in the development of the neural crest progenitor population. Dev. Biol. *360*, 173–185.

Weston, J.A. (1963). A radioautographic analysis of the migration and localization of trunk neural crest cells in the chick. Dev. Biol. *6*, 279–310.

Weston, J.A., Butler, S.L. (1966). Temporal factors affecting localization of neural crest cells in the chicken embryo. Dev. Biol. *14*, 246–266.

Williams, R.M., Candido-Ferreira, I., Repapi, E., Gavriouchkina, D., Senanayake, U., Ling, I.T.C., Telenius, J., Taylor, S., Hughes, J., Sauka-Spengler, T. (2019). Reconstruction of the global neural crest gene regulatory network in vivo. Dev. Cell *51*, 255-276.e7.

Williams, R.M., Lukoseviciute, M., Sauka-Spengler, T., Bronner, M.E. (2022). Single-cell atlas of early chick development reveals gradual segregation of neural crest lineage from the neural plate border during neurulation. Elife *11*.

Wu, C.-Y., Hooper, R.M., Han, K., Taneyhill, L.A. (2014). Migratory neural crest cell αN-catenin impacts chick trigeminal ganglia formation. Dev. Biol. *392*, 295–307.

Wu, C.-Y., Taneyhill, L.A. (2019). Cadherin-7 mediates proper neural crest cell-placodal neuron interactions during trigeminal ganglion assembly. Genesis *57*, e23264.

Xu, H., Dude, C.M., Baker, C.V.H. (2008). Fine-grained fate maps for the ophthalmic and maxillomandibular trigeminal placodes in the chick embryo. Dev. Biol. *317*, 174–186.

Xu, Y., Lopes, C., Qian, Y., Liu, Y., Cheng, L., Goulding, M., Turner, E.E., Lima, D., Ma, Q. (2008). Tlx1 and Tlx3 coordinate specification of dorsal horn pain-modulatory peptidergic neurons. J. Neurosci. *28*, 4037–4046.

Yntema, C.L. (1944). Experiments on the origin of the sensory ganglia of the facial nerve in the chick. J. Comp. Neurol. *81*, 147–167.

Yook, J.I., Li, X.-Y., Ota, I., Hu, C., Kim, H.S., Kim, N.H., Cha, S.Y., Ryu, J.K., Choi, Y.J., Kim, J., Fearon, E.R., Weiss, S.J. (2006). A Wnt-Axin2-GSK3beta cascade regulates Snail1 activity in breast cancer cells. Nat. Cell Biol. *8*, 1398–1406.

York, J.R., McCauley, D.W. (2020). The origin and evolution of vertebrate neural crest cells. Open Biol. *10*, 190285.

Young, N.M., Hu, D., Lainoff, A.J., Smith, F.J., Diaz, R., Tucker, A.S., Trainor, P.A., Schneider, R.A., Hallgrímsson, B., Marcucio, R.S. (2014). Embryonic bauplans and the developmental origins of facial diversity and constraint. Development *141*, 1059–1063.

Yu, H.-H., Moens, C.B. (2005). Semaphorin signaling guides cranial neural crest cell migration in zebrafish. Dev. Biol. *280*, 373–385.

Zalc, A., Sinha, R., Gulati, G.S., Wesche, D.J., Daszczuk, P., Swigut, T., Weissman, I.L., Wysocka, J. (2021). Reactivation of the pluripotency program precedes formation of the cranial neural crest. Science *371*.

Zhu, Y., Li, X., Janairo, R.R.R., Kwong, G., Tsou, A.D., Chu, J.S., Wang, A., Yu, J., Wang, D., Li, S. (2019). Matrix stiffness modulates the differentiation of neural crest stem cells in vivo. J. Cell. Physiol. *234*, 7569–7578.

Chapter 3

Tlx3 regulates neuronal specification during trigeminal gangliogenesis

A modified version of this chapter was published as:

Urrutia, H.A., Stundl, J., Bronner, M.E. (2024). Tlx3 mediates neuronal differentiation and proper condensation of the developing trigeminal ganglion. *Dev. Biol*. *515*, 79–91.

https://doi.org/10.1016/j.ydbio.2024.07.005

3.1 Introduction

During development, formation of key structures within the vertebrate head such as cranial ganglia and sense organs requires coordinated migration and interactions between two distinct embryonic cell populations: the neural crest (NC) and the ectodermal placodes (Baker, 2006; Blentic et al., 2011; D'Amico-Martel, 1982; D'Amico-Martel and Noden, 1983; Hamburger, 1961; Jidigam and Gunhaga, 2013; Knecht and Bronner-Fraser, 2002; Le Douarin and Kalcheim, 1999; Saint--Jeannet and Moody, 2014; Shiau et al., 2008; Steventon et al., 2014; Theveneau et al., 2013). The cranial ganglia are important sensory components of the peripheral nervous system, responsible for relaying somatosensation from different sensory organs to the brain (Baker, 2006; Hamburger, 1961; Lwigale, 2001; Sanders, 2010; reviewed in Vermeiren et al., 2020).

The largest of the cranial ganglia, the trigeminal is arguably the best studied cranial ganglion due to its size, accessibility within the developing embryo, and dual NC and placodal origin (D'Amico-Martel and Noden, 1983; Hamburger, 1961; Moody and Heaton, 1983a, 1983b). The trigeminal ganglion consists of three sensory branches (ophthalmic, maxillary, and mandibular), which are comprised of sensory neurons, as well as motor axons, and glial cells (Fig. 3.1A) (Begbie and Graham, 2001; D'Amico-Martel and Noden, 1983; Hamburger, 1961; Moody and Heaton, 1983a, 1983b; Moody et al., 1989; Serbedzija et al., 1992). Previous studies have demonstrated that formation of the ganglion requires several discrete steps, during which NC and placode cells interact, aggregate, condense, and differentiate to generate the lobes of the trigeminal ganglion (Akitaya and Bronner-Fraser, 1992; D'Amico-Martel and Noden, 1983; Gammill et al., 2007; Hamburger, 1961; Saint-Jeannet and Moody, 2014; Schwarz et al., 2008; Shiau and Bronner-Fraser, 2009; Shiau et al., 2008; Steventon et al., 2014).

In the chick embryo, trigeminal placode cells begin ingression from the surface ectoderm at Hamburger-Hamilton (HH)11–12 (D'Amico-Martel and Noden, 1983;

Hamburger and Hamilton, 1951). Placode cells then intermix with migrating NC cells, which initiate migration at HH9 (D'Amico-Martel and Noden, 1983; McCabe et al., 2009; Shiau et al., 2008). At the time of ingression, the placode cells already express neuronal markers before becoming post-mitotic (Begbie et al., 2002; Moody et al., 1989; Shiau et al., 2008). Differentiation of post-mitotic placode-derived neurons is first observed as HH16, as both NC and placodal cells condense to form the ophthalmic lobe of the trigeminal ganglion (d'Amico-Martel and Noden, 1980). Newly born neurons are positioned in the most distal region of both the ophthalmic and maxillo-mandibular lobes (Fig. 3.1A) (Begbie and Graham, 2001; D'Amico-Martel and Noden, 1983; Noden, 1978; Shiau et al., 2008). Additionally, NC cells contribute to the satellite glial cells that are distributed throughout the ganglia and Schwann cells along the nerve roots (D'Amico-Martel and Noden, 1983; Hamburger, 1961; Moody et al., 1989; Noden, 1975). Only later in development (~HH20-HH24) do NC cells begin to differentiate into sensory neurons within the proximal portion of the trigeminal ganglion (Fig. 3.1A) (Covell and Noden, 1989; d'Amico-Martel and Noden, 1980; Shiau et al., 2008).

Cellular and molecular crosstalk between NC and placode cells is known to be involved in trigeminal ganglion formation. In particular, tissue ablation experiments of either of these cell populations in chick embryos results in severe abnormalities of the trigeminal ganglion, demonstrating that NC-placode interactions are required for its proper formation and organization (D'Amico-Martel and Noden, 1983; Gammill et al., 2007; Hamburger, 1961; Lwigale, 2001; Moody and Heaton, 1983a, 1983b; Schwarz et al., 2008; Shiau and Bronner-Fraser, 2009; Shiau et al., 2008). At a molecular level, numerous adhesion and signaling molecules have been implicated in trigeminal ganglion formation, including N-cadherin in placodal cells, Cadherin-7 in NC cells, Neuropilin-2/Semaphorin-3F signaling in NC cells, and Slit1/Robo2 signaling between NC and placodal cells (Freter et al., 2013; Gammill et al., 2007; Shiau and Bronner-Fraser, 2009; Shiau et al., 2008; Theveneau et al., 2013; Wu et al., 2014). NC cells may function as "scaffolds", generating "corridors", and enabling

placode cells to integrate within the ganglion, while placode cells aid in the condensation of NC cells (Freter et al., 2013; Theveneau et al., 2013).

One transcription factor implicated in differentiation and fate specification of excitatory sensory neurons in both the central and peripheral nervous systems is the T-cell leukemia homeobox 3 (*Tlx3*) transcription factor, previously known as Hox11L2/Rnx (Cheng et al., 2004; Divya et al., 2016; Guo et al., 2012; Hornbruch et al., 2005; Kondo et al., 2008, 2011; Langenau et al., 2002; Logan et al., 1998, 2002; Monteiro et al., 2021; Shimomura et al., 2015; Uchiyama et al., 1999; Xu et al., 2008a). In the chick peripheral nervous system (PNS), *Tlx3* is expressed at HH15 in overlapping domains in placodally derived components of the trigeminal ganglion, serving as a post-mitotic selector gene that determines excitatory sensory neuronal fate (Cheng et al., 2004; Kondo et al., 2008; Logan et al., 1998). *Tlx3* also is expressed in dorsal root ganglia, sympathetic ganglia and enteric ganglia which arise from vagal and trunk neural crest cells (Kondo et al., 2008; Langenau et al., 2002; Logan et al., 1998; Shimomura et al., 2015). In the developing central nervous system (CNS), expression of *Tlx3* is present in two parallel bilateral stripes of neurons traveling rostrocaudally within the hindbrain and spinal cord, suggesting that this gene may also be involved in the development of neuronal circuitry (Cheng et al., 2004; Divya et al., 2016; Guo et al., 2012; Hornbruch et al., 2005; Logan et al., 2002; Monteiro et al., 2021). Notably, loss-of-function analysis in mice has revealed abnormalities in the ventral medulla and sensory neurons within the dorsal spinal cord and brainstem (Divya et al., 2016; Guo et al., 2012; Kondo et al., 2008; Qian et al., 2001).

Despite current understanding of the role of *Tlx3* in specification of sensory neurons within the PNS and CNS, little is known about whether its expression and function are limited to placode-derived neurons within the trigeminal ganglion or is a shared property of both the placode and neural crest components of the ganglion. Here we show that, in the chick embryo, *Tlx3* is expressed by NC cells and required for proper ganglion development. Moreover, ectopic expression of *Tlx3* leads to premature expression of neural markers, while its depletion results in improper

condensation and size reduction of the ganglion. Taken together, our data suggest that *Tlx3* is necessary for specification of neural crest- and placode-derived sensory neurons during development of the trigeminal ganglion.

3.2 Results

3.2.1 Both neural crest and placodal cells express Tlx3 within the developing trigeminal ganglion

Tlx3 expression was previously shown to be expressed in placodally- derived cells within the trigeminal ganglion and in NC cells of the dorsal root ganglion (Logan et al., 1998). To further characterize its spatiotemporal expression pattern during multiple stages of cranial neural crest and placode development, we performed whole-mount *in situ* hybridization. Whereas no *Tlx3* expression was detectable in either pre-migratory (HH9) or migratory (HH10) neural crest cells (Fig. 3.1B–C), expression was first detected in placode cells within the ophthalmic lobe of the trigeminal ganglion at HH14 (Fig. 3.1D). Additionally, expression of *Tlx3* was present in the central nervous system, particularly in the dorsolateral portions of the hindbrain, consistent with previous findings (Logan et al., 1998). *Tlx3* expression remained evident in the ophthalmic lobe of the developing trigeminal ganglion at HH16 (Fig. 3.1E). Although its expression was initially restricted to the ophthalmic lobe, expression of *Tlx3* extended into the maxillo-mandibular lobe of the trigeminal ganglion by HH17 (Fig. 3.1F). *Tlx3* expression was evident throughout both lobes of the ganglion by HH18, and its expression persisted as the embryo developed to later stages (Fig. 3.1G and Figs. S3.1A–B).

To better define *Tlx3* expression in the NC-derived components of the developing trigeminal ganglion, we examined transverse sections through the head of chick embryos at stages HH16, HH20, and HH22 and compared expression patterns between NC markers, such as SOX10 and HNK1, and TLX3 (Fig. 3.1A’-C′). SOX10,

a pan-neural crest marker, is an important member of the NC gene regulatory network, and crucial for proper specification, migration, and differentiation of NC cells into

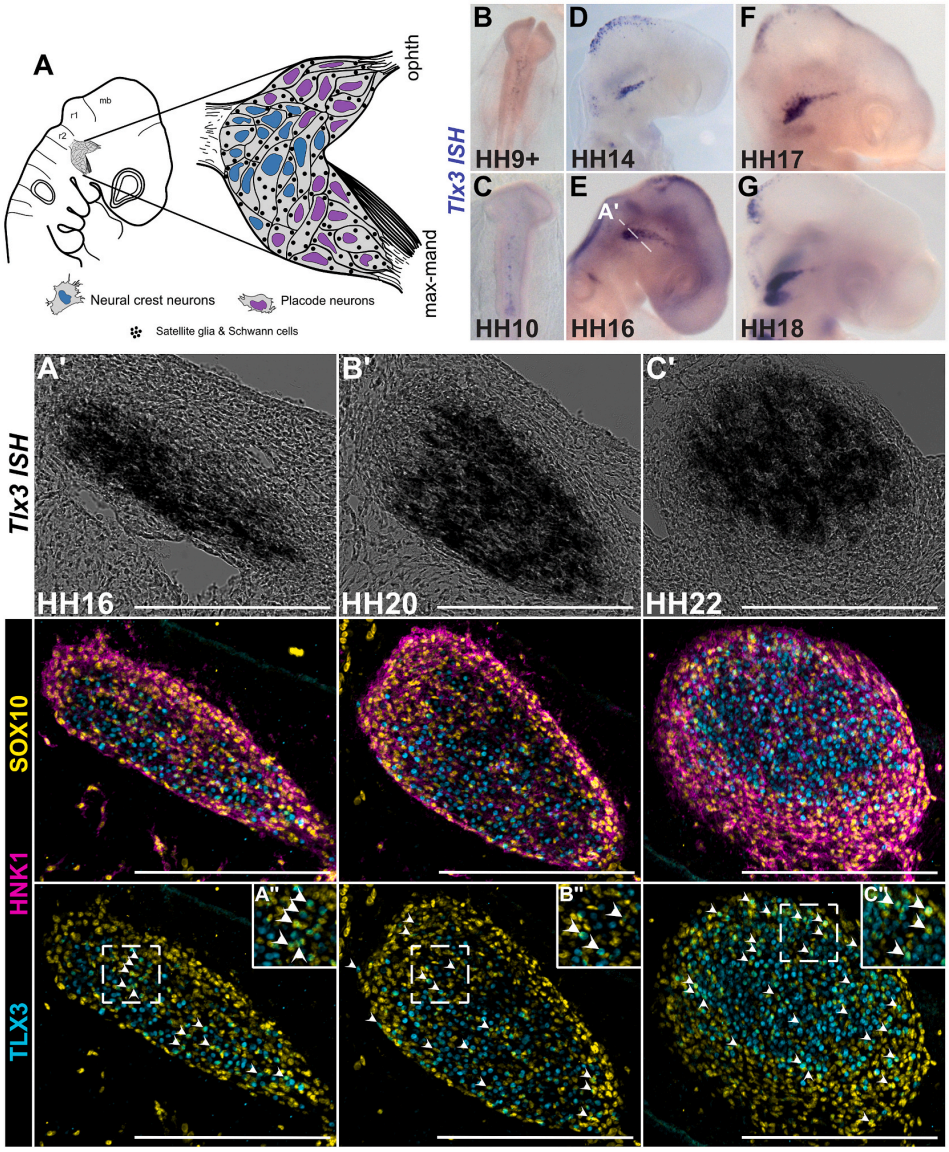

Fig. 3.1. *Tlx3* is expressed in cranial neural crest within the trigeminal ganglion. A. Schematic illustrating the trigeminal ganglion and associated cell types in a HH16 chick embryo. B-G. Representative images of chromogenic whole mount in situ hybridization for *Tlx3* in stage HH9+(B), HH10 (C), HH14 (D), HH16 (E), HH17 (F), HH18 (G) chick embryos. Dashed lines in E indicate cross section shown in A'. A′-C'. Representative transverse sections of chromogenic in situ hybridization for *Tlx3* and immunolabeling for SOX10 (yellow), HNK1 (magenta), and TLX3 (cyan) at stage HH16 (D), HH20 (Sup Fig.3.1A), and HH22 (Sup Fig. 3.1B) in stage-matched embryos. Dashed boxes in A′-C′ indicate zoomed areas in A″-C'' (inset). Immunolabeling for SOX10 (yellow) and TLX3 (cyan) reveals TLX3 expression in a subset of SOX10+neural crest cells, revealing overlapping domains of expression (filled arrows). Mb, midbrain; r1, rhombomere 1; r2, rhombomere 2; ophth, ophthalmic; max-mand, maxillo-mandibular. Scale bars represent 200 µm (A′-C′).

neurons and glia of the peripheral nervous system (reviewed in Martik and Bronner, 2017; Simoes-Costa and Bronner, 2015). HNK1 labels migratory NC cells that have delaminated from the neural tube and is maintained during migration and formation of ganglionic structures (Bronner-Fraser, 1986). Interestingly, transverse sections through HH16, HH20, and HH22 embryos revealed *Tlx3* expression in domains that overlapped with expression of both SOX10 and HNK1 (Fig. 3.1A'-C′). Additionally, immunohistochemical analysis at all three stages revealed TLX3 expression in SOX10+/HNK1+ NC cells (Fig. 3.1A'-C′ and Fig. S3.2A'-C′, filled arrowheads).

To perform direct lineage labeling of neural crest cells, we injected the fluorescent dye, cell tracker CM-DiI, into the lumen of the neural tube of HH9 chick embryos such that solution filled the neural tube from the posterior hindbrain to the level of the forebrain (Fig. 3.2A). We then allowed the injected embryos to develop and collected them 1-day post-injection (Fig. 3.2B). DiI-labeling of cranial migratory NC cells was clearly evident throughout the head, as visualized by whole mount imaging at HH16 (Fig. 3.2B). We then generated transverse 16-µm sections from the most rostral region of the head through the first pharyngeal arch, which were subsequently processed for *in situ* Hybridization Chain Reaction (HCR). At this time point, we observed a few *Tlx3* transcripts in NC cells that were not only DiI positive, but also expressing *Sox10* transcripts (Fig. 3.2C and Figs. S3.3A–C). We then repeated the *in situ* HCR at stage HH20 and observed numerous cells that contained *Tlx3* transcripts, some of which had both *Tlx3* and *Sox10* transcripts within the lobes of the developing trigeminal ganglion (Fig. 3.2D-D'). These results show that expression of *Tlx3* is not restricted to placode cells in the developing ganglion but is also enriched a subset of cranial NC-derived cells.

3.2.2 Ectopic Tlx3 expression in migrating neural crest cells delays emigration and results in premature expression of neural markers

Intriguingly, the onset of *Tlx3* expression in neural crest-derived cells occurs at HH16, correlating with onset of neurogenesis of excitatory sensory neurons. Accordingly, we next asked if ectopic expression of *Tlx3* would affect cranial NC migration and/or differentiation. To this end, we subcloned the full-length coding sequence of chick *Tlx3* with a C-terminal FLAG epitope into an expression vector under the control of a chick *Sox10* enhancer construct (Sox10E99) (Williams et al., 2019) which drives expression specifically in migratory cranial NC cells and also

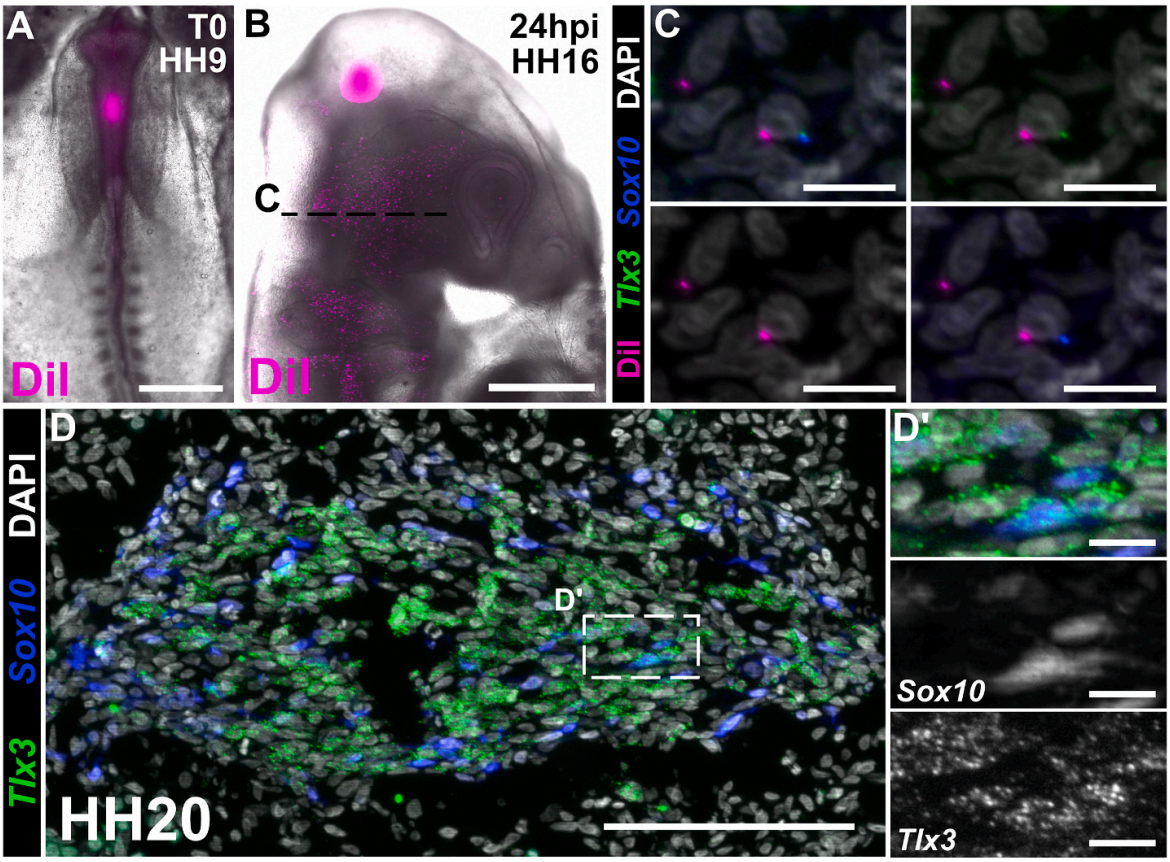

Fig. 3.2. Expression of *Tlx3* is enriched in a subset of cranial neural crest cells. A. Representative image of a whole mount HH9 DiI-labeled (magenta) chick embryo immediately post-injection (T0). B. Representative image of a whole mount HH16 chick embryo, 1 day post-injection (24hpi), revealing ample DiI-labeled (magenta) migratory cranial neural crest within the trigeminal ganglion. Dashed line in B indicates cross section shown in C. C. Hybridization chain reaction (HCR) reveals expression of *Tlx3* (green) transcripts in cells that are also DiI-labeled (magenta) and express *Sox10* (blue) transcripts. D. HCR analysis reveals co-expression of *Tlx3* (green) and *Sox10* (blue) within the developing trigeminal ganglion. Dashed box in D indicates zoomed area in D'. hpi, hours post-injection. Scale bars represent 500μm (A–B), 100 μm (D) and 10 μm (C and D′).

contains a downstream internal ribosome entry site (IRES)-driven nuclear eGFP for lineage tracing (Fig. 3.3B) (Betancur et al., 2010). Electroporation of this construct (Tlx3-FLAG) on the right side of gastrula stage HH4 chick embryos produced nuclear-localized FLAG immunolabeling, consistent with expected TLX3 localization and nuclear GFP expression; indicating successful protein expression specifically in migratory NC cells (Fig. 3.3A and C). The left side of the same embryo served as an

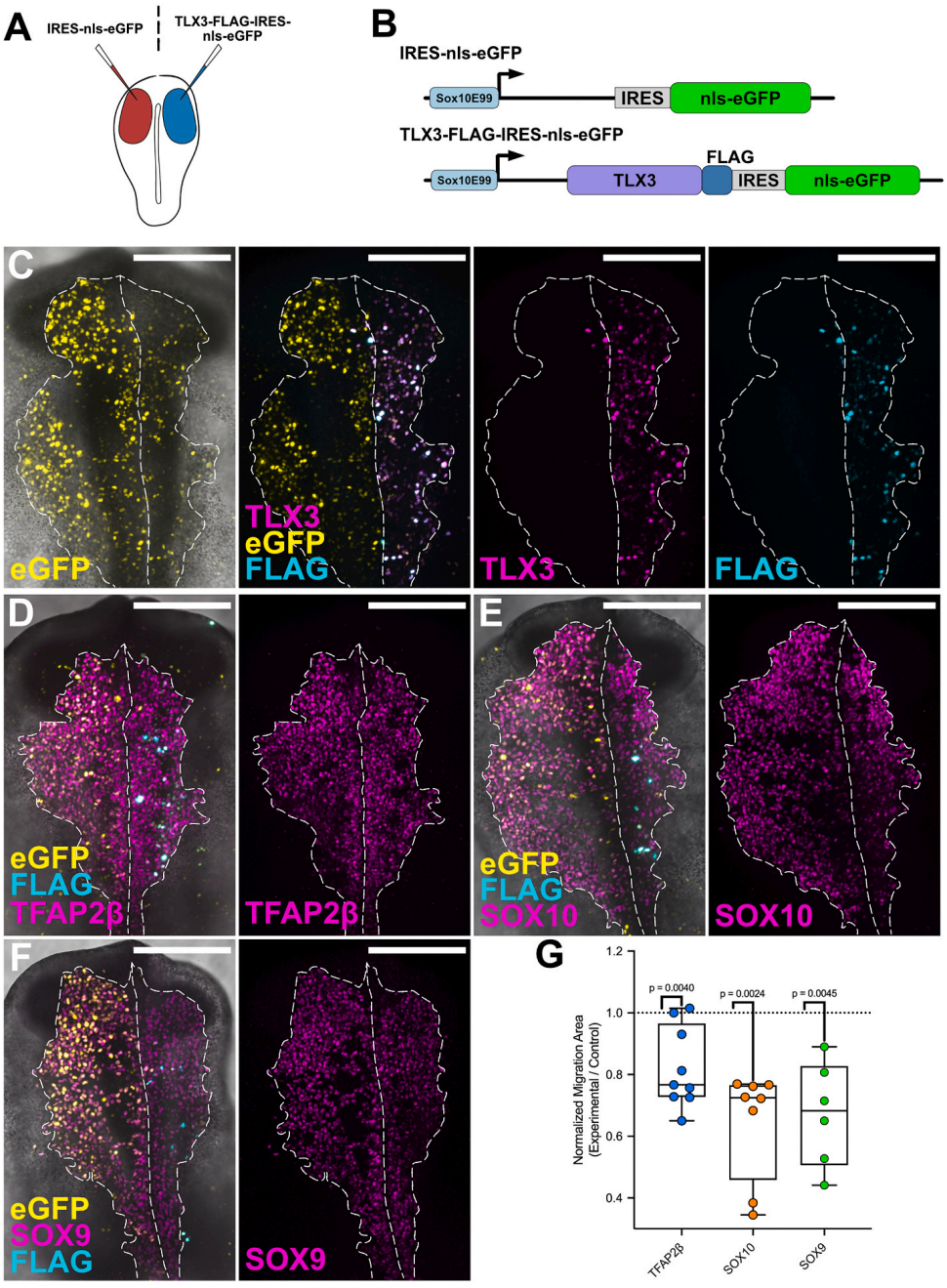

Fig. 3.3. Ectopic expression of *Tlx3* delays cranial neural crest emigration. A. Schematic representing the *ex ovo* experimental design to test the role of *Tlx3* in migratory cranial neural crest cells. Control (red) and experimental (blue) reagents were delivered bilaterally into HH4 chick embryos B. Schematic diagram of expression constructs used in this study. TLX3- FLAG (below) carries pTK-Sox10E99-mediated expression of a full length TLX3 protein tagged with a C-terminal FLAG epitope, followed by an internal ribosome entry site (IRES)-driven nuclear eGFP. IRES-nuclear-eGFP (above) serves as a control and is identical to the TLX3-FLAG construct without the TLX3-FLAG coding sequence (nls, nuclear localization signal). C–F. Gastrulating HH4 chick embryos were bilaterally electroporated with control IRES-nls-eGFP on the left side and TLX3-FLAG on the right side. C. Embryos were immunolabeled to display eGFP (yellow), FLAG (cyan), and TLX3 (magenta) expression at stage HH10. D-F. Immunohistochemistry for eGFP (yellow), FLAG (cyan), and TFAP2β/SOX10/SOX9 (magenta) reveals the effects of early migratory neural crest at HH10. G. Box and whisker quantitation of relative TLX3+neural crest migration normalized to electroporated control. Presented are ratios of normalized experimental migration distance divided by control migration distance. Each point represents an individual embryo (TFAP2β, n =9; SOX10, n =8; SOX9, n =6), and the p-value was determined by two-tailed, paired t-test. Scale bars represent 200 μm.

internal control and was electroporated with an equal concentration of a construct encoding only nuclear eGFP (Fig. 3.3A–C).

To assess the effect of ectopic *Tlx3* expression on cranial NC migration, embryos were allowed to develop to HH10 and screened for electroporation efficiency by eGFP expression. To assay effects of cranial NC migration, embryos were immunolabeled with antibodies against TFAP2β, SOX10, and SOX9, all markers of delaminating and early migrating NC cells (Fig. 3.3D–F). We also measured the relative distances that NC cells had migrated from the dorsal midline, compared to the contralateral control side of the same embryo. The results show that ectopic expression of *Tlx3* resulted in a notable reduction in NC migration area (Fig. 3.3G), suggesting that early expression of this gene interferes with migration. At HH10, no expression of neural markers, such as HuC/D, was evident (Fig. 3.4A).

To test whether ectopic *Tlx3* may affect initiation of NC migration, we next examined the expression of Cadherin-6B, down-regulation of which is critical for neural crest delamination from the neural tube (Dady et al., 2012; Rogers et al., 2013; Strobl-Mazzulla and Bronner, 2012; Taneyhill et al., 2007). By immunohistochemistry, we found a slight increase of Cadherin-6B in the dorsal neural tube at pre-migratory stages after ectopic expression of *Tlx3* (Fig. 4.4B), which may

account for the subsequent decrease in migration distance. In contrast, E-cadherin and N-cadherin appeared unchanged (Fig. 4.4C). Taken together, these data suggest that ectopic *Tlx3* expression may partially interfere with neural crest emigration, resulting in reduction in the distance migrated.

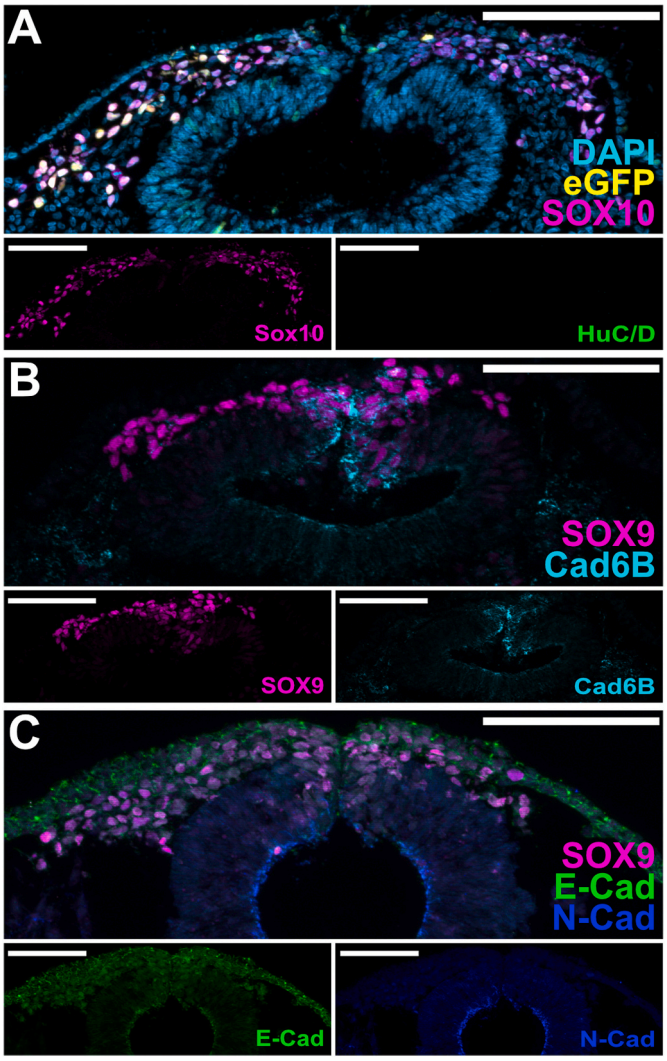

Fig. 3.4. Early ectopic expression of *Tlx3* affects initiation of cranial neural crest emigration. A-C. Representative transverse sections of embryos in Fig. 3. A. Immunolabeling for SOX10 (magenta) and HuC/D (green) reveals that ectopically expressing Tlx3 on the right side reduces neural crest migration compared to the left control side; no expression of HuC/D was detected at this stage. B. Immunohistochemistry reveals a slight increase in Cad6B (cyan) expression on the *Tlx3* overexpressing side, while a decrease was observed in SOX9+ (magenta) cells that failed to delaminate from the neural tube. C. Immuno-labeling of E-Cad (green) and N-Cad (blue) did not show a change in their expression upon ectopic expression of *Tlx3*. Cad6B, Cadherin-6B; E-Cad, E-Cadherin; N-Cad, N-Cadherin. Scale bars represent 100 μm

Differentiation of neural crest-derived sensory neurons in the trigeminal ganglion normally occurs at HH20. To test if ectopic expression of *Tlx3* promotes premature neurogenesis, we unilaterally electroporated HH8-9 (5 somites) embryos *in ovo* (Fig. 3.5A) and allowed embryos to develop to HH13. We screened for successful electroporation by eGFP expression (Fig. 3.5C, filled arrowheads) and immunolabeled for HuC/D expression, a pan-neuronal marker. Interestingly, we found that overexpression of *Tlx3* resulted in premature expression of

this neuronal marker only in electroporated neural crest cells, compared to the unelectroporated contralateral control side of the same embryo (compare Fig. 3.5B and C). Transverse sections through these embryos were immunolabeled for SOX10 to label NC cells and ISLET1 for placodal cells. The results revealed abundant HuC/D expression in SOX10 positive NC cells that ectopically expressed *Tlx3*, but not on the

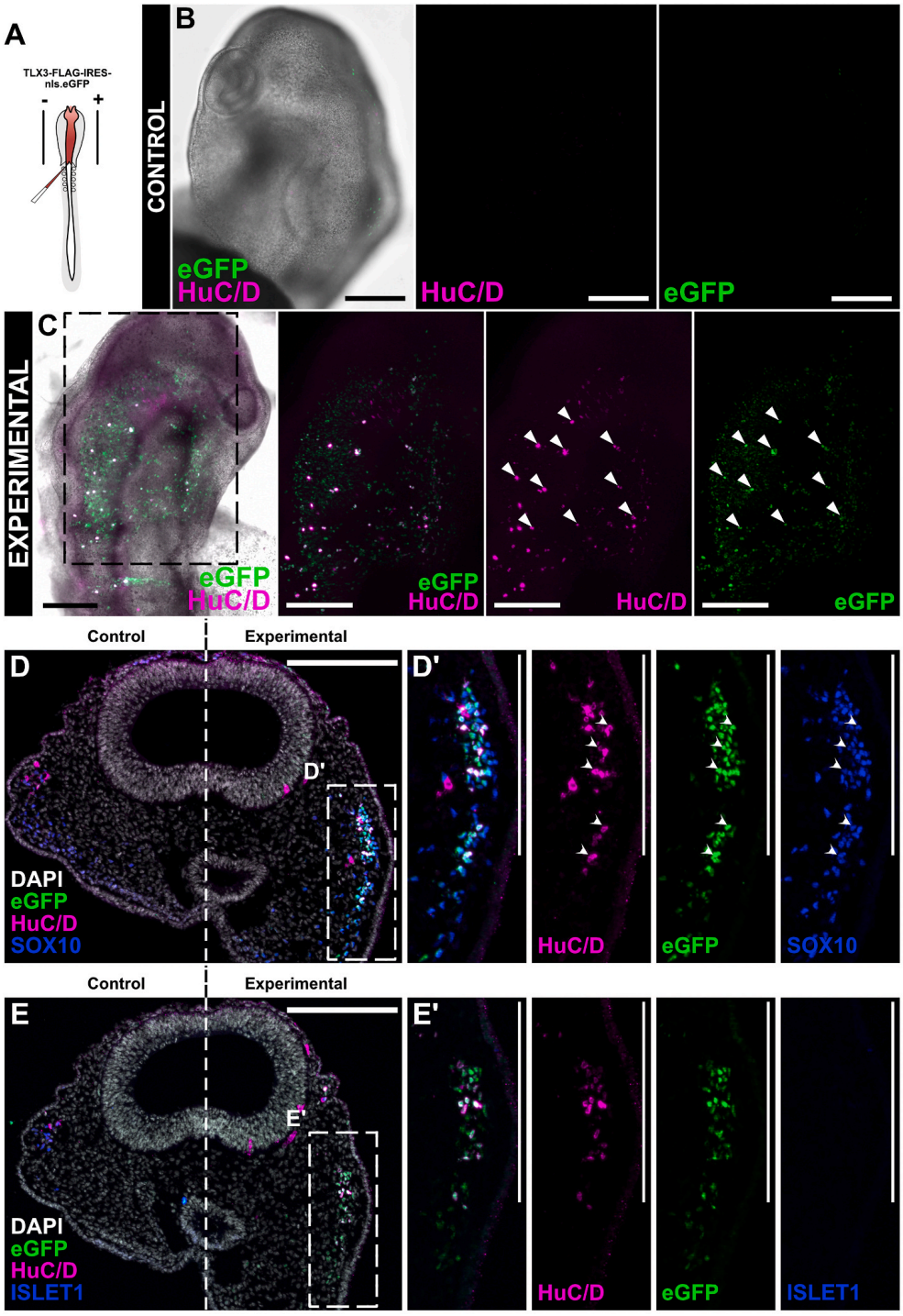

Fig. 3.5. Ectopic expression of *Tlx3* results in premature expression of neural markers at HH13. A. Schematic illustrating in ovo electroporation of experimental (red) reagents that were delivered unilaterally into HH8+(5 somites) chick embryos, in order to ectopically express *Tlx3* by specifically targeting neural crest cells. B–C. Embryos were unilaterally electroporated at HH8+, allowed to develop to HH13, and immunolabeled for HuC/D (magenta) and eGFP (green) expression (n=10) B. The non-electroporated control side of embryo displays no expression of HuC/D in the neural crest-derived cells at HH13. C. Immunolabeling for HuC/D (magenta) expression on the electroporated side of the embryo reveals premature expression of this neuronal marker in electroporated neural crest cells (closed arrowheads). Dashed box in C indicates zoomed area. D-E. Representative transverse sections of unilaterally electroporated embryos in (A–B). D. Immunolabeling for HuC/D (magenta) and SOX10 (blue) reveals HuC/D expression in SOX10+/TLX3+neural crest cells. E. Representative transverse sections of embryos unilaterally electroporated, immunolabeled for HuC/D (magenta) and ISLET1 (blue), reveals fewer ISLET1+/HuC/D+cells compared to SOX10+/HuC/D+(D) neural crest cells. D′-E'. Dashed boxes in C-D indicate zoomed in areas in C′-D'. Merged and Individual channel for HuC/D (magenta), eGFP (green), and SOX10 (D′)/ISLET1 (E′) (blue). Solid arrowheads indicate co-expression of HuC/D+/SOX10+neural crest cells. Scales bars represent 200 μm.

contralateral control side of the same embryo (Fig. 3.5D–E and Fig. 3.5D'-E′). ISLET1+/HuC/D+ placodal cells were observed on both sides of the embryos. These placode cells did not receive ectopic *Tlx3* but rather turn on neural markers even prior to ingression. However, their numbers were far fewer than the SOX10+/HuC/D +NC cells that ectopically expressed *Tlx3* (compare Fig. 3.5D-D′ and Fig. 3.5E-E′). In contrast to *Tlx3* over-expression, no SOX10+/HuC/D+ NC cells were observed after unilateral *in ovo* injection of a construct encoding nuclear eGFP alone (Fig. S3.4A-B′). These results suggest that ectopic *Tlx3* expression is sufficient to induce expression of neuronal marker, thus prematurely driving NC cells towards a neural fate.

3.2.3 Knock-down of *Tlx3* disrupts trigeminal ganglion development

To test whether expression of *Tlx3* is necessary for neurogenesis during ganglion development, we performed loss of function experiments by knocking down *Tlx3* using an antisense morpholino oligo (MO)-mediated approach. To this end, we first performed bilateral HH4 electroporation with our control or translation-blocking *Tlx3* specific MO (Fig. S3.5A). Electroporating these MOs into gastrula stage embryos results in loss of *Tlx3* in both NC and placodal populations. After culturing the embryos ex ovo until HH9 and HH10 to capture pre-migratory and migratory cranial

neural crest cells, respectively, we processed them for immunohistochemistry. Antibody staining for PAX7 revealed no notable migratory defects on the right experimental side, when compared to the left control side of the embryo (Figs. S3.5B–C). We then performed unilateral HH4 electroporation, with either our control MO or *Tlx3* MO, to determine if loss of *Tlx3* would affect neurogenesis during ganglion development (Fig. 3.6A). Following unilateral electroporation, these embryos were developed to ~HH16 and processed for immunolabeling. *Tlx3* knockdown resulted in an overall reduction in the expression of TLX3, within the ophthalmic lobe of the forming ganglion, when compared to the untreated contralateral control side (compare Fig. S3.6A' and Fig. S3.6B'). Expression of *Tlx3* only within the ophthalmic lobe at this particular stage is consistent with our whole-mount *in situ* hybridization results and previous findings (Logan et al., 1998). To further parse whether this affected the neural crest-derived component of the ganglion, we examined expression of SOX10 and observed a reduction in both the abundance of SOX10+ NC cells and in the overall size of the developing ganglion (compare Fig. S3.6A and Fig. S3.6B), that was statistically significant (Fig. 3.6L, lane 1). These results demonstrate that loss of *Tlx3* affects proper condensation and development of the trigeminal ganglion. Furthermore, global knockdown of *Tlx3* caused not only reduction of the ophthalmic lobe, but also resulted in failure of fusion between the ophthalmic and maxillo-mandibular lobe, compared to both the contralateral control side and control MO embryos (compare Fig. 3.6B', Fig. 3.6C and C′). We also observed a reduction in TUJ1 expression, which labels differentiating neurons, when compared to both control MO and untreated contralateral control sides (compare Fig. 3.6B', Fig. 3.6C and C'). These results suggest that loss of *Tlx3* not only affects neurogenesis but also proper gangliogenesis.

As a second method to knocking down *Tlx3*, we used our previously described single-CRISPR/Cas9 construct to genetically deplete this gene within the developing ganglion (Gandhi et al., 2021). To this end, we designed guide RNAs (gRNAs) targeting the coding sequence of *Tlx3* and unilaterally electroporated either control or *Tlx3* specific gRNA-CRISPR/Cas9 construct into HH4 embryos (Fig. 3.6A). These embryos were developed to ~HH16 and subsequently processed for immunolabeling.

Similar to MO-mediated knockdowns at later stages, CRISPR/Cas9 induced loss of *Tlx3* resulted in decreased expression of TLX3 within the ophthalmic lobe of the developing ganglion, compared to the contralateral control side (compare Fig. S3.6C' and Fig. S3.6D'). Additionally, *Tlx3* knockout resulted in a significant reduction in the abundance of SOX10+ cells, similar to effects noted with *Tlx3* MO knockdowns (compare Fig. S3.6C and Fig. S3.6D). We next looked at TUJ1 expression and, similarly to MO knockdowns, noted a significant reduction in its expression, when compared to both the contralateral control and control gRNA embryos (compare Fig. 3.6D', Fig. 3.6E and E'), with a statistically significant reduction in the overall size of the ganglion (Fig. 3.6L, lane 4). Interestingly, while CRISPR/Cas9-mediated loss of *Tlx3* resulted in a more penetrant phenotype, with complete loss of the ophthalmic lobe, MO-mediated loss of *Tlx3* caused a more notable overall size reduction of the trigeminal ganglion as a whole (Fig. 3.6L, compare lane 1 and lane 4). These differences are likely due to differences in timing of depletion of *Tlx3*. While CRISPR/Cas9 gives a penetrant phenotype through gene loss, it requires additional time to accumulate and produce mutations at desired sites within the genome. In contrast, translation blocking morpholinos immediately block mRNA translation of desired target genes, thus rapidly producing a phenotype but the tissue can sometimes compensate since there is no gene loss. Given that both approaches give similar phenotypes with subtle differences, the collective results suggest that *Tlx3* is necessary for neurogenesis and plays a vital role in the development of the trigeminal ganglion.

While global Tlx3 knock-down/knock-out clearly affects trigeminal ganglion formation, the above results cannot distinguish between the role of *Tlx3* in placodal versus neural crest portions of the trigeminal ganglion. To parse the individual contributions of each cell population, we next individually targeted NC or placode cells. To this end, we performed unilateral *in ovo* electroporation into either the neural tube (for neural crest specific knockout) or ectoderm (for placodal knockout) with either our *Tlx3* MO or *Tlx3*-gRNA-single-CRISPR/Cas9 constructs at HH8-9 (5 somites) for neural crest and HH12 (15 somites) for ectodermal electroporations (Fig.

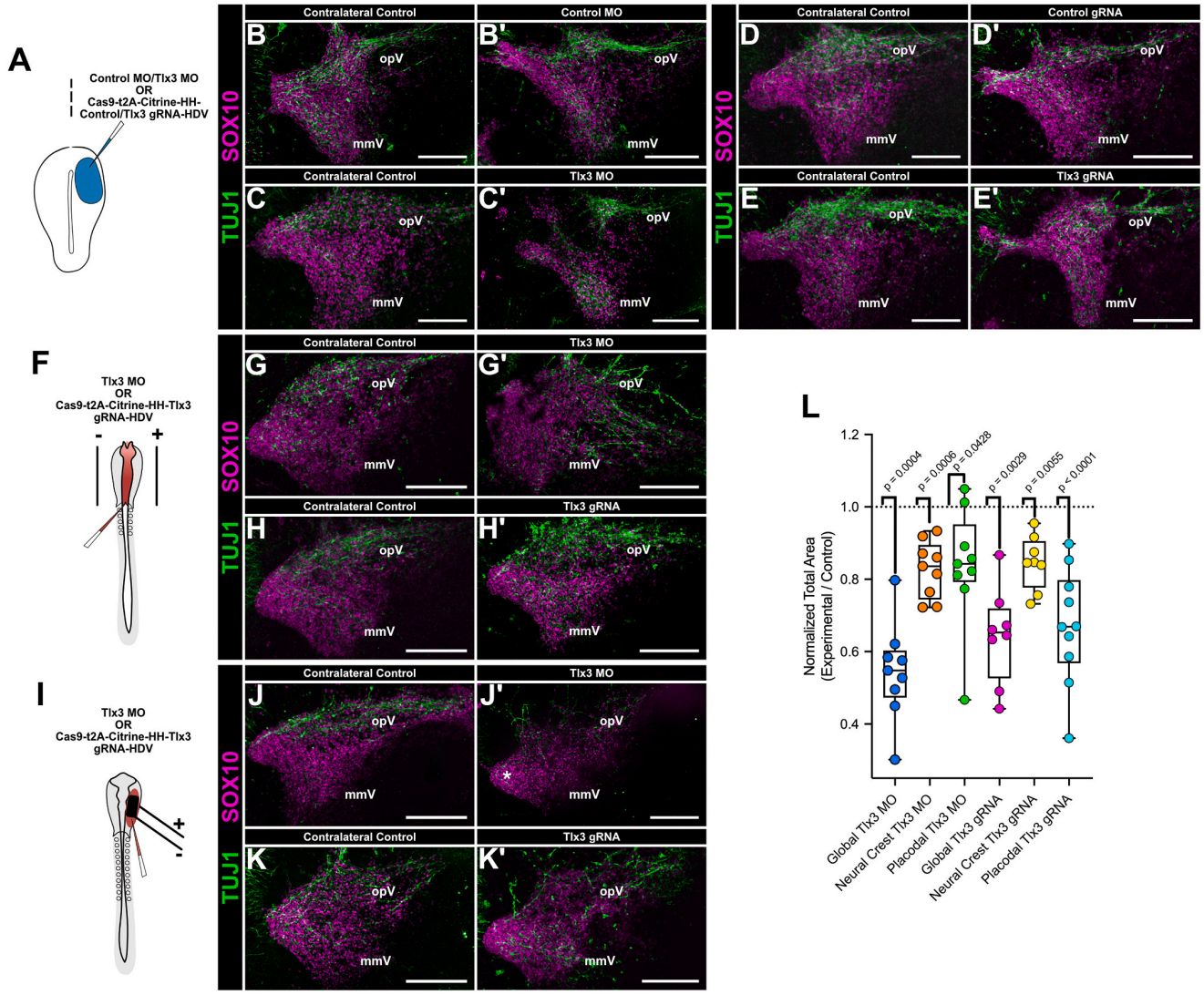

Fig. 3.6. Perturbation of *Tlx3* disrupts trigeminal ganglion development. A. Schematic diagram illustrating the *ex ovo* electroporation to test the effects of perturbing *Tlx3*. Control or experimental (blue) reagents were delivered unilaterally into gastrulating HH4 chick embryos. B-E'. Either control MO/*Tlx3* MO or control/*Tlx3* specific gRNA-CRISPR/Cas9 constructs were unilaterally electroporated on the right side of the embryo. B-E'. Immunohistochemistry for SOX10 (magenta) and TUJ1 (green) reveals the effects of global loss of *Tlx3* via MO or CRISPR/Ca9-mediated approach at HH16. F. Schematic illustrating in ovo electroporation of control or experimental (red) reagents were delivered unilaterally into HH8+(5 somites) chick embryos, in order to perturb *Tlx3* by specifically targeting neural crest cells. G-H'. Either a *Tlx3* MO or *Tlx3* specific gRNA-CRISPR/Cas9 constructs were introduced onto the right side of the embryo. Immunolabeling of SOX10 (magenta) and TUJ1 (green) reveals the effects of loss of *Tlx3* in neural crest cells at HH16. I. Schematic illustrating the *in ovo* experimental design to perturb *Tlx3*, specifically targeting placode cells. Control or experimental (red) reagents were delivered unilaterally into the ectoderm of HH12 (15 somites) chick embryos. J-K'. Either a *Tlx3* MO or *Tlx3* specific gRNA-CRISPR/Cas9 constructs were unilaterally electroporated on the right side of the embryo. Immunohistochemistry for SOX10 (magenta) and TUJ1 (green) reveals the effects of loss of *Tlx3*, specifically in placode cells at HH16. L. Box and whisker quantitation of relative trigeminal ganglion size normalized to contralateral control. Ratios represent normalized experimental area divided by contralateral control area. Each point represents an individual embryo (Global *Tlx3* MO, n =9; Neural crest *Tlx3* MO, n =9; Placode *Tlx3* MO, n=9; Global *Tlx3*, n =8; Neural crest *Tlx3* gRNA, n =8; Placode *Tlx3* gRNA, n =10), and the p-value was determined by two-tailed, paired t-test. Scale bars represent 200 μm.

3.6F and I, respectively). Following electroporations, these embryos were developed to ~HH16 and were subsequently processed for immunolabeling.

Morpholino-mediated knockdown of *Tlx3* in the NC resulted in ganglia that failed to properly condense and form a bi-lobed structure, compared to the contralateral control side where a bi-lobed ganglion is clearly evident (compare Fig. 3.6G and G′). Interestingly, this phenotype differed when compared to the global knockdown of *Tlx3* (compare Fig. 3.6C' and Fig. 3.6G'). Rather than an overall size reduction within two separate lobes, we mainly observed ganglia that had more dispersed SOX10+ NC and TUJ1+ placode cells. Additionally, while the ganglia failed to properly condense, the relative expression of SOX10 and TUJ1 appeared unchanged. This suggests that loss of *Tlx3* in the neural crest may not alter gene expression or affect NC migration, but rather may prevent the transition from an undifferentiated neural progenitor state to a post-mitotic sensory neuron precursor. Quantification revealed statistically significant differences in the total area of the trigeminal ganglion depending on the method of knock-down (Fig. 3.6L). Next, we examined the effects of *Tlx3* perturbation via our CRISPR/Cas9-mediated method, specifically targeting only the NC population (Fig. 3.6F). *Tlx3* loss of function in the NC population had a slightly different outcome, resulting in TUJ1 expression that was far more concentrated and fewer SOX10+ NC cells in the ophthalmic lobe of the ganglion, when compared to the contralateral control side (compare Fig. 3.6H and H′), suggesting that perturbing *Tlx3* reduced the number of SOX10+ NC cells but did not result in the entire loss of the lobe. Additionally, we examined the expression of NEUROG2 and NEUROD1, proneural genes expressed within the developing trigeminal ganglion, after loss of *Tlx3* within the NC population (Abu-Elmagd et al., 2001; Xu et al., 2008b; Zirlinger et al., 2002). Interestingly, we observed a reduction in the expression of these two genes within the developing ganglion (compare Fig. S3.7A and Fig. S3.7A'; compare Fig. S3.7B and Fig. S3.7B'). Intrigued by these findings, we hypothesized that while there may have been a reduction in the abundance of NC cells, formation of ophthalmic lobe was not entirely lost due to the placodal portion of the ganglion compensating and directing the remaining NC cells to the

ophthalmic lobe of the ganglion. Furthermore, loss of *Tlx3* also effected the expression of NEUROG2 and NEUROD1, further suggesting that *Tlx3* may influence proneural gene expression and specification within the ganglion. Quantification revealed that *Tlx3* loss of function in the NC did indeed result in a notable statistically significant phenotype (Fig. 3.6L, lane 5). Collectively, these results show that loss of *Tlx3* within the NC population impacts the development and proper formation of the trigeminal ganglion.

To further examine the individual contribution of each population within the trigeminal ganglion, we next examined the effects of knocking down *Tlx3* in the placodal population via our MO-mediated approach. Loss of *Tlx3* in the placodal population resulted in ganglia hat were not only reduced in overall size but also far more disorganized, when compared to the contralateral control side (compare Fig. 3.6J and J′). While it was clear that knocking down *Tlx3* reduced TUJ1 expression, it was also interesting that loss of *Tlx3* resulted in reduction of both the ophthalmic and maxillo-mandibular lobes (Fig. 3.6J'), indicating that loss of the placodal component resulted in ganglia that could not properly form its bi-lobed structure. Furthermore, we also observed a significant reduction in the expression of SOX10 and abundance of NC cells, indicating that the interactions between NC and placode cells was diminished such that both the ophthalmic and maxillo-mandibular lobe could not properly form, resulting only in the condensation of the NC at the most proximal region of the ganglion (Fig. 3.6J', asterisk), consistent with previous studies (D'Amico-Martel and Noden, 1983; Hamburger, 1961; Moody and Heaton, 1983a, 1983b; Shiau and Bronner-Fraser, 2009; Shiau et al., 2008). This reduction in size upon *Tlx3* knockdown was statistically significant at these developmental stages (Fig. 3.6L, lane 3).

We next examined the effects of perturbing *Tlx3* specifically in the placodal population via our CRISPR/Cas9-mediated method (Fig. 3.6I). We observed similar results in the placodal component of the trigeminal ganglion as with the MO-mediated approach. There was a notable loss of TUJ1 within the ophthalmic lobe and a

diminution overall of the ganglion size, both in the ophthalmic and maxillo-mandibular lobe, when compared to the contralateral control (compare Fig. 3.6K' and Fig. 3.6K). In addition to examining TUJ1 expression, we also examined the expression of NEUROG2 and NEUROD1. Loss of *Tlx3* within the placodal population also reduced expression of both NEUROG2 and NEUROD1 (compare Fig. S3.7C and Fig. S3.7C'; compare Fig. S3.7D and Fig. S3.7D'). Even though a similar phenotype was observed between both the MO and CRISPR/Cas9-mediated approach, we noted some differences in the expression of TUJ1. In general, loss of *Tlx3* in the placodal population resulted in reduced ganglia size and more dispersed SOX10+ NC and TUJ1+ placodal cells that failed to condense within the ophthalmic lobe.

Taken together, our results suggest that *Tlx3* is necessary for gangliogenesis in both neural crest and placodal cells during trigeminal ganglion development.

3.3 Discussion

Reciprocal interactions between NC and placodal cells have been shown to be necessary for the proper formation of the cranial trigeminal ganglion, relying on intimate and coordinated communication between the two populations (D'Amico-Martel and Noden, 1983; Gammill et al., 2007; Hamburger, 1961; Lwigale, 2001; Moody and Heaton, 1983a, 1983b; Shiau and Bronner-Fraser, 2009; Shiau et al., 2008; Theveneau et al., 2013). Previous studies have demonstrated that ablation of either cell population results in notable defects and abnormal development of the trigeminal ganglion. While placode-ablated embryos exhibit dispersed or smaller ganglia, NC-ablated embryos result in ganglia that do not properly connect to the hindbrain and fail to integrate into a bi-lobed structure (Hamburger, 1961; Shiau et al., 2008; Stark et al., 1997). Additionally, it has been shown that disruption of neural crest migration due to changes in signaling cues plays a crucial role in trigeminal condensation. Multiple cues, such as Neuropilin/Semaphorin, Robo/Slit, and Cxcr4/Sdf1 interactions represent molecular mechanisms by which neural crest and placodal cells signal one another during migration and facilitate condensation (Gammill et al., 2007; Shiau and

Bronner-Fraser, 2009; Shiau et al., 2008; Theveneau et al., 2013). Collectively, these studies have provided a clearer understanding of how mutual interactions between the neural crest and placode promote the coordinated morphogenesis required for proper cranial ganglion formation.

Many aspects of the transcriptional mechanisms underlying trigeminal ganglion formation remain unresolved. To tackle this question, here we demonstrate that *Tlx3* expression is pivotal in this process. Our results show that *Tlx3* expression is present in both neural crest and placodal cells (Fig. 3.1 and Fig. S3.1) and plays an essential but non-overlapping roles in each population. By combining lineage labeling with *in situ* HCR, we find expression of *Tlx3* in a subset of neural crest cells at a time that correlates with the onset of condensation of the trigeminal ganglion (Fig. 3.2). Additionally, we demonstrate that expression of *Tlx3* accumulates in *Sox10*+ neural crest cells, at later developmental stages and is maintained in a subset of cranial neural crest-derived cells. We hypothesize that while differentiation of neural crest cells into sensory neurons occur later in development (~HH20-HH24) (Covell and Noden, 1989; D'Amico-Martel and Noden, 1980; Shiau et al., 2008) than in placode cells, the mechanism appear to be similar. Accordingly, this subset of cells may be primed at the onset of condensation by proneural factors that transition these cells from a progenitor state to a post-mitotic sensory neuroblast, a process that precedes terminal differentiation (Sharma et al., 2020). Importantly, perturbation of *Tlx3*, by either MO or CRISPR/Cas9-mediated methods diminishes the overall size and abundance of both the neural crest and placodal populations, as well as degree of neurogenesis within the developing ganglion (Fig. 3.6). Taken together, our results show that *Tlx3* plays a critical role in both placode- and neural crest-derived cells during trigeminal gangliogenesis.

Tlx3 has been implicated in differentiation and fate specification of excitatory sensory neurons in both the CNS and PNS (Cheng et al., 2004; Divya et al., 2016; Guo et al., 2012; Hornbruch et al., 2005; Kondo et al., 2008, 2011; Langenau et al., 2002; Logan et al., 1998, 2002; Monteiro et al., 2021; Shimomura et al., 2015; Uchiyama et

al., 1999; Xu et al., 2008a). These previous studies have demonstrated that expression of *Tlx3* serves as a post-mitotic selector gene, implicated in specification of excitatory sensory neurons. For example, ectopic expression of *Tlx3* is sufficient to repress GABAergic differentiation and promote upregulation of glutamatergic neuronal subtype genes, in turn inducing a glutamatergic neuronal fate (Begbie et al., 2002; Cheng et al., 2004; Divya et al., 2016; Guo et al., 2012; Hornbruch et al., 2005; Kondo et al., 2008, 2011; Langenau et al., 2002; Logan et al., 1998, 2002; Monteiro et al., 2021; Shimomura et al., 2015; Uchiyama et al., 1999; Xu et al., 2008a). Surprisingly, we found that ectopic activation of *Tlx3* in the neural crest results in initial migration delays and subsequently in premature expression of neuronal markers (Figs. 3.3 and 3.5). We hypothesize that *Tlx3* expression induces downstream expression of proneural genes, requiring up-regulation of these genes, that in turn promotes the transition from undifferentiated precursor cells to differentiated sensory neurons (Kondo et al., 2008, 2011; Monteiro et al., 2021; Sharma et al., 2020). Previous studies have demonstrated that perturbation of *Tlx3* influences neuronal decisions, in terms of excitatory versus inhibitory cell fates, within the CNS and PNS (Cheng et al., 2004; Kondo et al., 2008; Monteiro et al., 2021; Xu et al., 2008a). In particular, *Tlx3* knockout in mice results in prospective excitatory neurons transitioning and adopting an entirely different neuronal fate, expressing different terminal differentiation markers, and affecting the overall excitatory population within the developing spinal cord (Cheng et al., 2004; Monteiro et al., 2021). In addition to this, our results reveal that perturbation of *Tlx3*, either by MO or CRISPR/Cas9-mediated approach, severely affects trigeminal ganglion formation. Moreover, we find different effects when we specifically knock-out Tlx3 in the neural crest versus placode cells. In particular, our results show that loss of *Tlx3* in the neural crest-derived portion of the trigeminal ganglion results in a reduced abundance of neural crest cells, and failure of proper ganglion condensation (Fig. 3.6G' and Fig. 3.6H'). In contrast, loss of *Tlx3* in the placodal portion of the ganglion results in diminution of TUJ1 expression and a disorganized ganglion that is reduced in size (Fig. 3.6J' and Fig. 3.6K'). Interestingly, our *Tlx3* loss-of-function phenotype within the placodal population is consistent with previous observations. Specifically, loss of Neurog2 has been shown to result in

dispersed organization of neurons within the ophthalmic lobe of the ganglion, while loss of NeuroD1 influenced trigeminal ganglion development, partially resembling our placodal *Tlx3* loss-of-function phenotype (Bina et al., 2023), providing further support that *Tlx3* may enhance proneural gene expression and specification.

In summary, the present study demonstrates that *Tlx3* is expressed in both neural crest and placode-derived portions of the trigeminal ganglion, where it functions in proper specification of sensory neurons. After loss of function, we mainly observed effects within the ophthalmic lobe of the trigeminal ganglia, consistent with its temporal appearance first in the ophthalmic lobe prior to onset of expression in the maxillo-mandibular lobe. Interestingly, ectopic activation of *Tlx3* results in premature expression of neuronal markers, while perturbation of *Tlx3* disrupts both ganglion integration and development, with somewhat different effects in the placode versus neural crest. Taken together, we speculate that *Tlx3* may serve as a post-mitotic selector gene in both the neural crest and placode to ensure proper development and formation of the trigeminal ganglion. These results expand upon the previous roles of *Tlx3* in the peripheral nervous system to show that it not only influences neurogenesis but also may be required for proper aggregation of the chick trigeminal ganglion.

3.4 Materials and methods

3.4.1 Chicken embryos

Fertilized chicken embryos (*Gallus gallus*) were obtained from local commercial sources (Petaluma Egg Farm, Petaluma, CA) and incubated at 37°C in humidified incubators to the desired stages. Embryos were staged by Hamburger-Hamilton (HH) (Hamburger and Hamilton, 1951) staging method as indicated.

3.4.2 Construct design, cloning, and morpholinos

DNA constructs were produced by PCR reactions using AccuPrime high-fidelity DNA Taq polymerase (ThermoFisher) followed by standard purification (Qiagen), restriction enzyme digestion, and ligation (NEB). Full-length coding region of Tlx3 was amplified from HH16 cDNA, using primers provided in the Key Resource table (Table S1), inserting an upstream Kozak sequence and C-terminal FLAG epitope tag. The pTK-Sox10E99:Citrine enhancer vector (Williams et al., 2019) was then modified to replace the Citrine fluorescent protein with an Internal Ribosome Entry Sites (IRES)-driven nuclear eGFP. Tlx3-FLAG coding sequence was then cloned into the vector. All constructs produced in this study were later verified by Sanger sequencing (Laragen) and full plasmid sequencing (Primordium) prior to usage. Constructs for all experiments were used at a final concentration of 2.5 µg/µl, diluted in EB buffer. All translation-blocking morpholino oligomer (MO) were synthesized by Gene Tools, LLC, and sequence of all MOs used is this study are provided in the Key Resource table (Table S1). Standard control oligomer from Gene Tools, LLC (control MO) and Tlx3 MO were diluted with water and used at a final dose of 2.5 µM. To enable visualization of the injection solution, 0.5 µl of 2% red/blue food dye was added per 10 µl injection mix.

3.4.3 CRISPR/Cas9-mediated perturbations

Guide RNA (gRNA) targets for *Tlx3* were generated and obtained using the CHOPCHOP tool (Labun et al., 2019, 2021). Two gRNAs targeting the coding sequence of exon 2 and exon 3 were generated and are provided in the Key Resource table (Table S1). The protospacers were cloned into the single-CRISPR/Cas9 construct, according to the protocol published by Gandhi et al. (2021). The single-plasmids were designed to contain the Cas9 sequence, citrine, and gene-specific gRNA. The control single-plasmid used in this study contains a synthetic DNA construct not found in the chicken genome, in place of the gene-specific guide, sequence provided in Key Resource table (Table S1). Each vector was later verified by Sanger sequencing (Laragen) prior to usage. All single CRISPR/Cas9 constructs used for all experiments were used at final concentration of 2.5 µg/µl, diluted in EB

buffer. To enable visualization of the injection solution, 0.5 µl of 2% red/blue food dye was added per 10 µl injection mix.

3.4.4 Electroporations

For *ex ovo* experiments, embryos were incubated 19–20 h to obtain stage HH4, whereas for *in ovo* experiments, embryos were either incubated 28–30 h to obtain stages HH8-HH9- or 40–45 h to obtain HH12-HH12+. *Ex ovo* electroporations were performed as previously described (Sauka-Spengler and Barembaum, 2008) by passing five 5.8 V pulses for 50 ms at 100 ms intervals. Embryos were then cultured in 1 ml albumin supplemented with 1% penicillin/streptomycin (PenStrep) at 37.5◦C. The following day, embryos were screened for transfection efficiency (high fluorescence intensity), and unhealthy and/or poorly transfected embryos were discarded. For *in ovo* experiments, all constructs were introduced at stages HH8-HH9- or HH12-HH12+. Platinum electrodes were placed vertically or horizontally across the chick embryo delivering five 13 V pulses for 50 ms at 100 ms intervals as previously described (Shiau et al., 2008). Incubation was then continued for ~18–24 h to reach stages HH13-14 or ~28–36 h to reach stages HH15-16.

3.4.5 Lineage tracing

For neural crest lineage tracing injections, cell tracker CM-DiI (Thermo Scientific) was diluted 1:2 with 10% sucrose (Stundl et al., 2023) and loaded into a thin pulled glass needle pipette. DiI solution was then injected into the closing neural tube at the hindbrain level through the opening in the hindbrain of HH9 chick embryos, filling the posterior hindbrain to the level of the forebrain. Embryos were then covered with sterile surgical tape and incubated at 37◦C for 1-day, after which the surviving embryos were dissected out and fixed with 4% paraformaldehyde overnight at 4◦C. Fixed embryos were then embedded for cryosectioning at 16 µm, processed for hybridization chain reaction, and subsequently imaged.

3.4.6 Cyosectioning

Whole-mount embryos were fixed in 4% paraformaldehyde (PFA) overnight at 4◦C, followed by three washes in 1 ×PBS at room temperature. Embryos were then washed in 5% sucrose in PBS at room temperature for 1 h and then stored in 15% sucrose in PBS overnight at 4◦C. Embryos were subsequently incubated in 7.5% gelatin for 4–16 h at 39◦C, then flash-frozen in liquid nitrogen and stored at− 80◦C. Transverse frozen sections were taken and allowed to dry overnight at room temperature. Gelatin was removed by incubating slides in PBS at 42◦C for 10 min, and coverslips were mounted with Fluoromount-G (SouthernBiotech).

3.4.7 *In situ* hybridization

Whole-mount in situ hybridization for Tlx3 was performed as previously described (Kerosuo and Bronner, 2016; Sim˜ oes-Costa and Bronner, 2015; Simoes-Costa and Bronner, 2016). Briefly, embryos were fixed in 4% PFA overnight at 4◦C, dehydrated, and stored in 100% methanol at −20◦C before processing. Embryos were then rehydrated with PBS-DEPC/0.1% Tween-20 (PBSTw), treated with 10 μg/ml Proteinase K at room temperature, washed successively with 2 mg/ml glycine/PBSTw and PBSTw, followed with 4% PFA/0.2% glutaraldehyde at room temperature. Following multiple washes of PBSTw, embryos were incubated with hybridization solution (containing 50% formamide, 1.3X SSC, pH 5, 5 mM EDTA, pH 8, 200 μg/ml yeast tRNA, 0.2% Tween-20, 0.5% CHAPS, and 100 μg/ml heparin) (Hybe) for at least 3 h before addition of probe at 70◦C in Hybe. Embryos were incubated with *Tlx3* probe, diluted in Hybe, for at least 16 h at 70◦C. After probe hybridization, embryos were washed several times in Hybe at 70◦C, then in MABT (1X maleic acid buffer/0.1% Tween-20) at room temperature. Embryos were then blocked in 20% sheep serum/2% Boehringer blocking reagent (BBR) in MABT for several hours before addition of anti-digoxigenin–AP antibody (1:2000; Fab fragments;

11093274910; Roche). Following overnight antibody incubation at 4◦C, embryos were then washed with MABT before chromogenic detection by NBT/BCIP. cDNA templates used for antisense RNA probe of *Tlx3* were obtained from HH16 chick cDNA. Antisense Tlx3 RNA probe, an 849 bp fragment, was synthesized using a T7 RNA polymerase (Promega) and then purified with Illustra ProbeQuant G-50 Micro Columns (GE Healthcare). Embryos were imaged, subsequently processed for cryosectioning at 16 μm.

3.4.8 Hybridization chain reaction

Hybridization chain reaction (HCR) v3 was performed using the protocol suggested by Molecular Technologies (Choi et al., 2018) with minor modifications. Briefly, embryos were fixed in 4% PFA overnight at 4◦C, washed in PBSTw, dehydrated, and stored in 100% methanol overnight at− 20◦C. The following day, embryos were rehydrated and processed for cryosectioning. Following sectioning, slides were treated with proteinase-K for 10 min, and incubated with 12 pmol of Tlx3 probe (B3 initiator) and Sox10 probe (B4 initiator) dissolved in hybridization buffer overnight at 37◦C. The subsequent day, following several washes in hybridization probe wash buffer and 0.1% 5x–SSC–Tween, embryos were incubated in 30 pmol of amplifier hairpins H1 and H2 labeled with Alexa488 and Alexa647 diluted in amplification buffer at room temperature overnight. The following day, embryos were washed in 0.1% 5x–SSC–Tween and imaged. All probes were designed and ordered through Molecular Technologies. Embryos were processed for cryosectioning at 16 μm and subsequently imaged.

3.4.9 Immunohistochemistry

Embryos were fixed in 4% PFA in sodium phosphate buffer for 20 min at room temperature, washed in 0.5 M Tris-HCl/1.5 M NaCl/10 mM CaCl2/0.5% Triton X-100 in TBS (TBSTr), blocked in 10% donkey serum in TBSTr for 2 h at room

temperature, and incubated in primary antibody solution at 4°C for two nights. On the third day, embryos were washed in TBSTr (30 min per wash, six washes) and incubated in secondary antibody solution for two nights at 4◦C. Following the secondary antibody incubation, embryos were washed in TBSTr (30 min per wash, six washes) and processed for imaging and then for cryosectioning. The following primary antibodies and concentrations were used: Guinea Pig anti-TLX3 (1:1000; a gift from T. Müller and C. Birchmeier, Max-Delbrück-Centrum for Molecular Medicine, Germany); Goat anti-GFP (1:500; Rockland, Cat# 600-101-215); Mouse IgG1 anti-PAX7 (1:10; DSHB, Cat# PAX7); Mouse IgG1 anti-Cadherin-6B (1:5; DSHB, Cat# CCD6B-1); rabbit IgG anti-SOX9 (1:1000; Sigma-Aldrich, Cat# AB5535); Mouse IgG1 anti-FLAG (1:500; Sigma-Aldrich, Cat# F1804); Rat anti-N-Cadherin (1:50, DSHB, Cat# MNCD2); Mouse IgM anti-HNK-1 (1:5, DSHB, Cat# 3H5); Mouse IgG2b anti-ISLET1 (1:100, DSHB, Cat# 40.2D6); Rabbit anit-Sox10 (1:500, Sigma-Aldrich, Cat# HPA068898); Mouse IgG1 anti-AP2β (1:250, Santa Cruz Biotechnology, Cat# sc-390119); Mouse IgG2A anti-TUJ1 (1:250, Biolegend, Cat# 801201); Mouse IgG2B anti-HuC/D (1:250, Invitrogen, Cat# A21271); Mouse IgG2A E-Cadherin (1:50, BD Bioscience, Cat# 610181); Rabbit anti-NeuroD1 (1:100, LifeSpan BioSciences Cat# LS-C331294); Mouse IgG2A anti-Neurog2 (1:50, Santa Cruz Biotechnology, Cat# sc-293430). Primary antibodies were detected by Alexa Fluor 488-, 568-, or 647-conjugated donkey secondary antibodies (1:500; Molecular Probes). For transverse sectioning, immunolabeled embryos were sectioned at a thickness of 12 μm.

3.4.10 Microscopy

Whole-mount and transverse section images were acquired at room temperature using a Zeiss Imager.M2 with an ApoTome.2 module, Axiocam 506 color and monochromatic cameras, and Zen 2 Blue software (ZEISS). Transverse section imaging was also preformed using a Zeiss LSM 980 with an inverted microscope and Fast Airyscan 2. Whole-mount images were acquired as wide-field views or displayed as a maximum intensity projection of Z-stacks, with a Plan Apochromat 10 x

objective/0.45 NA (ZEISS), and embryos were imaged in 1X TBSTr. Transverse sections were acquired as a single optical plane or maximum intensity projections of Z-stacks, using a Plan Apochromat 20 x objective/0.8 NA (ZEISS), and were imaged in Fluoromount-G (SouthernBiotech). Images were pseudocolored and minimally processed for brightness and contrast using Fiji (Schindelin et al., 2012). Image analysis and display preparation were performed using Fiji (Schindelin et al., 2012).

3.4.11 Image and statistical analysis

Images were analyzed and prepared for displaying using Fiji (Schindelin et al., 2012). For each whole-mount image, neural crest migration area was determined by manually drawing regions of interest (ROIs) surrounding the neural crest along a 400 μm length of the midbrain and measuring the area. This analysis approach has been used routinely to identify changes in migration area (Hutchins and Bronner, 2018, 2019; Piacentino and Bronner, 2018; Piacentino et al., 2021; Schiffmacher et al., 2018). Measurements were made for both sides at the same axial level, and then the electroporated experimental length was divided by the electroporated control length to calculate the relative maximum migration distance. Knockdown electroporations of chick embryos are heterogeneous and mosaic; as such, we performed analysis over large ROIs that encompass many cells within the trigeminal ganglion. For this analysis approach, ROIs were manually drawn to measure fluorescence intensity, size area, and to define boundaries for multiple-cell fluorescence intensity measurements. Fluorescence measurements, corrected total cellular fluorescence, values were calculated and normalized as previously described (Piacentino and Bronner, 2018).

Statistical analyses were performed using GraphPad Prism9. P-values are indicated in the text, and a cutoff of $P < 0.05$ was used to determine significance. All datasets were tested for normal distribution with a Kolmogorov–Smirnov test. Normalized distributed data were analyzed with parametric tests (t-test or one-way ANOVA). The specific tests used are reported in in the corresponding figure legends. All analyses show pooled biological replicates from at least three independent

experiments. Data are presented as mean values, with error bars indicating SEM. Number of embryos/samples and replicates are indicated in figure legends and/or text. Data distribution was assumed to be normal but was not formally tested.

3.5 Author contributions statement

Hugo A. Urrutia: Writing – Original draft, Visualization, Project administration, Methodology, Investigation, Funding acquisition, Formal analysis, Data curation, Conceptualization. Jan Stundl: Writing – review & editing, Methodology, Investigation. Marianne E. Bronner: Writing – Original draft, Supervision, Project administration, Investigation, Funding acquisition, Formal analysis, Data curation, Conceptualization.

3.6 Declaration of competing interest

The authors declare no competing or financial interests.

3.7 Acknowledgement

We would like to thank Drs. Thomas Müller and Carmen Birchmeier for providing TLX3 antibodies. We'd also like to thank Dr. Mike Piacentino and Ayyappa Raja Desingu Rajan for their helpful discussion during the course of our study. Lastly, we would like to thank the Caltech Biological Imaging Facility, supported by the Caltech Beckman Institute and the Arnold and Mabel Beckman Foundation, for confocal microscopy support. Funding for this work is supported by the National Institutes of Health (NIH) grants R01DE027568 to M.E.B. and F31DE031154 to H.A.U.

3.8 Key Resource Table

REAGENT or RESOURCES	SOURCE	IDENTIFIER
Antibodies		
Guinea Pig anti-TLX3	T. Müller and C. Birchmeier, Max-Delbrück-Centrum for Molecular Medicine, Germany	N/A
Goat polyclonal IgG anti-GFP	Rockland	Cat# 600-101-215
Mouse monoclonal IgG1 anti-PAX7	Developmental Studies Hybridoma Bank (DSHB)	Cat# PAX7; RRID:AB_528428
Mouse monoclonal IgG1 anti-CDH6	Developmental Studies Hybridoma Bank (DSHB)	Cat #CCD6B-1
Rabbit Polyclonal IgG anti-SOX9	Sigma-Aldrich	Cat #AB5535
Mouse monoclonal IgG1 anti-FLAG M2	Sigma-Aldrich	Cat #F1804
Mouse monoclonal IgG2a anti-CDH2	Developmental Studies Hybridoma Bank (DSHB)	Cat #MNCD2
Mouse monoclonal IgGM anti-HNK1	Developmental Studies Hybridoma Bank (DSHB)	Cat #3H5
Mouse monoclonal IgG1 anti-ISLET1	Developmental Studies Hybridoma Bank (DSHB)	Cat #40.2D6
Rabbit Polyclonal IgG anti-SOX10	Sigma-Aldrich	Cat #HPA068898
Mouse monoclonal IgG1 anti-AP2β	Santa Cruz Biotechnology	Cat #sc-390119
Mouse monoclonal IgG2a anti-TUJ1	BioLegend	Cat #801201
Mouse monoclonal IgG2a anti-HuC/D	Invitrogen	Cat# A21271
Mouse monoclonal IgG2a anti-CDH1	BD Bioscince	Cat #610181
Experimental Model		
Fertilized chicken eggs, Gallus gallus, breed: Rhode Island Red	Petaluma Egg Farm, Petaluma, CA	N/A

Oligonucleotides		
Morpholino: Control MO CCTCTTACCTCAGTTACAATTTATA	Gene Tool, LLC, This Paper	N/A
Morpholino: Tlx3 MO CGCAGCCCCGCGCCCGCTATAAA	Gene Tool, LLC, This Paper	N/A
CRISPR/Cas9 gRNA Target: Control GCACTGCTACGATCTACACC	(Gandhi et al., 2021)	N/A
CRISPR/Cas9 gRNA Target: *TLX3.2* TTCGTCAAGGAGCGCTTCAC	CHOPCHOP, This paper	N/A
CRISPR/Cas9 gRNA Target: *TLX3.3* ATGCGCCGCGTCACCGTGAA	CHOPCHOP, This paper	N/A
Primer: NheI TLX3 FWD: AAAAAGCTAGCGCCACCATGGAGCCGGC GGCGGGCGC	IDT, This paper	N/A
Primer: TLX3_FLAGtag PacI REV: AACGTTAATTAACTACTTGTCGTCATCGTC TTTGTAGTCGCCGGAGCCGACGAGGGAGG TGACCGGCG	IDT, This paper	N/A
Primer: NheI PacI MCS_IRES_nlseGFP FWD: AAAAGCTAGCAGGATTAATTAACTCGAGG TCGATCGACGGTA	IDT, This paper	N/A
Primer: eGFP FseI REV: AAAGGCCGGCCTTACTTGTACAGCTCGTC CATGC	IDT, This paper	N/A
Tlx3 mRNA ISH Probe GCTGACGCCCTTCACGGTGACGCGGCGCA TCGGACACCCGTACCAGAACCGCACCCCG CCGAAGCGCAAGAAGCCGCGCACGTCCTT CTCCCGCGTGCAGATCTGCGAGCTGGAGA AGCGCTTCCACCGGCAGAAGTACCTCGCG TCGGCCGAGCGCGCGGCCCTGGCCAAGTC GCTGAAGATGACGGACGCGCAGGTGAAG ACGTGGTTCCAGAACCGGCGCACGAAGTG GCGGCGGCAGACGGCGGAGGAGCGGGAG GCCGAGCGGCAGCAGGCGAGCCGGCTGA TGCTGCAGCTGCAGCACGACGCCTTCCAG AAGTCGCTCAACGAGTCGATCCAGCCCGA CCCGCTGTGTCTGCACAACTCGTCGCTGTT CGCGCTGCAGAACCTGCAGCCCTGGGAGG AGGAGAGCGCCAAGATCCCGCCGGTCAC CTCCCTCGTCTGA	(Logan et al., 1998)	N/A

Recombinant DNA		
Plasmid: pTK-SOX10-enh-99::Citrine	(Williams et al., 2019)	Addgene plasmid #130588
Plasmid: pTK-SOX10E99::TLX3-FLAG-IRES-nls-eGFP	This paper	N/A
Plasmid: pTK-SOX10E99::IRES-nls-eGFP	This paper	N/A
Plasmid: pCAG::Cas9-2a-Citrine-HH-ControlgRNA-HDV	(Gandhi et al., 2021)	N/A
Plasmid: pCAG::Cas9-2a-Citrine-HH-TLX3.2gRNA-HDV	This paper	N/A
Plasmid: pCAG::Cas9-2a-Citrine-HH-TLX3.3gRNA-HDV	This paper	N/A
Software and Algorithms		
Benchling		https://benchling.com/
Fiji v1.53c	(Schindelin et al., 2012)	https://imagej.net/Fiji
CHOPCHOP	(Labun et al., 2019; Labun et al., 2021)	https://chopchop.cbu.uib.no
Custom measurement macros for Fiji	This paper	N/A

3.9 References

Akitaya, T. and Bronner-Fraser, M. (1992). Expression of cell adhesion molecules during initiation and cessation of neural crest cell migration. Dev. Dyn. *194*, 12–20.

Baker, C. (2006). Neural Crest and Cranial Ectodermal Placodes. In Developmental Neurobiology, pp. 67–127. New York: Kluwer Academic Publishers-Plenum Publishers.

Begbie, J. and Graham, A. (2001). Integration between the epibranchial placodes and the hindbrain. Science *294*, 595–598.

Begbie, J., Ballivet, M. and Graham, A. (2002). Early steps in the production of sensory neurons by the neurogenic placodes. Mol. Cell. Neurosci. *21*, 502–511.

Betancur, P., Bronner-Fraser, M. and Sauka-Spengler, T. (2010). Genomic code for Sox10 activation reveals a key regulatory enhancer for cranial neural crest. Proc. Natl. Acad. Sci. U. S. A. *107*, 3570–3575.

Blentic, A., Chambers, D., Skinner, A., Begbie, J. and Graham, A. (2011). The formation of the cranial ganglia by placodally-derived sensory neuronal precursors. Mol. Cell. Neurosci. *46*, 452–459.

Bronner-Fraser, M. (1986). Analysis of the early stages of trunk neural crest migration in avian embryos using monoclonal antibody HNK-1. Dev. Biol. *115*, 44–55.

Cheng, L., Arata, A., Mizuguchi, R., Qian, Y., Karunaratne, A., Gray, P. A., Arata, S., Shirasawa, S., Bouchard, M., Luo, P., et al. (2004). Tlx3 and Tlx1 are post-mitotic selector genes determining glutamatergic over GABAergic cell fates. Nature Neuroscience *7*, 510–517.

Choi, H. M. T., Schwarzkopf, M., Fornace, M. E., Acharya, A., Artavanis, G., Stegmaier, J., Cunha, A. and Pierce, N. A. (2018). Third-generation in situ hybridization chain reaction: multiplexed, quantitative, sensitive, versatile, robust. Development *145*.

Covell, D. A., Jr and Noden, D. M. (1989). Embryonic development of the chick primary trigeminal sensory-motor complex. J. Comp. Neurol. *286*, 488–503.

Dady, A., Blavet, C. and Duband, J.-L. (2012). Timing and kinetics of E- to N-cadherin switch during neurulation in the avian embryo. Dev. Dyn. *241*, 1333–1349.

d'Amico-Martel, A. and Noden, D. M. (1980). An autoradiographic analysis of the development of the chick trigeminal ganglion. J. Embryol. Exp. Morphol. *55*, 167–182.

D'Amico-Martel, A. (1982). Temporal patterns of neurogenesis in avian cranial sensory and autonomic ganglia. Am. J. Anat. *163*, 351–372.

D'Amico-Martel, A. and Noden, D. M. (1983). Contributions of placodal and neural crest cells to avian cranial peripheral ganglia. Am. J. Anat. *166*, 445–468.

Divya, T. S., Lalitha, S., Parvathy, S., Subashini, C., Sanalkumar, R., Dhanesh, S. B., Rasheed, V. A., Divya, M. S., Tole, S. and James, J. (2016). Regulation of Tlx3 by Pax6 is required for the restricted expression of Chrnα3 in Cerebellar Granule Neuron progenitors during development. Sci. Rep. *6*, 30337.

Freter, S., Fleenor, S. J., Freter, R., Liu, K. J. and Begbie, J. (2013). Cranial neural crest cells form corridors prefiguring sensory neuroblast migration. Development *140*, 3595–3600.

Gammill, L. S., Gonzalez, C. and Bronner-Fraser, M. (2007). Neuropilin 2/semaphorin 3F signaling is essential for cranial neural crest migration and trigeminal ganglion condensation. Dev. Neurobiol. *67*, 47–56.

Gandhi, S., Li, Y., Tang, W., Christensen, J. B., Urrutia, H. A., Vieceli, F. M., Piacentino, M. L. and Bronner, M. E. (2021). A single-plasmid approach for genome editing coupled with long-term lineage analysis in chick embryos. Development *148*,.

Guo, Z., Zhao, C., Huang, M., Huang, T., Fan, M., Xie, Z., Chen, Y., Zhao, X., Xia, G., Geng, J., et al. (2012). Tlx1/3 and Ptf1a control the expression of distinct

sets of transmitter and peptide receptor genes in the developing dorsal spinal cord. J. Neurosci. *32*, 8509–8520.

Hamburger, V. (1961). Experimental analysis of the dual origin of the trigeminal ganglion in the chick embryo. J. Exp. Zool. *148*, 91–123.

Hamburger, V. and Hamilton, H. L. (1951). A series of normal stages in the development of the chick embryo. J. Morphol. *88*, 49–92.

Hornbruch, A., Ma, G., Ballermann, M. A., Tumova, K., Liu, D. and Cairine Logan, C. (2005). A BMP-mediated transcriptional cascade involving Cash1 and Tlx-3 specifies first-order relay sensory neurons in the developing hindbrain. Mech. Dev. *122*, 900–913.

Hutchins, E. J. and Bronner, M. E. (2018). Draxin acts as a molecular rheostat of canonical Wnt signaling to control cranial neural crest EMT. J. Cell Biol. *217*, 3683–3697.

Hutchins, E. J. and Bronner, M. E. (2019). Draxin alters laminin organization during basement membrane remodeling to control cranial neural crest EMT. Dev. Biol. *446*, 151–158.

Jidigam, V. K. and Gunhaga, L. (2013). Development of cranial placodes: Insights from studies in chick. Dev. Growth Differ. *55*, 79–95.

Kerosuo, L. and Bronner, M. E. (2016). CMyc regulates the size of the premigratory neural crest stem cell pool. Cell Rep. *17*, 2648–2659.

Knecht, A. K. and Bronner-Fraser, M. (2002). Induction of the neural crest: A multigene process. Nat. Rev. Genet. *3*, 453–461.

Kondo, T., Sheets, P. L., Zopf, D. A., Aloor, H. L., Cummins, T. R., Chan, R. J. and Hashino, E. (2008). Tlx3 exerts context-dependent transcriptional regulation and promotes neuronal differentiation from embryonic stem cells. Proc. Natl. Acad. Sci. U. S. A. *105*, 5780–5785.

Kondo, T., Matsuoka, A. J., Shimomura, A., Koehler, K. R., Chan, R. J., Miller, J. M., Srour, E. F. and Hashino, E. (2011). Wnt signaling promotes neuronal differentiation from mesenchymal stem cells through activation of Tlx3. Stem Cells *29*, 836–846.

Labun, K., Montague, T. G., Krause, M., Torres Cleuren, Y. N., Tjeldnes, H. and Valen, E. (2019). CHOPCHOP v3: Expanding the CRISPR web toolbox beyond genome editing. Nucleic Acids Res. *47*, W171–W174.

Labun, K., Krause, M., Torres Cleuren, Y. and Valen, E. (2021). CRISPR genome editing made easy through the CHOPCHOP website. Curr. Protoc. *1*, e46.

Langenau, D. M., Palomero, T., Kanki, J. P., Ferrando, A. A., Zhou, Y., Zon, L. I. and Look, A. T. (2002). Molecular cloning and developmental expression of Tlx (Hox11) genes in zebrafish (Danio rerio). Mech. Dev. *117*, 243–248.

Le Douarin, N. and Kalcheim, C. (1999). Developmental and cell biology series: The neural crest series number *36*. 2nd ed. Cambridge, England: Cambridge University Press.

Logan, C., Wingate, R. J., McKay, I. J. and Lumsden, A. (1998). Tlx-1 and Tlx-3 homeobox gene expression in cranial sensory ganglia and hindbrain of the chick embryo: Markers of patterned connectivity. J. Neurosci. *18*, 5389–5402.

Logan, C., Millar, C., Bharadia, V. and Rouleau, K. (2002). Onset of Tlx-3 expression in the chick cerebellar cortex correlates with the morphological development of fissures and delineates a posterior transverse boundary. J. Comp. Neurol. *448*, 138–149.

Lwigale, P. Y. (2001). Embryonic origin of avian corneal sensory nerves. Dev. Biol. *239*, 323–337.

Martik, M. L. and Bronner, M. E. (2017). Regulatory logic underlying diversification of the neural crest. Trends Genet. *33*, 715–727.

McCabe, K. L., Sechrist, J. W. and Bronner-Fraser, M. (2009). Birth of ophthalmic trigeminal neurons initiates early in the placodal ectoderm. J. Comp. Neurol. *514*, 161–173.

Monteiro, F. A., Miranda, R. M., Samina, M. C., Dias, A. F., Raposo, A. A. S. F., Oliveira, P., Reguenga, C., Castro, D. S. and Lima, D. (2021). Tlx3 exerts direct control in specifying excitatory over inhibitory neurons in the dorsal spinal cord. Front Cell Dev Biol *9*, 642697.

Moody, S. A. and Heaton, M. B. (1983a). Developmental relationships between trigeminal ganglia and trigeminal motoneurons in chick embryos. I. Ganglion development is necessary for motoneuron migration. J. Comp. Neurol. *213*, 327–343.

Moody, S. A. and Heaton, M. B. (1983b). Developmental relationships between trigeminal ganglia and trigeminal motoneurons in chick embryos. II. Ganglion axon ingrowth guides motoneuron migration. J. Comp. Neurol. *213*, 344–349.

Moody, S. A., Quigg, M. S. and Frankfurter, A. (1989). Development of the peripheral trigeminal system in the chick revealed by an isotype-specific anti-beta-tubulin monoclonal antibody. The Journal of Comparative Neurology *279*, 567–580.

Noden, D. M. (1978). The control of avian cephalic neural crest cytodifferentiation. Dev. Biol. *67*, 296–312.

Piacentino, M. L. and Bronner, M. E. (2018). Intracellular attenuation of BMP signaling via CKIP-1/Smurf1 is essential during neural crest induction. PLoS Biol. *16*, e2004425.

Piacentino, M. L., Hutchins, E. J. and Bronner, M. E. (2021). Essential function and targets of BMP signaling during midbrain neural crest delamination. Dev. Biol. *477*, 251–261.

Qian, Y., Fritzsch, B., Shirasawa, S., Chen, C. L., Choi, Y. and Ma, Q. (2001). Formation of brainstem (nor)adrenergic centers and first-order relay visceral sensory neurons is dependent on homeodomain protein Rnx/Tlx3. Genes Dev. *15*, 2533–2545.

Rogers, C. D., Saxena, A. and Bronner, M. E. (2013). Sip1 mediates an E-cadherin-to-N-cadherin switch during cranial neural crest EMT. J. Cell Biol. *203*, 835–847.

Saint-Jeannet, J.-P. and Moody, S. A. (2014). Establishing the pre-placodal region and breaking it into placodes with distinct identities. Dev. Biol. *389*, 13–27.

Sanders, R. D. (2010). The trigeminal (V) and facial (VII) cranial nerves: Head and face sensation and movement. Psychiatry (Edgmont) *7*, 13–16.

Sauka-Spengler, T. and Barembaum, M. (2008). Gain- and loss-of-function approaches in the chick embryo. Methods Cell Biol. *87*, 237–256.

Schiffmacher, A. T., Adomako-Ankomah, A., Xie, V. and Taneyhill, L. A. (2018). Cadherin-6B proteolytic N-terminal fragments promote chick cranial neural crest cell delamination by regulating extracellular matrix degradation. Dev. Biol. *444*, S237–S251.

Schindelin, J., Arganda-Carreras, I., Frise, E., Kaynig, V., Longair, M., Pietzsch, T., Preibisch, S., Rueden, C., Saalfeld, S., Schmid, B., et al. (2012). Fiji: An open-source platform for biological-image analysis. Nat. Methods *9*, 676–682.

Schwarz, Q., Vieira, J. M., Howard, B., Eickholt, B. J. and Ruhrberg, C. (2008). Neuropilin 1 and 2 control cranial gangliogenesis and axon guidance through neural crest cells. Development *135*, 1605–1613.

Serbedzija, G. N., Bronner-Fraser, M. and Fraser, S. E. (1992). Vital dye analysis of cranial neural crest cell migration in the mouse embryo. Development *116*, 297–307.

Sharma, N., Flaherty, K., Lezgiyeva, K., Wagner, D. E., Klein, A. M. and Ginty, D. D. (2020). The emergence of transcriptional identity in somatosensory neurons. Nature *577*, 392–398.

Shiau, C. E. and Bronner-Fraser, M. (2009). N-cadherin acts in concert with Slit1-Robo2 signaling in regulating aggregation of placode-derived cranial sensory neurons. Development *136*, 4155–4164.

Shiau, C. E., Lwigale, P. Y., Das, R. M., Wilson, S. A. and Bronner-Fraser, M. (2008). Robo2-Slit1 dependent cell-cell interactions mediate assembly of the trigeminal ganglion. Nat. Neurosci. *11*, 269–276.

Shimomura, A., Patel, D., Wilson, S. M., Koehler, K. R., Khanna, R. and Hashino, E. (2015). Tlx3 promotes glutamatergic neuronal subtype specification through direct interactions with the chromatin modifier CBP. PLoS One *10*, e0135060.

Simões-Costa, M. and Bronner, M. E. (2015). Establishing neural crest identity: A gene regulatory recipe. Development *142*, 242–257.

Simoes-Costa, M. and Bronner, M. E. (2016). Reprogramming of avian neural crest axial identity and cell fate. Science *352*, 1570–1573.

Stark, M. R., Sechrist, J., Bronner-Fraser, M. and Marcelle, C. (1997). Neural tube-ectoderm interactions are required for trigeminal placode formation. Development *124*, 4287–4295.

Steventon, B., Mayor, R. and Streit, A. (2014). Neural crest and placode interaction during the development of the cranial sensory system. Dev. Biol. *389*, 28–38.

Strobl-Mazzulla, P. H. and Bronner, M. E. (2012). A PHD12-Snail2 repressive complex epigenetically mediates neural crest epithelial-to-mesenchymal transition. J. Cell Biol. *198*, 999–1010.

Stundl, J., Martik, M. L., Chen, D., Raja, D. A., Franěk, R., Pospisilova, A., Pšenička, M., Metscher, B. D., Braasch, I., Haitina, T., et al. (2023). Ancient vertebrate dermal armor evolved from trunk neural crest. Proc. Natl. Acad. Sci. U. S. A. *120*, e2221120120.

Taneyhill, L. A., Coles, E. G. and Bronner-Fraser, M. (2007). Snail2 directly represses cadherin6B during epithelial-to-mesenchymal transitions of the neural crest. Development *134*, 1481–1490.

Theveneau, E., Steventon, B., Scarpa, E., Garcia, S., Trepat, X., Streit, A. and Mayor, R. (2013). Chase-and-run between adjacent cell populations promotes directional collective migration. Nat. Cell Biol. *15*, 763–772.

Uchiyama, K., Otsuka, R. and Hanaoka, K. (1999). CHox11L2, a Hox11 related gene, is expressed in the peripheral nervous system and subpopulation of the spinal cord during chick development. Neurosci. Lett. *273*, 97–100.

Vermeiren, S., Bellefroid, E. J. and Desiderio, S. (2020). Vertebrate sensory ganglia: Common and divergent features of the transcriptional programs generating their functional specialization. Front Cell Dev Biol *8*, 587699.

Williams, R. M., Candido-Ferreira, I., Repapi, E., Gavriouchkina, D., Senanayake, U., Ling, I. T. C., Telenius, J., Taylor, S., Hughes, J. and Sauka-Spengler, T. (2019). Reconstruction of the global neural crest gene regulatory network in vivo. Dev. Cell *51*, 255-276.e7.

Wu, C.-Y., Hooper, R. M., Han, K. and Taneyhill, L. A. (2014). Migratory neural crest cell αN-catenin impacts chick trigeminal ganglia formation. Dev. Biol. *392*, 295–307.

Xu, Y., Lopes, C., Qian, Y., Liu, Y., Cheng, L., Goulding, M., Turner, E. E., Lima, D. and Ma, Q. (2008). Tlx1 and Tlx3 coordinate specification of dorsal horn pain-modulatory peptidergic neurons. J. Neurosci. *28*, 4037–4046.

3.10 Supplementary Figures

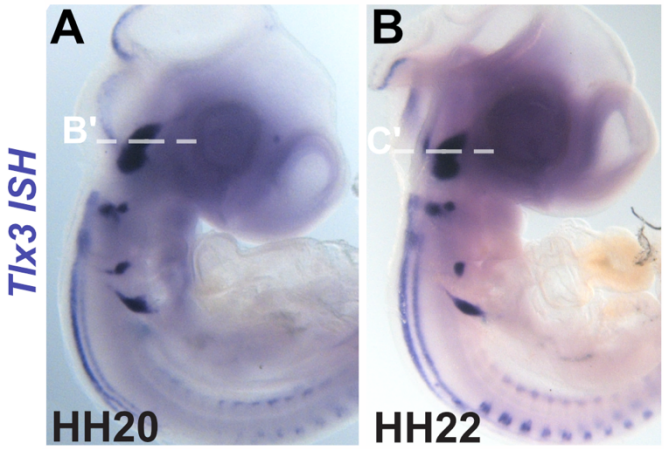

Fig S3.1. *Tlx3* expression persists within the trigeminal ganglion at later developmental stages. A-B. Representative images of chromogenic whole mount *in situ* hybridization for *Tlx3* in stage HH20 (A) and HH22 (B) chick embryos. Dashed lines in A and B (labeled B' and C', respectively) indicate cross section shown in Fig 1B' and 1C'.

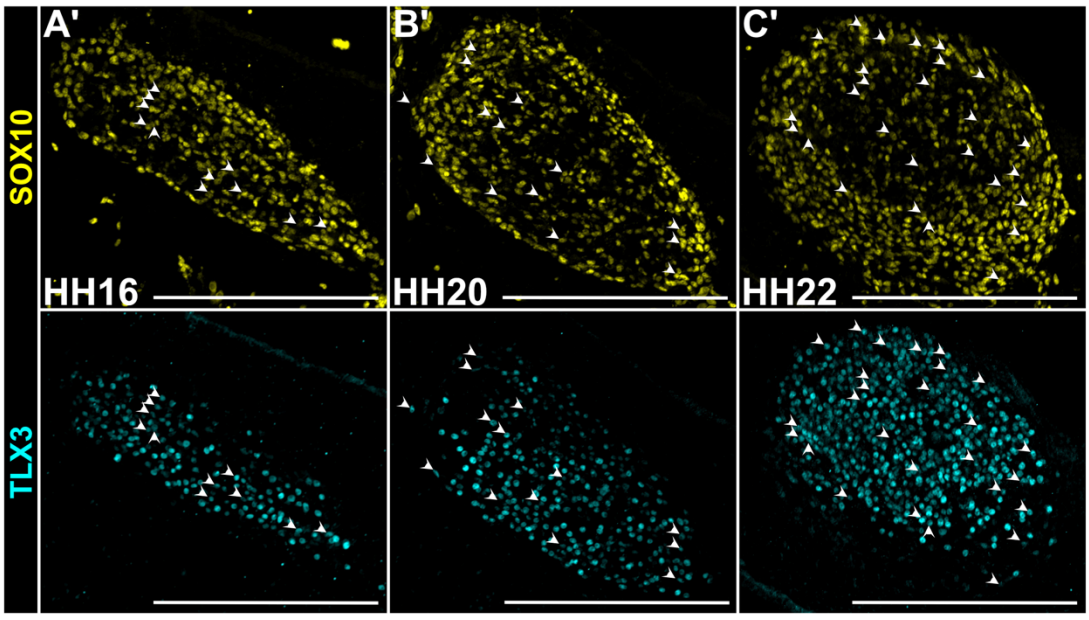

Fig S3.2. TLX3 is expressed in cranial neural crest cells within the developing ganglion. A'-C'. Representative transverse sections of immunolabeled for SOX10 (yellow) and TLX3 (cyan) at stage HH16 (D), HH20 (Sup Fig.1A), and HH22 (Sup Fig. 1B) in stage-matched embryos. Immunolabeling for SOX10 (yellow) and TLX3 (cyan) reveals TLX3 expression in a subset of SOX10+ neural crest cells, revealing overlapping domains of expression (filled arrows). Scale bars represent 200 μm.

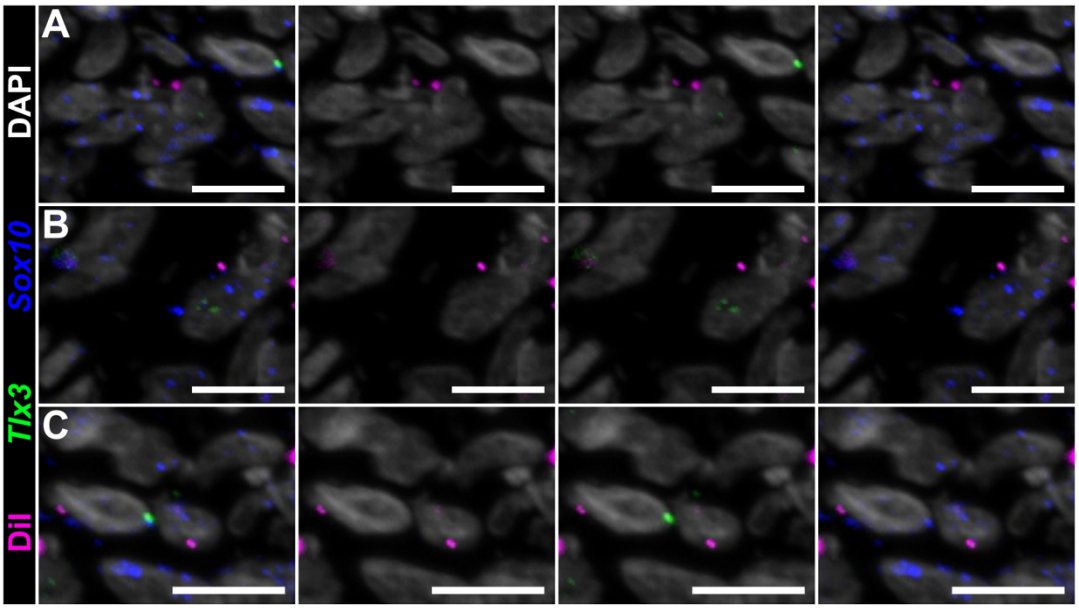

Fig S3.3. *Tlx3* is expressed in a subset of DiI-labeled cranial neural crest cells. A-C. HCR reveals expression of *Tlx3* (green) transcripts in additional cells that also express *Sox10* (blue) transcripts and are DiI-labeled (magenta). Scale bars represent 10 μm.

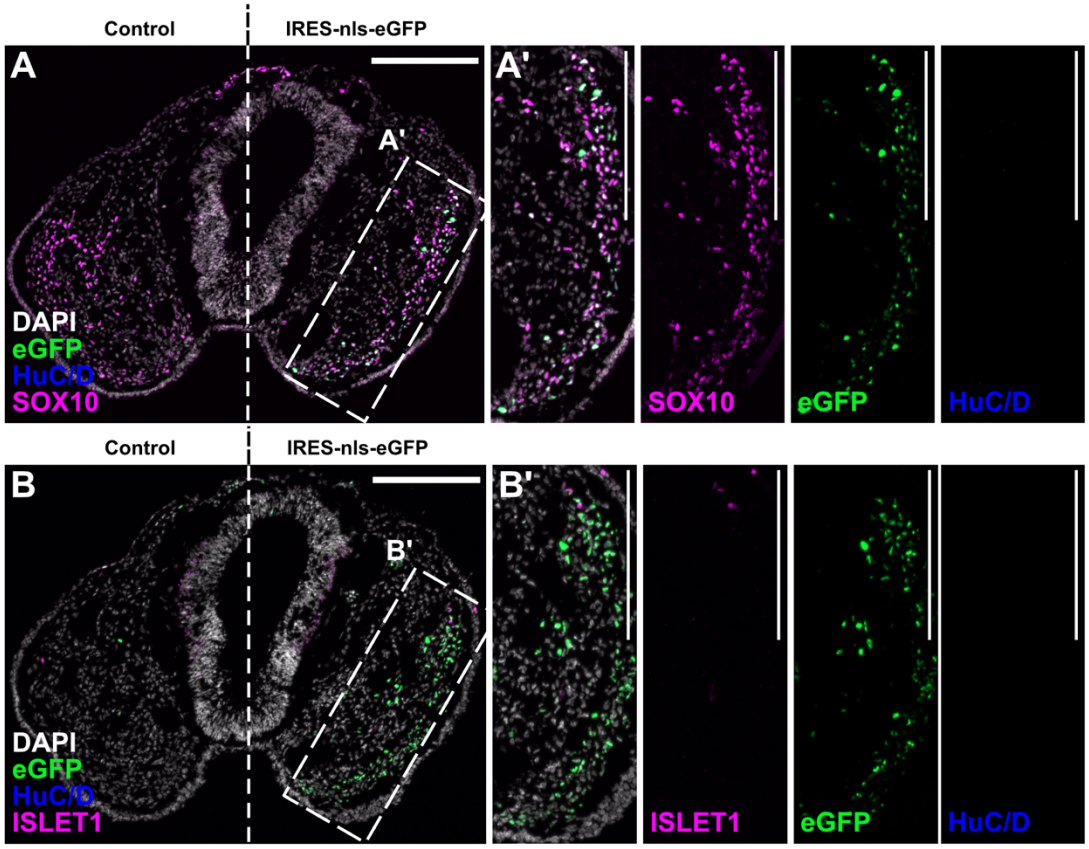

Fig S3.4. Premature neuronal expression is not evident in the absence of *Tlx3* expression. A-B. Representative transverse sections of unilaterally electroporated control (IRES-nls-eGFP) embryos and immunolabeled for SOX10 or ISLET1 (magenta), eGFP (green), and HuC/D (blue) expression (n=8). Immunolabeling on these sections reveals lack of HuC/D+ neural crest cells at stage HH13. A'-B'. Dashed boxes in A-B indicate zoomed in areas in A'-B'. Merged and Individual channel for SOX10 (A')/ISLET1 (B') (magenta), eGFP (green), and HuC/D (blue). Scales bars represent 200 μm.

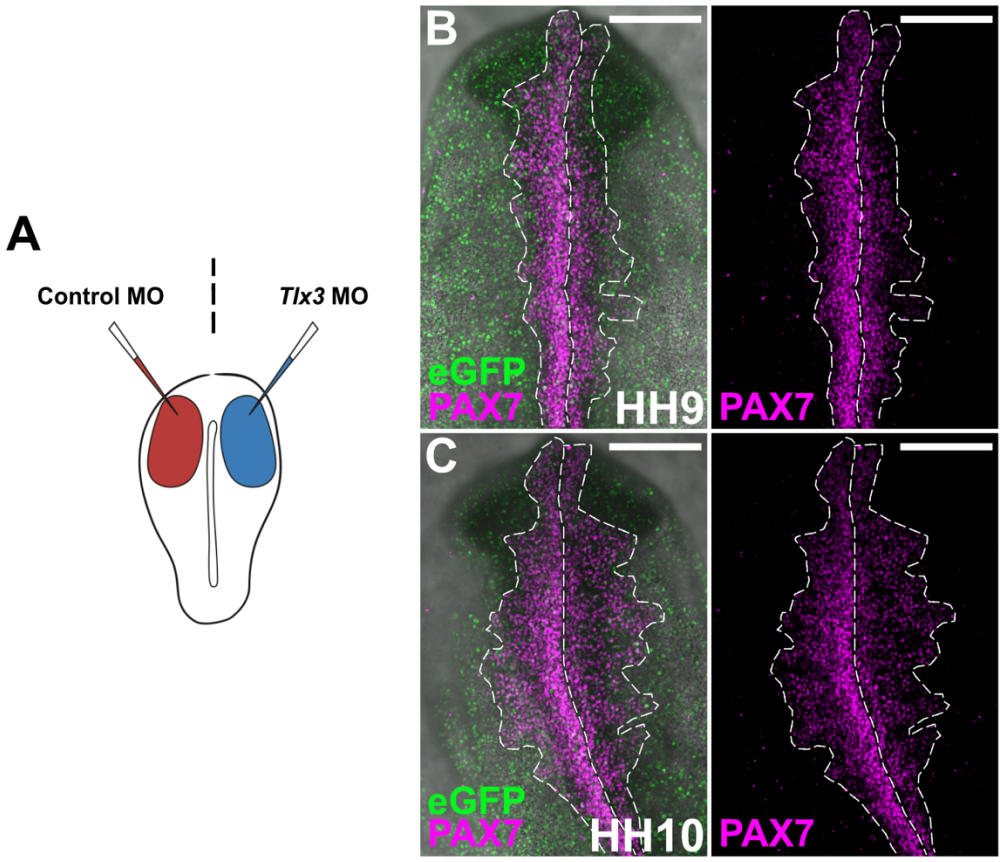

Fig S3.5. Perturbation of *Tlx3* by MO at early stages does not alter migration. A. Schematic representing the *ex ovo* experimental design to test the effects of perturbing *Tlx3*. Control (red) and experimental (blue) reagents were delivered bilaterally into HH4 chick embryos. B-C. Gastrulating HH4 chick embryos were bilaterally electroporated with control MO on the left side and *Tlx3* MO on the right side. B-C. Embryos were immunolabeled to display PAX7 (magenta) expression at stage HH9-10. Immunohistochemistry for PAX7 (magenta) reveals no effects at pre-migratory or early migratory neural crest at HH9-10 (Pre-migratory stage - HH9, n=6; Migratory stage - HH10, n=5). Scale bars represent 200 μm.

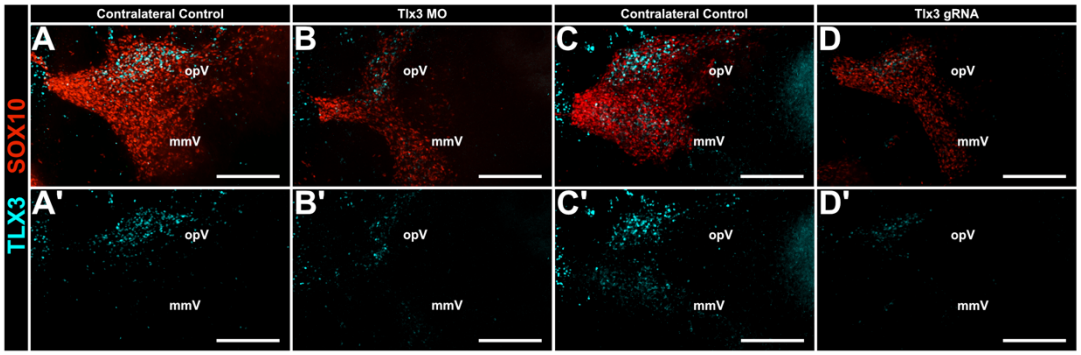

Fig S3.6. Perturbation of *Tlx3* disrupts its expression during/in trigeminal ganglion development. A-D'. Gastrulating HH4 chick embryos were unilaterally electroporated with either *Tlx3* MO or *Tlx3* specific gRNA-CRISPR/Cas9 constructs on the right side of the embryo (*Tlx3* MO, n=10; *Tlx3* gRNA-CRISPR/Cas9, n=10). A-D'. Immunohistochemistry for SOX10 (red) and TLX3 (cyan) reveal the effects on the global loss of TLX3 via MO or CRISPR/Ca9-mediated approach at HH16. A-A' & C-C'. Immunohistochemistry for SOX10 (red) and TLX3 (cyan) reveal the expression of these two proteins on the contralateral control side of the embryo. Scales bars represent 200 μm.

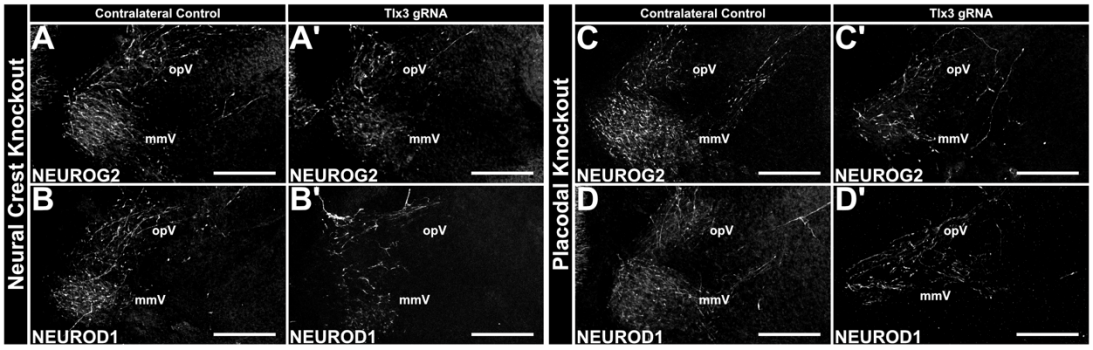

Fig S3.7. Perturbation of *Tlx3* disrupts the expression of proneural genes. A-D'. Gastrulating HH4 chick embryos were unilaterally electroporated with *Tlx3* specific gRNA-CRISPR/Cas9 constructs on the right side of the embryo (*Tlx3* gRNA-CRISPR/Cas9; experimental reagents). A-B'. Experimental reagents were delivered unilaterally into HH8+ (5 somites) chick embryos, in order to perturb *Tlx3* by specifically targeting neural crest cells (n=5). Immunolabeling of NEUROG2 (A-A') (white) or NEUROD1 (B-B') (white) reveals the effects of loss of *Tlx3* in neural crest cells at HH16. C-D'. Experimental reagents were delivered unilaterally into the ectoderm of HH12 (15 somites) chick embryos (n=6). Immunohistochemistry for NEUROG2 (C-C') (white) or NEUROD1 (D-D') (white) reveals the effects of loss of *Tlx3*, specifically in placode cells at HH16. Immunohistochemistry for NEUROG2 (A & C) (white) or NEUROD1 (B & D) (white) reveal the expression of these two proteins on the contralateral control side of the embryo. Scales bars represent 200 μm.

Chapter 4

Cxcl14 mediates proper trigeminal ganglion formation

A modified version of this chapter is currently *in preparation* as:

Urrutia, H.A.*, Gao, J.*, Bronner, M.E. (2025). Placode-derived orphan chemokine CXCL14 interacts with CXCR4 to mediate proper trigeminal ganglion formation. ***In preparation***.

4.1 Introduction

Chemokines are small, secreted ligands known for their roles in regulating cell migration in the immune response, cancer and embryogenesis (Kasemeier-Kulesa et al., 2010; Kucia et al., 2004; Olesnicky Killian et al., 2009). For example, the directional migration of both cranial and cardiac neural crest during development is influenced by *Cxcl12*, also known Stromal cell derived factor (*Sdf1*), present in the branchial arches (Escot et al., 2013; Olesnicky Killian et al., 2009). CXCR4 is a receptor for CXCL12 that is expressed in the neural folds as well as on migrating neural crest cells. Initially, it was thought that CXCL12 and CXCR4 form an exclusive pair, but it was subsequently found that CXCL12 also may bind to CXCR7 (Balabanian et al., 2005; Bleul et al., 1996; Boldajipour et al., 2008; Chen et al., 2015; Halasy et al., 2023; Levoye et al., 2009; Memi et al., 2013). During germ cell migration, CXCL12 signals through CXCR4, while CXCR7 functions as a "decoy" receptor, sequestering the ligand and potentially generating a CXCL12 gradient that directs migrating germ cells (Boldajipour et al., 2008).

Beyond their role in forming the skeletal elements in the ventral portion of the face, cranial neural crest cells also contribute to cranial sensory ganglia, the largest of which is the trigeminal ganglion. In vertebrates, the trigeminal ganglion, the largest of all cranial sensory ganglia, is comprised of two distinct cell populations: neural crest and ectodermal placodal cells, with neurons arising from both populations (D'Amico-Martel and Noden, 1983). The formation of ganglia from neural crest and placodal populations follows several discrete steps and interactions between these two embryonic cell types is essential for proper gangliogenesis. Several cell-cell and cell-matrix interactions have been implicated as molecular mediators for the condensation of the trigeminal ganglion (Halmi et al., 2024, 2022; Shah and Taneyhill, 2015; Shiau et al., 2008; Shiau and Bronner-Fraser, 2009; Wu and Taneyhill, 2019). Yet while these previous studies have provided novel insights into cranial ganglion formation, the underlying molecular mechanisms mediating neural crest–placodal aggregation and condensation remains largely unexplored.

The trigeminal ganglion arises lateral to the neural tube via critical interactions between ectodermal placodal and cranial neural crest derived cells. Chemokine signaling is thought to play a role in this process. For example, in zebrafish, CXCR4-CXCL12 interactions has been implicated in migration to the branchial arches as well as proper positioning of the trigeminal sensory ganglion (Knaut et al., 2003; Olesnicky Killian et al., 2009). In *Xenopus*, neural crest cells expressing CXCR4 are attracted toward the cranial placodes which express the ligand, CXCL12 (Theveneau et al., 2013, 2010). This interaction activates Rac1 signaling in neural crest cells at the front of the collectively migrating group, which are repelled upon contact. Together, this creates a coordinated migratory pattern between neural crest and placode cells, termed "chase and run." However, in chick embryos, CXCL12 is expressed in the ectoderm of the branchial arches, which is quite distant from the site of trigeminal ganglion formation. This raises the intriguing possibility that in addition to CXCL12, other factors, including unidentified chemokines, may also play a role in trigeminal ganglion formation.

In contrast to extensive information about CXCL12, little is known about the expression or function of CXCL14 during embryonic development. CXCL14 is a novel orphan chemokine with known roles in immune cell migration and anti-microbial effects (Dai et al., 2015; Lu et al., 2016; Westrich et al., 2020). Its expression has been noted in several epithelial tissue and its loss correlates with malignancy (Giacobbi et al., 2024; Gordon et al., 2011; Sjöberg et al., 2016; Westrich et al., 2020, 2019). While CXCL14 has been suggested to interact with CXCR4, CXCR7, LRP1, or CXCL12, supporting evidence remains contradictory (Atanes et al., 2019; Collins et al., 2017; Miyajima et al., 2024; Sand et al., 2015). CXCL14 has been proposed to signal via the MAPK/Erk1/2 pathway (Waldemer-Streyer et al., 2017), potentially influencing the cell cycle and epithelial-to-mesenchymal transition (EMT).

Here we explore the role of *Cxcl14* in forming trigeminal ganglion of the chick embryo. In screening for genes whose onset of expression correlates with the timing

of ganglion condensation in the chick embryo, we noted that *Cxcl14* is expressed at the onset of aggregation, as neural crest and placode cells are extensively interacting. Intriguingly, *Cxcl14* expression was largely restricted to ectodermal cells including the placodal precursors and migrating placode cells. In contrast, *Cxcr4* was exclusively expressed by neural crest cells, whereas its proposed ligand, *Cxcl12*, was expressed in the branchial arches, some distance away from the forming ganglion primordium. Importantly, loss of *Cxcl14*, including specifically in placode cells, disrupted ganglion formation, leading to abnormal gangliogenesis and defective axonal projection. Taken together, we propose that CXCL14, produced by placodal cells, may bind to the receptor CXCR4 on cranial neural crest cells to properly pattern the forming trigeminal ganglion. This work not only potentially identifies a receptor-ligand interaction between CXCL14 and CXCR4 but also demonstrate a unique role for this interaction in trigeminal neurogenesis.

4.2 Results

4.2.1 *Cxcl14* is expressed by trigeminal placode cells during interactions with cranial neural crest cells that express *Cxcr4*

To better understand potential receptor-ligand interactions during cranial neural crest migration and onset of ganglion formation in the chick embryo, we examined the gene expression patterns of receptors *Cxcr4* and *Cxcr7* relative to chemokines *Cxcl12* and *Cxcl14* using *in situ* Hybridization Chain Reaction (HCR) (Choi et al., 2018). Cranial neural crest cells undergo EMT to delaminate from the neural tube at Hamburger and Hamilton stage (HH) 9, subsequently emigrating away. At HH9, *Cxcr4* expression is evident in pre-migratory neural crest cells and persists in migratory cranial neural crest cells from HH10-HH13 (Fig. 4.1A-C).

As neural crest cells emigrate from the neural tube, *Cxcl14* is expressed in the dorsal neural tube, in a non-overlapping pattern with *Cxcr4*. Indeed, at HH9-10,

Cxcl14 is confined to the neural tube just caudal to the emigrating neural crest domain (Fig. 4.1A' and 1B', arrowheads). By HH13, *Cxcl14* expression shifts and becomes evident on what appeared to be ingressing placodal cells that are intermingled with *Cxcr4* expressing neural crest cells (Fig. 4.1C-C'). Additionally, *Cxcl14* expression remains evident in the distal regions of the developing trigeminal ganglion at HH16. This is consistent with the final location of placode-derived neurons identified in previous studies (Fig. 4.1D-D') (Begbie and Graham, 2001; D'Amico-Martel and Noden, 1983; Noden, 1978; Shiau et al., 2008).

In contrast to *Cxcr4*, *Cxcr7* was not expressed in pre-migratory or migratory neural crest cells (Fig. S4.1A) or in the condensing trigeminal ganglion anlage (Fig. S4.1B-C). Instead, *Cxcr7* was highly expressed in the frontonasal process, where its expression overlapped with *Cxcl12* (Fig. S4.1B-C). Interestingly, *Cxcl12* expression did not overlap with that of *Cxcr4* in the cranial region; rather it was predominantly expressed in the frontonasal process, quite a distant from *Cxcr4*- expressing cranial neural crest cells (compare Fig. 4.1C-D & Fig. S4.1B-C). This expression pattern in the cranial neural crest is in stark contrast to the cardiac region, where *Cxcl12* expression is immediately adjacent to and in front of the migrating cardiac neural crest cell front at HH13 and persists adjacent to the cardiac neural crest stream within the caudal branchial arches (compare Fig. 4.1C & Fig. S4.1B).

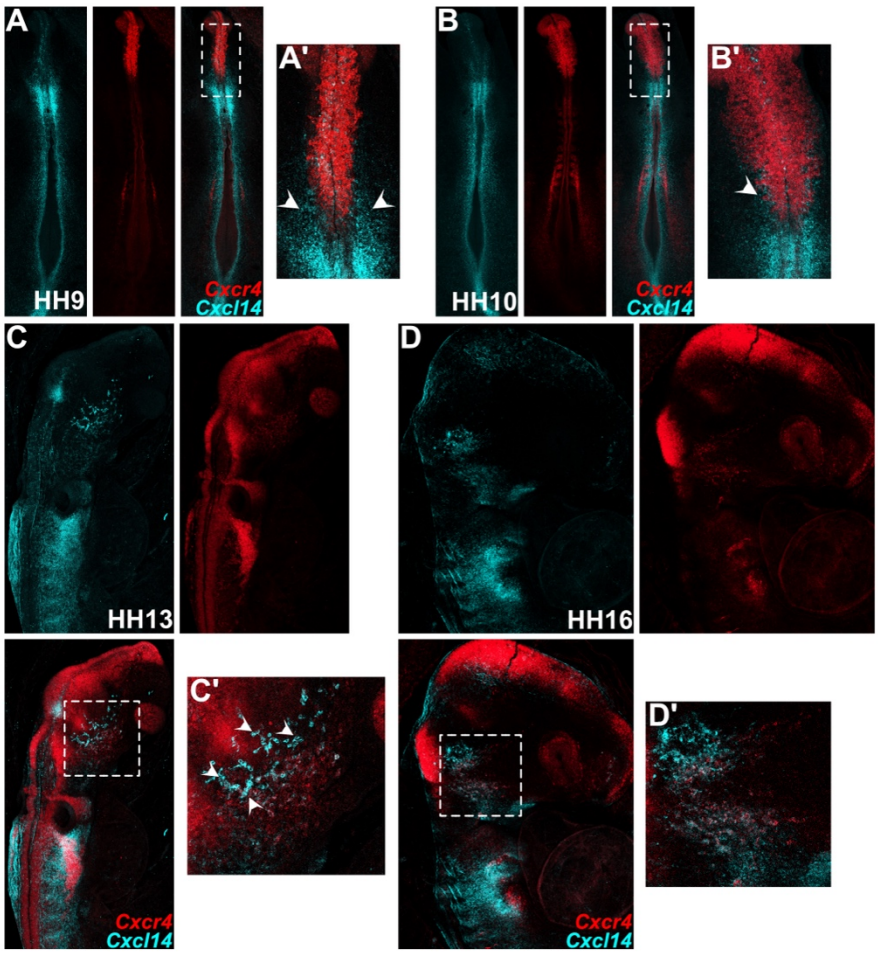

Fig. 4.1. *Cxcl14* is expressed in placodal cells and within the trigeminal ganglion. A-D. Representative images of chromogenic whole mount Hybridization chain reaction (HCR) *in situ* hybridization for *Cxcr4* (red) and *Cxcl14* (cyan) in stage HH9(A), HH10 (B), HH13 (C), HH16 (D) chick embryos. Dashed box in A-D indicates zoomed area in 'A′-D'. (inset). HCR for *Cxcr4* (red) and *Cxcl14* (cyan) reveals expression of *Cxcl14* in subset of cells, nonoverlapping domains of expression are labeled with filled arrowhead.

To determine the cell type that expresses *Cxcl14* at high resolution, we performed *ex ovo* electroporations, labeling the ectoderm and presumptive placode cells with an ectodermal enhancer, and looked for co-expression of *Cxcl14* transcripts. Transverse sections through HH13 embryos revealed *Cxcl14* transcripts in presumptive placode cells adjacent to SOX10+ expressing neural crest cells (Fig. 4.2A & 4.2A', arrowheads). These results revealed that *Cxcl14* expressing cells predominantly originate from the placodal population, as co-expression of membrane-

bound eGFP and *Cxcl14* was most prevalent following electroporation (Fig. 4.2A'-D', arrowheads).

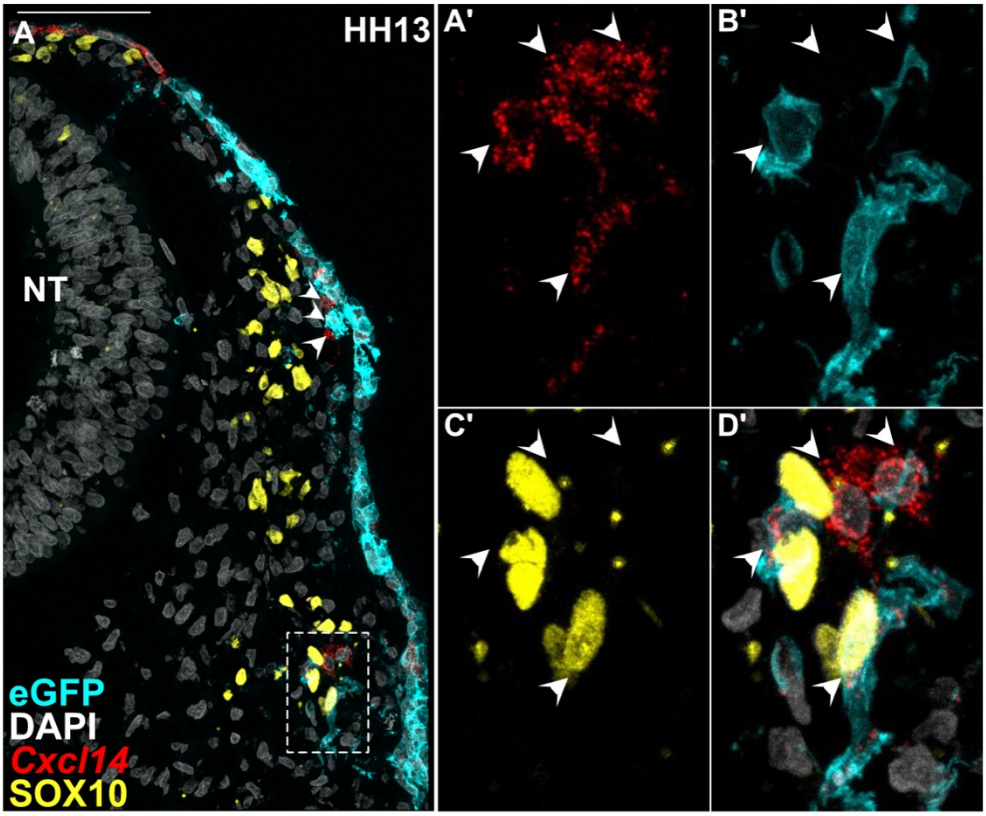

Fig. 4.2. Expression of *Cxcl14* is enriched in a subset of ectodermal placodal cells A. Representative image of a transverse section at HH13. Hybridization chain reaction (HCR) reveals expression of *Cxcl14* (red) transcripts localizing with cells that are also eGFP-labeled with an ectodermal enhancer (cyan). Immunolabeling for SOX10 (yellow) reveal neural crest cells expressing SOX10. A'-D'. Dashed box in A indicates zoomed area in A'-D'. Scale bars represent 50μm (A), NT, neural tube.

Taken together, these results suggest a possible interaction between *Cxcr4* and *Cxcl14* in the developing trigeminal ganglion. Interestingly, *Cxcl12* expression correlates with the presence of *Cxcr7* expression in the cranial region. Thus, in contrast to *Xenopus* embryos in which the *Cxcl12* has been shown to mediate interactions between cranial neural crest and placode cells, we find that *Cxcl12* is not expressed at the right place and time to account for this function in trigeminal ganglion formation in the developing chick embryo.

4.2.2 Loss of *Cxcl14* disrupts trigeminal ganglion formation

Next, we examined the effects of *Cxcl14* perturbation using CRISPR/Cas9-mediated knockouts. To achieve this, we utilized our single-CRISPR/Cas9 construct (Gandhi et al., 2021) to deplete *Cxcl14* in the developing chick embryo. Guide RNAs (gRNAs) targeting the coding sequence of *Cxcl14* were electroporated unilaterally into HH4 embryos, enabling for a global *Cxcl14* knockout (Fig. 4.3A). Following electroporation, treated embryos were allowed to develop to HH16, a stage when placode-derived neurons have extended axons, but neural crest-derived cells have yet to differentiate (Begbie et al., 2002; D'Amico-Martel and Noden, 1980; Moody et al., 1989; Shiau et al., 2008). To assess trigeminal ganglion formation, we performed immunolabeling using SOX10 to identify neural crest cells and TUJ1 to label placode-derived neurons and axonal processes.

Examination of the experimental (knockout) side of the embryo revealed defects in ganglion formation when compared to the control contralateral side of the same embryo. Specifically, neural crest-derived cells in both the ophthalmic and maxillomandibular lobes appeared more broadly dispersed following loss of *Cxcl14* (Fig. 4.3C-C''). Additionally, placode-derived neuronal processes appeared somewhat misdirected and less bundled when compared to the contralateral control side (Compare Fig. 4.3B-B'' & 4.3C-C''). To quantify these effects, we analyzed the degree of dispersion of SOX10-expressing neural crest-derived cells and TUJ1-expressing placods-derived neurons. The results revealed a significant increase in the dispersion and total area occupied by both neural crest- and placode-derived cells (Fig. 4.3D-E), affecting the ganglion as whole. Interestingly, when evaluating this effect in different ganglionic lobes, the ophthalmic lobe exhibited a more severe phenotype than the maxillomandibular lobe (Fig. 4.3C-C'').

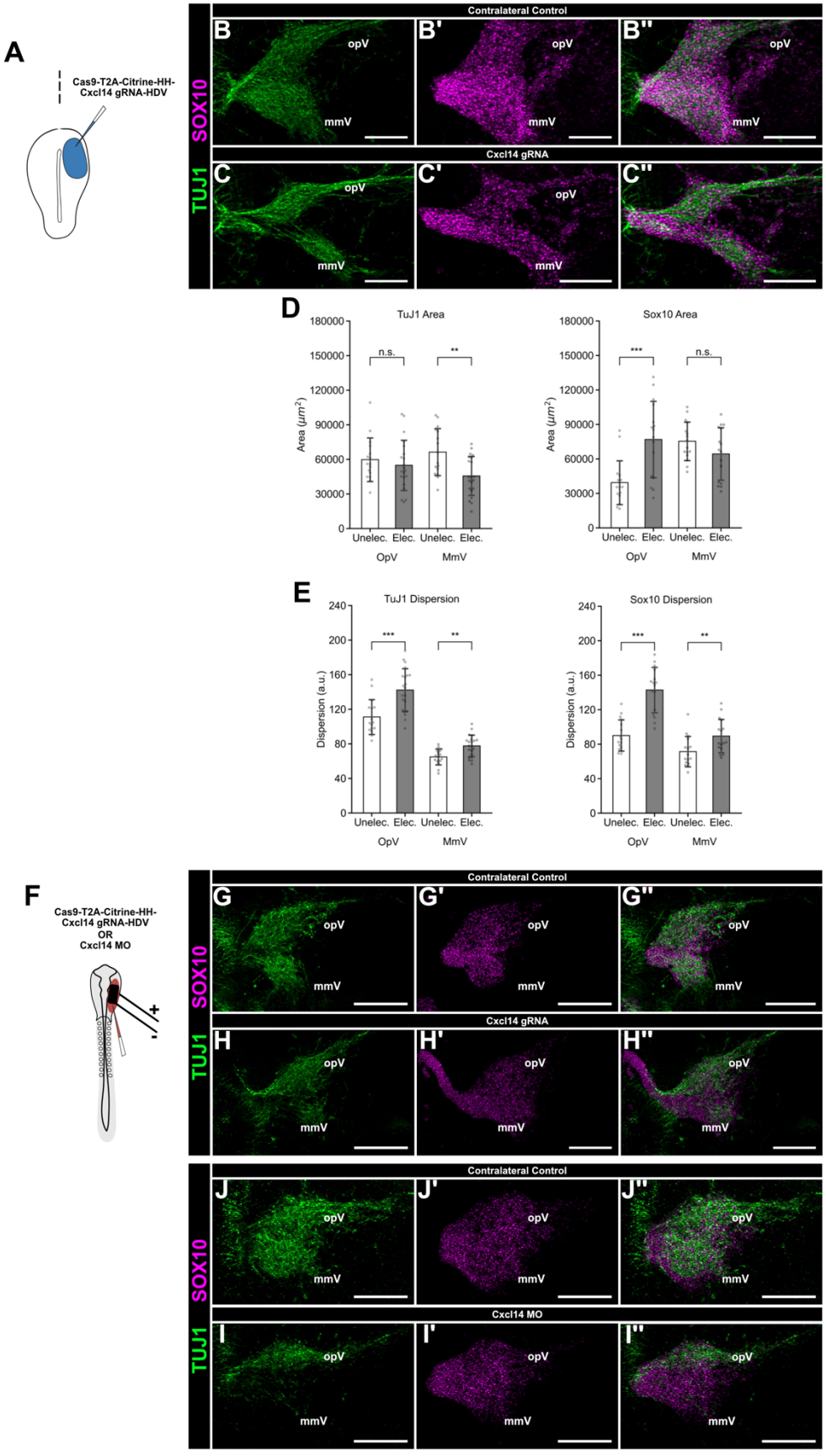
A
Cas9-T2A-Citrine-HH-Cxcl14 gRNA-HDV
Contralateral Control
Cxcl14 gRNA
SOX10
TUJ1
B
B'
B''
C
C'
C''
opV
mmV
D
TuJ1 Area
Sox10 Area
Area (μm²)
n.s.
**
***
Unelec.
Elec.
OpV
MmV
E
TuJ1 Dispersion
Sox10 Dispersion
Dispersion (a.u.)
F
Cas9-T2A-Citrine-HH-Cxcl14 gRNA-HDV
OR
Cxcl14 MO
+
-
G
G'
G''
H
H'
H''
Cxcl14 MO
J
J'
J''
I
I'
I''

Fig. 4.3. Perturbation of *Cxcl14* disrupts trigeminal ganglion development. A. Schematic diagram illustrating the *ex ovo* electroporation to test the effects of perturbing *Cxcl14*. Experimental (blue) reagents were delivered unilaterally into gastrulating HH4 chick embryos. B-C''. *Cxcl14* specific gRNA-CRISPR/Cas9 construct was unilaterally electroporated on the right side of the embryo. B-C''. Immunohistochemistry for SOX10 (magenta) and TUJ1 (green) reveals the effects of global loss of *Cxcl14* via CRISPR/Ca9-mediated approach at HH16. D-E. Quantitation of relative trigeminal ganglion size normalized to contralateral control. Ratios represent normalized experimental area divided by contralateral control area. Each point represents an individual embryo and the p-value was determined by two-tailed, paired t-test. F. Schematic illustrating the *in ovo* experimental design to perturb *Cxcl14*, specifically targeting placode cells. Experimental (red) reagents were delivered unilaterally into the ectoderm of HH11 (13 somites) chick embryos. G-I''. Either a *Cxcl14* MO or *Cxcl14* specific gRNA-CRISPR/Cas9 construct were introduced onto the right side of the embryo. Immunolabeling of SOX10 (magenta) and TUJ1 (green) reveals the effects of loss of *Cxcl14* in within the trigeminal ganglion, specifically in placode cells at HH16. Scale bars represent 200 μm.

We next examined the effects of perturbing *Cxcl14* specifically in the placodal population. To specifically knock out *Cxcl14* in the ectoderm, which normally expresses this chemokine, we electroporated *in ovo* the ectoderm with our single-CRISPR/Cas9 construct at HH11 (Fig. 4.3F). The results revealed increased dispersion of neural crest-derived cells in the maxillomandibular lobe but not in the ophthalmic lobe of the trigeminal ganglion (compare Fig. 4.3G-G'' and Fig. 4.3H-H''). Similarly, placode-derived cells occupied a reduced area, but only in the maxillomandibular lobe. Given that it takes several hours after electroporation to generate the Cas9 protein, this is consistent with the developmental timing of the trigeminal ganglion, as the ophthalmic lobe forms earlier than the maxillomandibular lobe. In addition to increased dispersion, we also noted abnormal extensions of neural crest cells away from the main body of the ganglion. In contrast to the neural crest component, the placode-derived cells appear relatively normal with no increase in dispersion (Fig. 4.3I-J). As a secondary approach, we performed *in ovo* electroporations to achieve Morpholino-mediated knockdown of *Cxcl14*. The results were morphologically similar to those obtained with the CRISPR construct, albeit not as penetrant (compare Fig. 4.3H-H'' and Fig. 4.3I-I''). Collectively, these results show that loss of *Cxcl14* impacts the condensation and proper formation of the trigeminal ganglion.

Taken together, our results reveal a new *in vivo* developmental role for *Cxcl14* during trigeminal ganglion development.

4.3 Discussion

In our search for signaling factors involved in trigeminal ganglion formation, we found that the orphan chemokine *Cxcl14* is expressed by ectodermal placode cells precisely as the trigeminal ganglion begins to condense via interactions with neural crest cells. Moreover, loss of *Cxcl14*, either globally or specifically in the ectoderm, causes abnormalities in trigeminal ganglion formation. Surprisingly, these results contradict the existing model, which suggests that interactions between *Cxcr4* and *Cxcl12* drive neural crest and ectodermal placodal interactions. This model, originally based on *Xenopus* studies, proposes that *Cxcr4-Cxcl12* interactions create a "chase and run" mechanism between neural crest and placode cells, facilitating neural crest migration throughout the embryonic head (Theveneau et al., 2013, 2010). In the chick embryo, we find that this scenario fits well with the migration pattern of cardiac neural crest cells in the neck region of the embryo. These cells interact with epibranchial placode cells as they migrate to the heart (Halasy et al., 2023; Kuratani and Tanaka, 1990; Tani-Matsuhana et al., 2023). Our expression analysis suggests a close interaction between neural crest cells expressing *Cxcr4* and epibranchial placode cells expressing *Cxcl12*, leading to migration into the heart. Consistent with this, chick *Cxcl12* is critical for guiding cardiac neural crest cells to the heart (Gandhi et al., 2020; Tani-Matsuhana et al., 2023). In contrast, our study finds no evidence of *Cxcl12* expression near cranial neural crest cells migrating toward the trigeminal ganglion. Instead, *Cxcl12* is expressed in the ectoderm of branchial arches 1 and 2, near cells expressing *Cxcr7*. Conversely, *Cxcl14* expression in chick placode cells at HH13 correlates strongly with *Cxcr4* expression in migrating cranial neural crest cells. On this basis, we hypothesize that an interaction between *Cxcr4* expressing neural crest cells and *Cxcl14* expressing placode cells is critical for proper condensation of the trigeminal ganglion. Consistent with this, our results show that loss of *Cxcl14* disrupts ganglion formation, with the most severe effects on the neural crest-derived component of the ganglion.

While our findings highlight an important role for chemokine signaling in trigeminal ganglion formation, other pathways have also been shown to be critical for gangliogenesis. For example, *Robo2* on placodal cells and *Slit1* on neural crest cells are known to mediate trigeminal placode-neural crest interactions (Shiau et al., 2008; Shiau and Bronner-Fraser, 2009). In addition, previous studies have demonstrated that trigeminal ganglion formation are mediated, in part, by cadherin-based adhesions. Notably, Cadherin-7 and N-Cadherin are expressed in neural crest and placode cells, respectively, during formation of the chick trigeminal ganglia (Halmi et al., 2022; Hatta et al., 1987; Nakagawa and Takeichi, 1995; Shiau and Bronner-Fraser, 2009; Wu and Taneyhill, 2019). Overall, the interactions between Cadherin-7, expressed in neural crest cells, and N-Cadherin, present in placodal neurons, is required for coalescing of neural crest and placodal neurons during trigeminal ganglion formation (Wu et al., 2014; Wu and Taneyhill, 2019).

In summary, this present study demonstrates that the orphan chemokine *Cxcl14* is expressed in placode-derived cells during prior to ingression and at the onset of aggregation, allowing for the extensive interactions during formation of the trigeminal ganglion of the chick embryo. In contrast, *Cxcr4* was exclusively expressed by neural crest cells, whereas its proposed ligand *Cxcl12* was expressed in the branchial arches, some distance away from the forming ganglion primordium. Additionally, CRISPR-Cas9 mediated knockout of *Cxcl14*, specifically in the placodal cells, results in loss of the maxillary mandibular lobe and reduction in the ophthalmic lobe of the trigeminal ganglion. Taken together, we speculate that *Cxcl14*, made by placodal cells, may facilitate interactions with migratory cranial neural crest at the onset of condensation of the trigeminal ganglion, in turn driving the proper gangliogenesis.

4.4 Materials and methods

4.4.1 Chicken embryos

Fertilized chicken embryos (*Gallus gallus*) were obtained from local commercial sources (Petaluma Egg Farm, Petaluma, CA) and incubated at 37°C in humidified incubators to the desired stages. Embryos were staged by Hamburger-Hamilton (HH) (Hamburger and Hamilton, 1951) staging method as indicated.

4.4.2 Construct design, cloning, and morpholinos

DNA constructs were produced by PCR reactions using AccuPrime high-fidelity DNA Taq polymerase (ThermoFisher) followed by standard purification (Qiagen), restriction enzyme digestion, and ligation (NEB). Full-length sequence of the ectodermal enhancer, LNFG, was amplified from a previous construct and inserted into the pTK backbone, upstream of a Memb-bound eGFP. All constructs produced in this study were later verified by Sanger sequencing (Laragen) and full plasmid sequencing (Primordium) prior to usage. Constructs for all experiments were used at a final concentration of 2.5 μg/μl, diluted in EB buffer. All translation-blocking morpholino oligomer (MO) were synthesized by Gene Tools, LLC. Standard control oligomer from Gene Tools, LLC (control MO) and *Cxcl14* MO were diluted with water and used at a final dose of 2.5 μM. To enable visualization of the injection solution, 0.5 μl of 2% red/blue food dye was added per 10 μl injection mix.

4.4.3 CRISPR/Cas9-mediated perturbations

Guide RNA (gRNA) targets for *Cxcl14* were generated and obtained using the CHOPCHOP tool (Labun et al., 2019, 2021). One gRNA targeting the coding sequence of *Cxcl14* was generated and the protospacer were cloned into the single-CRISPR/Cas9 construct, according to the protocol published by Gandhi et al. (2021).

The final vector was later verified by Sanger sequencing (Laragen) prior to usage. All single CRISPR/Cas9 construct used for all experiments were used at final concentration of 2.5 μg/μl, diluted in EB buffer. To enable visualization of the injection solution, 0.5 μl of 2% red/blue food dye was added per 10 μl injection mix.

4.4.4 Electroporations

For *ex ovo* experiments, embryos were incubated 19–20 h to obtain stage HH4, whereas for *in ovo* experiments, embryos were either incubated 33 h to obtain stages HH11. *Ex ovo* electroporations were performed as previously described (Sauka-Spengler and Barembaum, 2008) by passing five 5.8 V pulses for 50 ms at 100 ms intervals. Embryos were then cultured in 1 ml albumin supplemented with 1% penicillin/streptomycin (PenStrep) at 37.5◦C. The following day, embryos were screened for transfection efficiency (high fluorescence intensity), and unhealthy and/or poorly transfected embryos were discarded. For *in ovo* experiments, all constructs were introduced at stages HH11 Platinum electrodes were placed vertically or horizontally across the chick embryo delivering five 13 V pulses for 50 ms at 100 ms intervals as previously described (Shiau et al., 2008). Incubation was then continued for ~18–24 h to reach stages HH13-14 or ~28–36 h to reach stages HH15-16.

4.4.5 Cyosectioning

Whole-mount embryos were fixed in 4% paraformaldehyde (PFA) overnight at 4◦C, followed by three washes in 1 ×PBS at room temperature. Embryos were then washed in 5% sucrose in PBS at room temperature for 1 h and then stored in 15% sucrose in PBS overnight at 4◦C. Embryos were subsequently incubated in 7.5% gelatin for 4–16 h at 39◦C, then flash-frozen in liquid nitrogen and stored at− 80◦C. Transverse frozen sections were taken and allowed to dry overnight at room

temperature. Gelatin was removed by incubating slides in PBS at 42◦C for 10 min, and coverslips were mounted with Fluoromount-G (SouthernBiotech).

4.4.6 Hybridization chain reaction

Hybridization chain reaction (HCR) v3 was performed using the protocol suggested by Molecular Technologies (Choi et al., 2018) with minor modifications. Briefly, embryos were fixed in 4% PFA overnight at 4◦C, washed in PBSTw, dehydrated, and stored in 100% methanol overnight at− 20◦C. The following day, embryos were rehydrated and processed for cryosectioning. Following sectioning, slides were treated with proteinase-K for 10 min, and incubated with 12 pmol of *Cxcl14* probe (B9 initiator) dissolved in hybridization buffer overnight at 37◦C. The subsequent day, following several washes in hybridization probe wash buffer and 0.1% 5x–SSC–Tween, embryos were incubated in 30 pmol of amplifier hairpins H1 and H2 labeled with Alexa647 diluted in amplification buffer at room temperature overnight. The following day, embryos were washed in 0.1% 5x–SSC–Tween and imaged. All probes were designed and ordered through Molecular Technologies. Embryos were processed for cryosectioning at 16 μm and subsequently imaged.

4.4.7 Immunohistochemistry

Embryos were fixed in 4% PFA in sodium phosphate buffer for 20 min at room temperature, washed in 0.5 M Tris-HCl/1.5 M NaCl/10 mM CaCl2/0.5% Triton X-100 in TBS (TBSTr), blocked in 10% donkey serum in TBSTr for 2 h at room temperature, and incubated in primary antibody solution at 4°C for two nights. On the third day, embryos were washed in TBSTr (30 min per wash, six washes) and incubated in secondary antibody solution for two nights at 4◦C. Following the secondary antibody incubation, embryos were washed in TBSTr (30 min per wash, six washes) and processed for imaging and then for cryosectioning. The following primary antibodies and concentrations were used: Goat anti-GFP (1:500; Rockland,

Cat# 600-101-215); Rabbit anit-Sox10 (1:500, Sigma-Aldrich, Cat# HPA068898); Primary antibodies were detected by Alexa Fluor 488-, 568-, or 647-conjugated donkey secondary antibodies (1:500; Molecular Probes). For transverse sectioning, immunolabeled embryos were sectioned at a thickness of 12 μm.

4.4.8 Microscopy

Whole-mount and transverse section images were acquired at room temperature using a Zeiss Imager.M2 with an ApoTome.2 module, Axiocam 506 color and monochromatic cameras, and Zen 2 Blue software (ZEISS). Transverse section imaging was also preformed using a Zeiss LSM 900 with an inverted microscope. Whole-mount images were acquired as wide-field views or displayed as a maximum intensity projection of Z-stacks, with a Plan Apochromat 10 x objective/0.45 NA (ZEISS), and embryos were imaged in 1X TBSTr. Transverse sections were acquired as a single optical plane or maximum intensity projections of Z-stacks, using a Plan Apochromat 40 x objective/1.3 NA (ZEISS), and were imaged in Fluoromount-G (SouthernBiotech). Images were pseudocolored and minimally processed for brightness and contrast using Fiji (Schindelin et al., 2012). Image analysis and display preparation were performed using Fiji (Schindelin et al., 2012).

4.4.9 Image and statistical analysis

Images were analyzed and prepared for displaying using Fiji (Schindelin et al., 2012). For each whole-mount image, neural crest migration area was determined by manually drawing regions of interest (ROIs) surrounding the neural crest along a 400 μm length of the midbrain and measuring the area. This analysis approach has been used routinely to identify changes in migration area (Hutchins and Bronner, 2018, 2019; Piacentino and Bronner, 2018; Piacentino et al., 2021; Schiffmacher et al., 2018). Measurements were made for both sides at the same axial level, and then the electroporated experimental length was divided by the electroporated control length

to calculate the relative maximum migration distance. Knockdown electroporations of chick embryos are heterogeneous and mosaic; as such, we performed analysis over large ROIs that encompass many cells within the trigeminal ganglion. For this analysis approach, ROIs were manually drawn to measure fluorescence intensity, size area, and to define boundaries for multiple-cell fluorescence intensity measurements. Fluorescence measurements, corrected total cellular fluorescence, values were calculated and normalized as previously described (Piacentino and Bronner, 2018).

Statistical analyses were performed using GraphPad Prism9. P-values are indicated in the text, and a cutoff of $P < 0.05$ was used to determine significance. All datasets were tested for normal distribution with a Kolmogorov–Smirnov test. Normalized distributed data were analyzed with parametric tests (t-test or one-way ANOVA). The specific tests used are reported in in the corresponding figure legends. All analyses show pooled biological replicates from at least three independent experiments. Data are presented as mean values, with error bars indicating SEM.

4.5 Author contributions statement

Hugo A. Urrutia: Writing – Original draft, Visualization, Project administration, Methodology, Investigation, Funding acquisition, Formal analysis, Data curation, Conceptualization. Junpeng Gao: Writing – review & editing, Methodology, Investigation. Marianne E. Bronner: Writing – Original draft, Supervision, Project administration, Investigation, Funding acquisition, Formal analysis, Data curation, Conceptualization.

4.6 Declaration of competing interest

The authors declare no competing or financial interests.

4.7 Acknowledgement

Funding for this work is supported by the National Institutes of Health (NIH) grants R01DE027568 to M.E.B. and F31DE031154 to H.A.U.

4.8 References

Atanes, P., Hawkes, R.G., Olaniru, O.E., Ruz-Maldonado, I., Amisten, S., Persaud, S.J., 2019. CXCL14 inhibits insulin secretion independently of CXCR4 or CXCR7 receptor activation or cAMP inhibition. Cell. Physiol. Biochem. 52, 879–892.

Balabanian, K., Lagane, B., Infantino, S., Chow, K.Y.C., Harriague, J., Moepps, B., Arenzana-Seisdedos, F., Thelen, M., Bachelerie, F., 2005. The chemokine SDF-1/CXCL12 binds to and signals through the orphan receptor RDC1 in T lymphocytes. J. Biol. Chem. 280, 35760–35766.

Bleul, C.C., Fuhlbrigge, R.C., Casasnovas, J.M., Aiuti, A., Springer, T.A., 1996. A highly efficacious lymphocyte chemoattractant, stromal cell-derived factor 1 (SDF-1). J. Exp. Med. 184, 1101–1109.

Boldajipour, B., Mahabaleshwar, H., Kardash, E., Reichman-Fried, M., Blaser, H., Minina, S., Wilson, D., Xu, Q., Raz, E., 2008. Control of chemokine-guided cell migration by ligand sequestration. Cell 132, 463–473.

Chen, Q., Zhang, M., Li, Y., Xu, D., Wang, Y., Song, A., Zhu, B., Huang, Y., Zheng, J.C., 2015. CXCR7 mediates neural progenitor cells migration to CXCL12 independent of CXCR4. Stem Cells 33, 2574–2585.

Choi, H.M.T., Schwarzkopf, M., Fornace, M.E., Acharya, A., Artavanis, G., Stegmaier, J., Cunha, A., Pierce, N.A., 2018. Third-generation in situ hybridization chain reaction: Multiplexed, quantitative, sensitive, versatile, robust. Development 145. https://doi.org/10.1242/dev.165753

Collins, P.J., McCully, M.L., Martínez-Muñoz, L., Santiago, C., Wheeldon, J., Caucheteux, S., Thelen, S., Cecchinato, V., Laufer, J.M., Purvanov, V., Monneau, Y.R., Lortat-Jacob, H., Legler, D.F., Uguccioni, M., Thelen, M.,

Piguet, V., Mellado, M., Moser, B., 2017. Epithelial chemokine CXCL14 synergizes with CXCL12 via allosteric modulation of CXCR4. FASEB J. 31, 3084–3097.

Dai, C., Basilico, P., Cremona, T.P., Collins, P., Moser, B., Benarafa, C., Wolf, M., 2015. CXCL14 displays antimicrobial activity against respiratory tract bacteria and contributes to clearance of Streptococcus pneumoniae pulmonary infection. J. Immunol. 194, 5980–5989.

D'Amico-Martel, A., Noden, D.M., 1983. Contributions of placodal and neural crest cells to avian cranial peripheral ganglia. Am. J. Anat. 166, 445–468.

Escot, S., Blavet, C., Härtle, S., Duband, J.-L., Fournier-Thibault, C., 2013. Misregulation of SDF1-CXCR4 signaling impairs early cardiac neural crest cell migration leading to conotruncal defects. Circ. Res. 113, 505–516.

Gandhi, S., Ezin, M., Bronner, M.E., 2020. Reprogramming axial level identity to rescue neural-crest-related congenital heart defects. Dev. Cell 53, 300-315.e4.

Gandhi, S., Li, Y., Tang, W., Christensen, J.B., Urrutia, H.A., Vieceli, F.M., Piacentino, M.L., Bronner, M.E., 2021. A single-plasmid approach for genome editing coupled with long-term lineage analysis in chick embryos. Development 148. https://doi.org/10.1242/dev.193565

Giacobbi, N.S., Mullapudi, S., Nabors, H., Pyeon, D., 2024. The chemokine CXCL14 as a potential immunotherapeutic agent for cancer therapy. Viruses 16, 302.

Gordon, C.T., Wade, C., Brinas, I., Farlie, P.G., 2011. CXCL14 expression during chick embryonic development. Int. J. Dev. Biol. 55, 335–340.

Halasy, V., Szőcs, E., Soós, Á., Kovács, T., Pecsenye-Fejszák, N., Hotta, R., Goldstein, A.M., Nagy, N., 2023. CXCR4 and CXCL12 signaling regulates the development of extrinsic innervation to the colorectum. Development 150. https://doi.org/10.1242/dev.201289

Halmi, C.A., Leonard, C.E., McIntosh, A.T., Taneyhill, L.A., 2024. N-cadherin facilitates trigeminal sensory neuron outgrowth and target tissue innervation. bioRxiv. https://doi.org/10.1101/2024.05.20.594965

Halmi, C.A., Wu, C.-Y., Taneyhill, L.A., 2022. Neural crest cell-placodal neuron interactions are mediated by Cadherin-7 and N-cadherin during early chick trigeminal ganglion assembly. F1000Res. 11, 741.

Hamburger, V., 1961. Experimental analysis of the dual origin of the trigeminal ganglion in the chick embryo. J. Exp. Zool. 148, 91–123.

Hatta, K., Takagi, S., Fujisawa, H., Takeichi, M., 1987. Spatial and temporal expression pattern of N-cadherin cell adhesion molecules correlated with morphogenetic processes of chicken embryos. Dev. Biol. 120, 215–227.

Kasemeier-Kulesa, J.C., McLennan, R., Romine, M.H., Kulesa, P.M., Lefcort, F., 2010. CXCR4 controls ventral migration of sympathetic precursor cells. J. Neurosci. 30, 13078–13088.

Knaut, H., Werz, C., Geisler, R., Nüsslein-Volhard, C., Tübingen 2000 Screen Consortium, 2003. A zebrafish homologue of the chemokine receptor Cxcr4 is a germ-cell guidance receptor. Nature 421, 279–282.

Kucia, M., Jankowski, K., Reca, R., Wysoczynski, M., Bandura, L., Allendorf, D.J., Zhang, J., Ratajczak, J., Ratajczak, M.Z., 2004. CXCR4-SDF-1 signalling, locomotion, chemotaxis and adhesion. J. Mol. Histol. 35, 233–245.

Kuratani, S., Tanaka, S., 1990. Peripheral development of the avian vagus nerve with special reference to the morphological innervation of heart and lung. Anat. Embryol. (Berl.) 182, 435–445.

Levoye, A., Balabanian, K., Baleux, F., Bachelerie, F., Lagane, B., 2009. CXCR7 heterodimerizes with CXCR4 and regulates CXCL12-mediated G protein signaling. Blood 113, 6085–6093.

Lu, J., Chatterjee, M., Schmid, H., Beck, S., Gawaz, M., 2016. CXCL14 as an emerging immune and inflammatory modulator. J. Inflamm. (Lond.) 13, 1.

Memi, F., Abe, P., Cariboni, A., MacKay, F., Parnavelas, J.G., Stumm, R., 2013. CXC chemokine receptor 7 (CXCR7) affects the migration of GnRH neurons by regulating CXCL12 availability. J. Neurosci. 33, 17527–17537.

Miyajima, R., Tanegashima, K., Naruse, N., Denda, M., Hara, T., Otaka, A., 2024. Identification of low-density lipoprotein receptor-related protein 1 as a

CXCL14 receptor using chemically synthesized tetrafunctional probes. ACS Chem. Biol. 19, 551–562.

Nakagawa, S., Takeichi, M., 1995. Neural crest cell-cell adhesion controlled by sequential and subpopulation-specific expression of novel cadherins. Development 121, 1321–1332.

Olesnicky Killian, E.C., Birkholz, D.A., Artinger, K.B., 2009. A role for chemokine signaling in neural crest cell migration and craniofacial development. Dev. Biol. 333, 161–172.

Sand, L.G.L., Scotlandi, K., Berghuis, D., Snaar-Jagalska, B.E., Picci, P., Schmidt, T., Szuhai, K., Hogendoorn, P.C.W., 2015. CXCL14, CXCR7 expression and CXCR4 splice variant ratio associate with survival and metastases in Ewing sarcoma patients. Eur. J. Cancer 51, 2624–2633.

Shah, A., Taneyhill, L.A., 2015. Differential expression pattern of Annexin A6 in chick neural crest and placode cells during cranial gangliogenesis. Gene Expr. Patterns 18, 21–28.

Shiau, C.E., Bronner-Fraser, M., 2009. N-cadherin acts in concert with Slit1-Robo2 signaling in regulating aggregation of placode-derived cranial sensory neurons. Development 136, 4155–4164.

Shiau, C.E., Lwigale, P.Y., Das, R.M., Wilson, S.A., Bronner-Fraser, M., 2008. Robo2-Slit1 dependent cell-cell interactions mediate assembly of the trigeminal ganglion. Nat. Neurosci. 11, 269–276.

Sjöberg, E., Augsten, M., Bergh, J., Jirström, K., Östman, A., 2016. Expression of the chemokine CXCL14 in the tumour stroma is an independent marker of survival in breast cancer. Br. J. Cancer 114, 1117–1124.

Tani-Matsuhana, S., Kawata, Y., Inoue, K., 2023. The cardiac neural crest gene MafB ectopically directs CXCR4 expression in the trunk neural crest. Dev. Biol. 495, 1–7.

Theveneau, E., Marchant, L., Kuriyama, S., Gull, M., Moepps, B., Parsons, M., Mayor, R., 2010. Collective chemotaxis requires contact-dependent cell polarity. Dev. Cell 19, 39–53.

Theveneau, E., Steventon, B., Scarpa, E., Garcia, S., Trepat, X., Streit, A., Mayor, R., 2013. Chase-and-run between adjacent cell populations promotes directional collective migration. Nat. Cell Biol. 15, 763–772.

Waldemer-Streyer, R.J., Reyes-Ordoñez, A., Kim, D., Zhang, R., Singh, N., Chen, J., 2017. Cxcl14 depletion accelerates skeletal myogenesis by promoting cell cycle withdrawal. NPJ Regen. Med. 2.

Westrich, J.A., Vermeer, D.W., Colbert, P.L., Spanos, W.C., Pyeon, D., 2020. The multifarious roles of the chemokine CXCL14 in cancer progression and immune responses. Mol. Carcinog. 59, 794–806.

Westrich, J.A., Vermeer, D.W., Silva, A., Bonney, S., Berger, J.N., Cicchini, L., Greer, R.O., Song, J.I., Raben, D., Slansky, J.E., Lee, J.H., Spanos, W.C., Pyeon, D., 2019. CXCL14 suppresses human papillomavirus-associated head and neck cancer through antigen-specific CD8+ T-cell responses by upregulating MHC-I expression. Oncogene 38, 7166–7180.

Wu, C.-Y., Hooper, R.M., Han, K., Taneyhill, L.A., 2014. Migratory neural crest cell αN-catenin impacts chick trigeminal ganglia formation. Dev. Biol. 392, 295–307.

Wu, C.-Y., Taneyhill, L.A., 2019. Cadherin-7 mediates proper neural crest cell-placodal neuron interactions during trigeminal ganglion assembly. Genesis 57, e23264.

4.9 Supplementary Figures

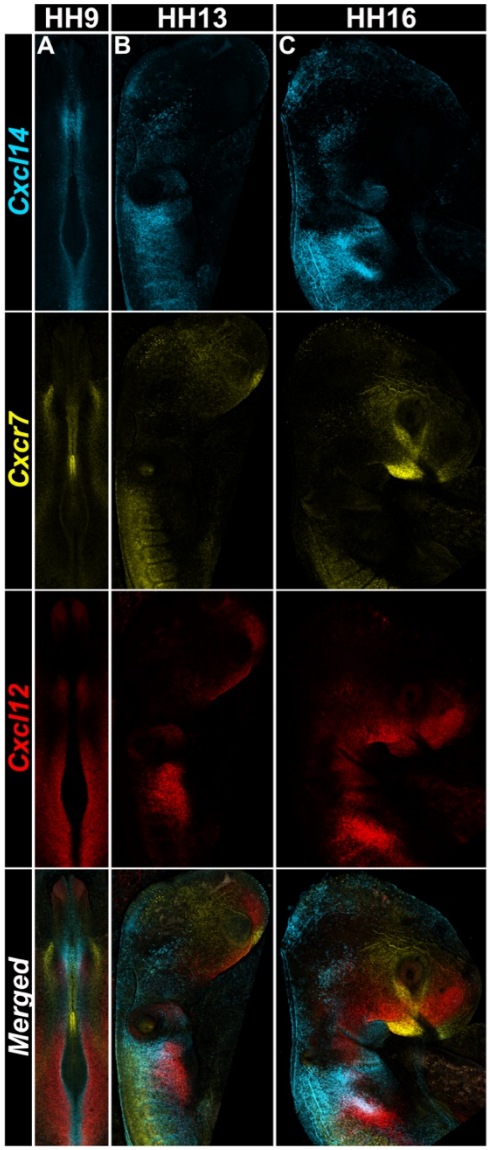

Fig S4.1. Expression patterns of *Cxcr7* and *Cxcl12* across a range of developmental stages from HH9 to HH16. A-C. Representative images of whole mount HCR *in situ* hybridization for *Cxcr7*, *Cxcl12*, and *Cxcl14* at stages HH9 (A), HH13 (B) and HH15 (C) chick embryos.

Chapter 5

Conclusion

The experimental studies presented in this thesis provide further insights into the cellular mechanisms underlying the assembly and condensation of neural crest and placodal cells into distinct cranial sensory ganglia. The results demonstrate that, from ingression of placodal cells to the formation a properly condensed ganglion, these two cell populations are highly interdependent, engaging in extensive interactions *in vivo* that culminate in proper trigeminal gangliogenesis.

To determine the transcriptional changes that govern trigeminal gangliogenesis, we screened for genes whose expression coincides with the onset of ganglion condensation in the developing chick embryo. We were able to draw clearer conclusions regarding the roles and interactions required during these critical developmental stages. Previous studies have shown that ablating either cell population results in significant defects and abnormal trigeminal ganglion development (Shiau et al., 2008). Specifically, embryos lacking placodal cells exhibit smaller or dispersed ganglia, whereas the absence of neural crest cells leads to ganglia that fail to properly connect to the hindbrain and do not integrate into a bi-lobed structure (Shiau et al., 2008). These findings emphasize the necessity of interactions between these two distinct cell populations and suggest that bi-directional neural crest–placode signaling plays a crucial role in mediating ganglion formation.

As a potential downstream mechanism, the role of the proneural transcription factor *Tlx3* was tested during trigeminal gangliogenesis. *Tlx3* has been implicated in the differentiation and fate specification of excitatory sensory neurons in both the central and peripheral nervous systems. Previous studies have identified *Tlx3* as a post-mitotic selector gene essential for specifying excitatory sensory neuronal identity. In the chick peripheral nervous system, *Tlx3* is expressed at HH15 in overlapping

domains within placodally derived components of the trigeminal ganglion, where it functions as a post-mitotic selector gene directing excitatory sensory neuronal fate (Cheng et al., 2004; Kondo et al., 2008; Logan et al., 1998). Despite these insights, it remained unclear whether *Tlx3* expression and function were restricted to placode-derived neurons or if neural crest-derived neurons within the trigeminal ganglion also share this property. To address this question, we utilized a combination of lineage labeling and *in situ* hybridization in the chick embryo and demonstrated that neural crest-derived cells contributing to the cranial trigeminal ganglion express *Tlx3* at critical time points corresponding to the onset of ganglion condensation. Notably, loss of *Tlx3* function *in vivo* reduces the overall size and abundance of neurons within the trigeminal ganglion, whereas ectopic expression of *Tlx3* in migrating cranial neural crest cells results in premature neuronal differentiation. Taken together, these findings highlight a crucial role for *Tlx3* in neural crest-derived cells during chick trigeminal gangliogenesis.

Additionally, the concurrent expression of *Cxcl14* in placodal cells and its potential cognate receptor *Cxcr4* expressed in migratory neural crest cells during trigeminal ganglion development led us to investigate whether this ligand-receptor pair may mediate neural crest-placode interactions. Focusing on the initial stages of their interactions, we examined the function of the orphan chemokine *Cxcl14* during trigeminal gangliogenesis. Our results reveal that while *Cxcl14* is expressed in various regions of the developing embryo, its expression is also evident in the cranial region at the onset of ganglion condensation. We found that *Cxcl14* expression is primarily restricted to ectodermal cells, including placodal precursors and migratory placodal cells. Loss of *Cxcl14*, specifically in placodal cells, *in vivo* resulted in severely disorganized ganglion formation, leading to defects in both gangliogenesis and axonal projection. These results indicate that CXCL14, produced by placodal cells, binds to the receptor CXCR4 on cranial neural crest cells to guide the proper organization of the forming trigeminal ganglion. This work not only establishes a receptor-ligand interaction between CXCL14 and CXCR4 but also reveals a previously unrecognized role for this interaction in trigeminal neurogenesis.

In summary, the results of this thesis have identified molecular players involved in neural crest–placode interactions during the formation of chick cranial sensory ganglia. We hypothesize that cranial gangliogenesis follow at least four distinct but overlapping steps: (1) migratory cranial neural crest cells emigrate to the site of the ganglion assembly; (2) placodal cells are specified and begin differentiating into neurons within the ectoderm; (3) placodal neuroblasts ingress into the ganglion anlage; and (4) interactions between migratory cranial neural crest and placodal neurons at the ectoderm–mesenchyme interface drive the condensation of these intermixed populations into discrete ganglion structure. It is worth mentioning that several of these steps are interactive. For example, the production and ingression of placodal neurons from the surface ectoderm continue throughout most of gangliogenesis, and ongoing interactions between neural crest and placodal cells are essential to this coordinated developmental process.

Our findings reveal a novel role for *Cxcl14* as a molecular cue produced by placodal cells. Its expression initiates in ectodermal placodal precursors and migratory placodal cells at the onset of trigeminal ganglion condensation. The early expression of this chemokine positions it in a prime location, influencing neighboring migratory cranial neural crest cells, which express its cognate receptor *Cxcr4*. Neural crest cells that first interact with placodal cells first respond to *Cxcl14*, and this signaling event then facilitate the proper condensation and assembly of the forming trigeminal ganglion (see Figure 5.1, for a schematic summary). While the downstream mechanisms of *Cxcr4–Cxcl14* dependent signaling in mediating condensation and differentiation neural crest- and placode-derived cell remains unclear, we speculate that placodal cells may influence the final fate (either neuronal or glial) of neural crest cells during trigeminal ganglion formation. We show that both neural crest-derived and placode-derived cells express the proneural transcription factor *Tlx3*, albeit at different time points corresponding to their respective developmental timeline.

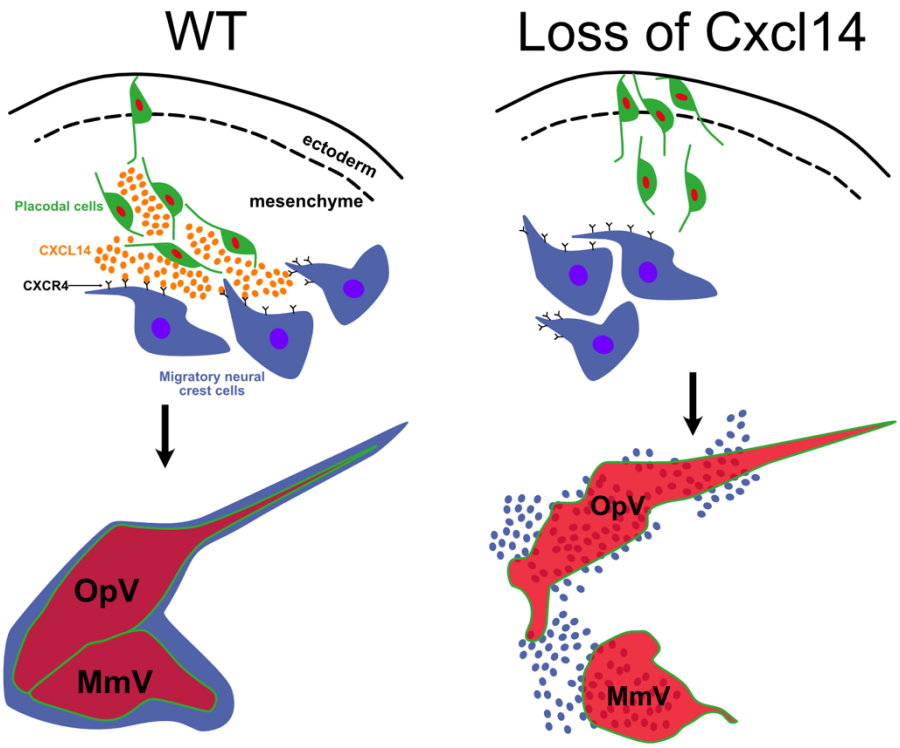

Figure 5.1. Schematic illustrating the possible role for *Cxcr4-Cxcl14* dependent signaling during cranial gangliogenesis. The main defect is depicted in *Cxcl14* deficient embryos as compared to wild type (WT) embryos. First, ingression appears to be delayed in *Cxcl14* deficient embryos, inhibiting placodal neurons at early stages of migration. Conversely, loss of *Cxcl14* could also result in loss of placodal neurons at early stages. At the time of condensation, loss of *Cxcl14* results in deficient placodal neurons not assembling in their normal positions and are more disorganized, while their axonal projections are also affected. Additionally, *Cxcl14* deficient embryos, have more dispersed neural crest cells, resulting in a defective ganglion, as compared to the WT. Perturbation of *Cxcl14* in placodal cells causes a migratory and condensation defects, which may possibly suggest a role for *Cxcl14* at different steps of ganglion formation.

These results suggest that ganglion coalescence and differentiation of neural crest-derived cells may be driven by *Cxcr4–Cxcl14* signaling that precedes and perhaps plays a role in initiation of *Tlx3* expression. Accordingly, we propose two possible models: (1) *Tlx3* expression in neural crest-derived cells occurs following its exposure to CXCL14, such that this chemokine-receptor interaction acts as a potential upstream cue for neuronal differentiation, while lack of *Cxcl14* may promote a glial fate. Thus, these two components form a coordinated developmental pathway, with *Cxcl14* signaling serving as a trigger that contributes to subsequent *Tlx3* activation, particularly in neural crest cells (Figure 5.2A). In an alternative scenario, (2) neural crest-derived cells may activate *Tlx3* independently or earlier, as part of an intrinsic

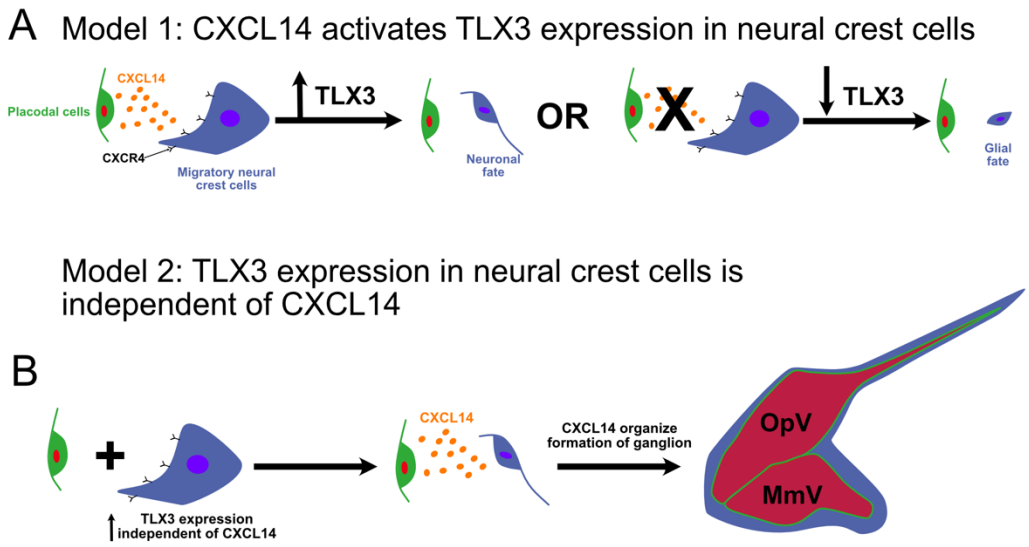

Figure 5.2. Schematic illustrating two possible models for *Cxcl14* and *Tlx3* mechanisms during trigeminal ganglion formation. Model 1 proposes that CXCL14 potentially activates the expression of *Tlx3* in neural crest cells, promoting neuronal differentiation. Conversely, lack of *Cxcl14* from placodal cells may in turn promote a glial fate, suggesting that these two components form a coordinated developmental pathway, with *Cxcr4-Cxcl14* signaling serves as a trigger that contributes to proneuronal differentiation in neural crest cells. Model 2 presents the alternative hypothesis, illustrating that neural crest-derived cells may activate *Tlx3* independently of CXCL14 exposure, representing a separate and distinct mechanism by which CXCL14 may instead guide the spatial organization of the ganglion by directing neural crest and placodal cells to their respective locations within the developing ganglion.

differentiation program initiated by other factors. In this model, *Cxcl14* and *Tlx3* represent separate and distinct mechanisms. CXCL14 may guide the spatial organization of the ganglion by directing placodal cells to distal regions and positioning neural crest cells appropriately based on their exposure to the chemokine (Figure 5.2B). Functionally, *Tlx3* acts as a post-mitotic selector gene required for the acquisition of excitatory sensory neuronal identity. Cells that fail to express *Tlx3 in vivo* show reduced neuronal differentiation and ganglion size, but do not appear to adopt a glial fate, suggesting that Tlx3 is necessary for excitatory neuron specification rather than a binary neuronal-versus-glial decision. Together, these results reveal a dynamic interplay between placodal signaling, chemokine guidance, and transcriptional programming that underlies the coordinated assembly of the trigeminal ganglion.

These findings provide additional molecular insights into the signaling mechanisms that facilitate neural crest–placode condensation during trigeminal ganglion formation. They underscore the importance of heterotypic cell interactions during cranial gangliogenesis for cellular condensation, further illustrating the critical interplay of cell–cell communication and condensation in the formation of complex structures in the developing vertebrate embryo.

5.2 Future perspectives

The work presented in this thesis lays a foundation for numerous questions surrounding the fascinating processes of cell–cell interactions and morphogenesis during cranial sensory ganglia formation. Many aspects of neural crest–placode interactions remain to be investigated to fully understand the intricate and complex process of cranial gangliogenesis. In this thesis, I have identified a critical role for *Tlx3* in neural crest-derived cells and demonstrated its essential function in proper chick trigeminal gangliogenesis. Initially described in placodally-derived neurons, *Tlx3* was originally believed to be restricted to this cell population within the trigeminal ganglion. However, it is now evident that *Tlx3* expression is necessary for the differentiation of excitatory neurons, though many aspects of how this transcription factor is activated and maintained in these cell populations remain to be fully elucidated. Since *Tlx3* expression first emerges in placodal cells, it would be valuable to investigate whether key factors present in placodal cells stimulate the specification and differentiation of neural crest cells toward a sensory neuronal fate. In particular, determining how *Tlx3* is activated and how it regulates trigeminal ganglion formation remain to be determined.

In looking for signals that may influence trigeminal ganglion formation, I have identified a novel role for *Cxcl14* and *Cxcr4* in mediating a key aspect of neural crest–placode interactions that regulate the proper organization of the trigeminal ganglion during its formation. Notably, *Cxcl14* expression precedes that of *Tlx3* and was largely restricted to ectodermal cells, including placodal precursors and migrating placodal

cells. In contrast, its putative receptor *Cxcr4* was exclusively expressed by neural crest cells. Canonically, *Cxcr4* have been proposed to interact with the ligand, *Cxcl12*; however, we only detected *Cxcl12* in the branchial arches, some distance away from the forming ganglion primordium. Importantly, loss of *Cxcl14*, including its specific depletion in placodal cells, disrupted ganglion formation, resulting in abnormal gangliogenesis and defective axonal projection. These findings not only highlight the receptor-ligand interaction between CXCL14 and CXCR4 but also demonstrate a unique role for this signaling axis in trigeminal neurogenesis. However, several aspects of these interactions remain poorly understood at the molecular level. These include the mechanisms underlying reciprocal or reverse signaling from neural crest to placodal cells, whether multiple signaling pathways are activated or downregulated upon CXCR4–CXCL14 interaction, and whether additional direct protein interactions mediate neural crest–placode interactions. Furthermore, since *Cxcr4* is expressed in neural crest cells, we cannot rule out the possibility that *Cxcl14* expression is activated and maintained once placodal cells ingress, leading to the subsequent downregulation of CXCR4 in neural crest cells. The integration of multiple signaling pathways likely governs the formation of the ganglion. Uncovering the molecular interactions of CXCR4 and CXCL14 at different developmental stages and within distinct regions of the forming ganglion is crucial for understanding how this signaling mechanism drives proper ganglion assembly.

Here, I present a few possible future directions stemming from this study to address some of these open questions. The study of neural crest–placode interactions not only elucidate critical processes in the development of the peripheral nervous system but also serves as a powerful model for investigating cell–cell signaling and subsequent cellular changes *in vivo*.

First, investigating *Cxcl14*-*Cxcr4* interactions at the protein level during gangliogenesis is a necessary step for gaining deeper insight into the function of this signaling pair. Previous studies focusing on *Cxcr4* have demonstrated that loss of this receptor affects neural crest migration, but it would be worthwhile to examine how the

loss of migratory neural crest cells may influence *Cxcl14* activation in placodal cells and is it dependent on neural crest proximity or interactions. It would also be crucial to determine if only CXCL14 directly interacts with CXCR4 or are there other chemokines that potentially dimerize with CXCL14 to bind to CXCR4. These would provide crucial understanding about the function of *Cxcl14* and whether other signaling pathways compensate for or modulate CXCR4–CXCL14 interactions.

Second, exploring the downstream signaling pathways activated by CXCR4–CXCL14 in neural crest cells would elucidate further intracellular mechanisms dictating the cellular changes that occur during gangliogenesis. The interaction between CXCR4 and CXCL14 may elicit different cellular responses at distinct stages of neural crest–placode interactions and characterizing these signaling events would provide a more comprehensive understanding of their roles in cranial ganglion formation.

Finally examining whether neural crest–placode interactions and the roles of CXCR4–CXCL14 signaling are evolutionarily conserved in cranial sensory gangliogenesis across other vertebrate species (e.g., mouse, zebrafish, and lamprey) could reveal broader biological significance. Comparative studies across species would provide valuable insights into how these signaling mechanisms have been conserved or diversified throughout vertebrate evolution. Taken together, the findings presented in this thesis open the door to many exciting future investigations and research directions. Further exploration of these molecular interactions and signaling pathways will continue to enhance our understanding of the fundamental mechanisms underlying cranial sensory ganglion formation and neural crest–placode interactions.